HAL
open science

Conception d'un distributeur de servocommande hydromécanique sous critères de coût et de mixabilité

Thibaut Marger

To cite this version:

Thibaut Marger. Conception d'un distributeur de servocommande hydromécanique sous critères de coût et de mixabilité. Génie mécanique [physics.class-ph]. Arts et Métiers ParisTech, 2010. Français. NNT : 2010ENAM0052 . pastel-00590711

HAL Id: pastel-00590711

https://pastel.hal.science/pastel-00590711v1

Submitted on 4 May 2011

HAL is a multi-disciplinary open access archive for the deposit and dissemination of scientific research documents, whether they are published or not. The documents may come from teaching and research institutions in France or abroad, or from public or private research centers.

L'archive ouverte pluridisciplinaire **HAL**, est destinée au dépôt et à la diffusion de documents scientifiques de niveau recherche, publiés ou non, émanant des établissements d'enseignement et de recherche français ou étrangers, des laboratoires publics ou privés.

2010-ENAM-0052

École doctorale n° 432 : Sciences des Métiers de l'Ingénieurs

Doctorat ParisTech

T H È S E

pour obtenir le grade de docteur délivré par

l'École Nationale Supérieure d'Arts et Métiers

Spécialité " Conception mécanique "

présentée et soutenue publiquement par

Thibaut MARGER

le 13 décembre 2010

Conception d'un distributeur de servocommande hydromécanique sous critères de coût et de mixabilité

Valve design of hydro-mechanical servoactuator under cost and mixability criteria

Directeur de thèse : **Jean-Claude CARMONA**
Co-encadrement de la thèse : **Jean-Charles MARE**
Co-encadrement de la thèse : **Valérie BUDINGER**
Co-encadrement de la thèse : **François MALBURET**

Jury

Mme. Valérie BUDINGER, Maître de conférences, DMIA, ISAE	Co-encadrant
M. Jean-Claude CARMONA, Professeur des universités, LSIS-INSM, Arts et Métiers ParisTech	Directeur
M. Bruno CHADUC, Ingénieur, Research & Development – Eurocopter	Invité
M. Rogelio FERRER, Docteur-Ingénieur, Research & Development - Eurocopter	Examinateur
M. Zbigniew KOSANECKI, Professeur, Institute des turbomachines, Université Technique de Lodz	Examinateur
M. Pascal LEGUAY, , Ingénieur, Research & Development – Eurocopter	Invité
M. François MALBURET, Maître de conférences, LSIS-INSM, Arts et Métiers ParisTech	Co-encadrant
M. Jean-Charles MARÉ, Professeur des universités, LGMT, INSA Toulouse-UPS	Co-encadrant
M. Patrick SEBASTIAN, Maître de Conférences HDR , TREFLE, Université Bordeaux 1	Rapporteur
M. Nicolae VASILIU, Professeur DR.Ing, HHMD, Université Politehnica de Bucarest	Rapporteur

T H È S E

Arts et Métiers ParisTech - Centre d'Aix-en-Provence
Nom de l'Unité de recherche

ParisTech
INSTITUT DES SCIENCES ET TECHNOLOGIES
PARIS INSTITUTE OF TECHNOLOGY

ARTS ET MÉTIERS ParisTech

Arts et Métiers ParisTech - Centre d'Aix-en-Provence
Nom de l'Unité de recherche

Remerciements

De nombreuses et enrichissantes rencontres ont eut lieu tout au long de la thèse. Chacune ayant participée à l'accomplissement de celle-ci par sa contribution, je tenais à les remercier.

Tout d'abord à mes encadrants de l'ENSAM, J.C. Carmona et F. Malburet pour leurs aides et soutiens quotidien. Ils m'ont notamment aidé à apprendre à évoluer au sein d'une grande entreprise tout en suivant des objectifs principalement donnés par le monde universitaire. Je ne peux parler de l'ENSAM sans mentionner le chef de l'équipe IMS P. Véron ainsi que M. Richard et F. Weider qui m'ont aidé à nager parmi les méandres administratifs. Evidemment j'ai une pensée toute particulière à toutes les personnes que j'ai pu y côtoyer pendant ces trois ans : T. Ripert, N. Lalande, P. Salvan-Guillotin, C. Lopez, M, Houry-Panchetti, A. Brindejonc, F. Boukari et R. Lou.

J'aimerais ensuite remercier mes autres encadrants universitaires J.C. Maré et V. Budinger qui m'ont énormément apporté par leurs conseils, leur présence et leur aide aussi bien technique que personnelle. Ils ont été des acteurs indispensables à la réussite de ce projet. J'en profite pour saluer le département avionique et système de l'ENSICA qui m'a très bien accueilli lors de mes déplacements sur Toulouse avec F. Deudon, O. Cherrier, S. Bidon, O. Besson, ainsi que les dames de la maison des élèves qui se sont occupées de mon logement avec diligence. Mes déplacements à l'INSA bien que moins fréquents ont toujours été cordial grâce au très bon accueil des différentes personnes y travaillant : M. Budinger, Jonathan et Wissam.

Je ne peux bien évidemment pas oublier les nombreuses personnes rencontrées au sein d'Eurocopter. Vincent S. qui m'a formé sur le sujet au début de ma thèse, puis Jean-Romain B. qui a pris sa suite et avec qui les échanges ont été quotidien, riche aussi bien personnellement que professionnellement. Pascal L. et Bruno C. ne sont évidemment pas à oublier pour leur aide continue et leur connaissance. Je ne peux faire sans mentionner toute l'équipe des commandes de vol si agréable, sympathique et dynamique : Christophes, Florian, Nicolas, Yohanne, Jean-Philippe, Zouhair, Michel, Patrice, Jean-Yves, Damien, Tanguy et Cédric. Je remercie également ceux que j'ai côtoyé au sein du laboratoire d'essai aussi bien les compagnons, que les techniciens et les ingénieurs, et en particulier à Enguerrand G. et Mathieu G. pour leur bonne humeur.

Je ne peux finir sans mentionner ma famille et mes amis qui m'ont été présent aussi bien durant les moments de reconnaissance que pendant les phases plus difficile.

Contents

Introduction 7
French synthesis 7
Thesis introduction 9
Chapitre 1 From helicopter flight controls to actuator components 13
1.1 - French synthesis 13
1.2 - Introduction 16
1.3 - Helicopter flight controls 16
1.3.1 - A rotor aircraft: the helicopter 16
1.3.2 - Helicopter architecture 17
1.4 - Architecture of a main servoactuator for light helicopters 23
1.4.1 - Architecture in nominal mode 23
1.4.2 - Architecture in degraded mode 25
1.5 - Architecture of the valve 26
1.5.1 - Architecture in nominal mode 26
1.5.2 - Architecture in degraded mode 29
1.6 - Conclusion 30
Chapitre 2 Models and tools for design and manufacturing 33
2.1 - French synthesis 33
2.2 - Introduction 38
2.3 - Servoactuator behavior 38
2.3.1 - Preliminary remarks on servohydraulic actuator 38
2.3.2 - Power requirements 40
2.3.3 - Jack-to-load adaptation 41
2.3.4 - Valve-to-jack adaptation 42
2.3.5 - Frequency requirements 42
2.4 - Non linear static valve model 43
2.4.1 - The valve characteristics 43
2.4.2 - Orifice valve model 48
2.4.3 - Parameters of the four ways, sliding spool valve 51
2.5 - Simulation tools 55
2.5.1 - Design of experiments 56
2.5.2 - Implementation of the valve quasi-static model 58
2.5.3 - Dynamic models of the servoactuator and of the valve 61
2.6 - Conclusion 64
Chapitre 3 Pre-design and manufacturing of the valve 67
3.1 - French Synthesis 67
3.2 - Introduction 71
3.3 - Specification of the servoactuator 71
3.3.1 - Specification from the existing servoactuator [17] 71
3.3.2 - New specifications 77
3.3.3 - Summary of the specifications 77
3.4 - Model based methodology for the valve pre-design 78
3.4.1 - Fixed parameters for the pre-design 78
3.4.2 - Equations for the pre-design 80
3.4.3 - Methodology and computation of the design parameters 83
3.5 - Asymptotic method for valve manufacturing 84

3.5.1 - Using the valve model to define the machining process 85
3.5.2 - Asymptotic pressure gain 86
3.5.3 - Link between the valve overlap and the valve parameters 88
3.5.4 - Parasitic influence of the rounded edge 90
3.5.5 - Experimental validation 92
3.6 - Design of the test bench 95
3.7 - Conclusion 100
Chapitre 4 Final design of the valve in the nominal mode 101
4.1 - French synthesis 101
4.2 - Introduction 106
4.3 - Valve design and valve model update from experiments 106
4.3.1 - DOE-based selection of the rectangular slot and restriction diameter 106
4.3.2 - Update of the dynamic valve model 114
4.4 - Valve design update for mixability over the full operating domain 118
4.4.1 - From rectangular to trapezoidal valve slot 119
4.4.2 - Model-based selection of the basis of the trapezoidal slot 121
4.4.3 - Experimental validation of the selected basis 125
4.5 - Servoactuator behavior 125
4.5.1 - Validation on the servoactuator 125
4.5.2 - Evolution of the project 128
4.6 - Conclusion 129
Conclusion 131
French synthesis 131
Thesis conclusion 133
Bibliography 137
Annex1: method to compute the speed gain curve from the flow gain test 139

Introduction

French synthesis

Cette thèse a été à l'initiative d'Eurocopter, un membre du groupe EADS (European Aeronautic Defence & Space) depuis 2000. Eurocopter est le leader mondial en termes de fabrication et suivi des hélicoptères civils et militaires. Très peu de pièces sont effectivement fabriquées par l'entreprise qui se concentre sur l'intégration mécanique et avionique des systèmes négociés à des fournisseurs, ne gardant en fabrication interne que les équipements clés comme la boite de transmission principale. Dans un souci de garder la maitrise des éléments clés, Eurocopter a souhaité acquérir un nouveau savoir-faire : le design et la fabrication des servocommandes principales nécessaires dans les commandes de vol.

Les servocommandes aident le pilote à contrôler l'appareil avec précision et peu d'effort au manche (<0.25daN). Sur un hélicoptère comme le dauphin, les charges exercées par les pales peuvent atteindre les 300daN. Dans ces conditions, un pilotage manuel serait impossible. Différentes sortes de servocommandes peuvent être utilisée : hydromécanique, électrohydraulique, électromécanique.

Ce travail concerne le design et la fabrication de servocommandes à entrée mécanique et puissance hydraulique. Ces servocommandes sont constituées de :

- Un levier d'entrée pour transmettre les ordres du pilote
- Un distributeur pour moduler la puissance
- Un piston pour transformer la puissance hydraulique en puissance mécanique
- Un corps et une tige pour transmettre la puissance mécanique
- Une liaison mécanique pour assurer le contrôle de la commande

Le distributeur est la pièce la plus coûteuse et la plus difficile à concevoir et à fabriquer de la servocommande. Cette pièce est également celle qui influence principalement les performances de l'actionneur.

Le principal objectif de la thèse est de concevoir une servocommande faible coût qui possède des performances similaires à une servocommande actuellement utilisée. La servocommande sélectionnée est celle de l'EC130, l'hélicoptère le plus vendu. C'est un appareil léger (<5tonnes) avec un circuit hydraulique fonctionnant à faible pression (35bar).

Cet objectif a été scindé en trois étapes :

- Modéliser une servocommande et en particulier l'étage pilote de celle-ci : le distributeur

- Concevoir le distributeur à partir de ce modèle
- Fabriquer des prototypes de servocommande et valider la conception grâce à des essais expérimentaux

Ces étapes ont été atteintes tout au long de la thèse et sont décrites dans les différents chapitres. Les deux premiers présentent principalement le fonctionnement général de l'hélicoptère, de la servocommande et du distributeur. Les deux derniers chapitres concernent les études réalisées pour répondre aux objectifs fixés par Eurocopter.

Le premier chapitre est une description descendante de l'hélicoptère au distributeur de servocommande. Il décrit tout d'abord les éléments principaux de l'appareil. Puis un centrage sur les comportements de la servocommande permet d'expliquer son fonctionnement dans les deux configurations d'utilisation possibles (nominal et dégradé). L'organe critique de la servocommande est le distributeur qui module la puissance hydraulique. Le fonctionnement de cette pièce est donc un point décisif vis-à-vis des performances de la servocommande. Comme celle-ci, le distributeur est décrit dans ses deux configurations de fonctionnement. Dans ce chapitre, des solutions techniques du futur design sont sélectionnées pour la servocommande et le distributeur afin de répondre aux exigences de l'application.

Le second chapitre présente les modèles et outils pour le design et la fabrication du distributeur de servocommande. Il commence avec la description du domaine fonctionnel de la servocommande, *i.e.* le plan caractéristique de puissance mécanique. Puis le domaine fonctionnel du distributeur est décrit par les trois courbes caractéristiques : le gain en débit, le gain en pression et la courbe de fuite. Ces courbes sont analysées afin de montrer le lien entre les caractéristiques du distributeur et les performances de la servocommande. Puis les équations du modèle de distributeur pour un orifice sont présentées en fonction des paramètres géométriques du distributeur et des caractéristiques du fluide. Ces paramètres sont ensuite analysés et leur plage de fonctionnement définie. La dernière partie du chapitre présente les outils pour la simulation et la conception : les plans d'expérience, l'implémentation du modèle quasi-statique de distributeur à partir du modèle d'écoulement à travers un orifice et le modèle dynamique de distributeur ainsi que de servocommande.

Le troisième chapitre concerne le pré-design et la fabrication des premiers distributeurs. Afin de satisfaire les exigences, les spécifications doivent être détaillées et quantifiées. Ces spécifications proviennent des servocommandes existantes déjà exploitées et sont complétées par de nouvelles concernant la mixabilité avec la servocommande existante et le débit maximal consommé par la servocommande. La méthode choisie pour le pré-design du distributeur est basé sur une exploitation de modèle. Celui-ci est fonction de différents paramètres : des paramètres fixes du fluide, de la servocommande et du distributeur et des

autres paramètres réglables, dit de « design », qui influencent les performances du distributeur et de la servocommande. La méthode consiste à calculer les paramètres de design à partir du modèle. Cette étude permet de définir un jeu de paramètres initial. Comme il est connu que les paramètres fixes de design sont définis avec certaines incertitudes, plusieurs distributeurs sont fabriqués autour du jeu de paramètres initial. Du fait des tolérances très strictes, la fabrication des distributeurs est une opération difficile. Aussi, une nouvelle méthode bas coûts est développée basée sur la représentation asymptotique de la courbe de gain en pression. Finalement, deux bancs d'essai sont réalisés afin de tester les distributeurs et servocommandes fabriqués.

Le quatrième chapitre présente le design final du distributeur en mode nominal. Les résultats expérimentaux ont été exploités grâce à un plan d'expérience afin de calculer les paramètres de design du distributeur réel. De plus ces essais sont utilisés pour recaler le modèle dynamique de distributeur et évaluer la mixabilité sur tout le domaine de fonctionnement. Les résultats de cette évaluation montrent que cette dernière exigence n'est pas atteinte. Afin de solutionner ce problème, une nouvelle géométrie de fente pour le distributeur est proposée. Le design est donc mis à jour grâce à une approche basée sur le modèle puis validé par des essais sur le nouveau distributeur. Finalement le distributeur est monté sur un prototype de servocommande qui est testé sur le banc dédié. Les résultats expérimentaux obtenus sont utilisés pour recaler le modèle dynamique de servocommande et pour vérifier toutes les exigences. Quelques légères modifications du design sont proposées d'un point de vue marketing : l'augmentation de la course levier et de la limite de consommation maximale afin d'augmenter la vitesse maximale à vide.

Thesis introduction

This thesis has been initiated by Eurocopter a member of EADS group (European Aeronautic Defence & Space) since 2000. Eurocopter is leader in manufacturing and supporting civil and military helicopters. The company integrates mechanical and avionic systems delivered by suppliers. Very few devices are manufactured by Eurocopter, for example the main gear box, which is a critical component of helicopters. OnlyEurocopter has wished to acquire a know-how in the design and manufacturing of another critical device: the main servoactuators used for the flight controls.

The servoactuators assist the pilot to control the helicopter with accuracy and small pilot loads (<0.25daN). On a helicopter like Dolphin, the load exerted by the blades can reach 300daN on the swashplate. Manual piloting would be impossible without the use of servoactuators. Different kind of servoactuators can be used to perform this force amplification function: hydro-mechanical, electro-hydraulic and electro-mechanical.

This work concerns the design and manufacturing of hydraulically supplied and mechanically signalled servoactuators. These actuators which power assist the pilot, are constituted by:

- An input lever to transmit the pilot order
- A valve to modulate the power delivered to the jack
- A jack to transform the hydraulic power in mechanical power
- A body and a rod to transmit the mechanical loads
- A mechanical linkage to realize the position control of the actuator.

The valve is the most costly servoactuator device. It is difficult to design and to manufacture. This device is also the one that mainly influences the servoactuator performance.

The thesis main objective is to design a low cost servoactuator which has similar performances as one of the servoactuators already in service. The selected servoactuator is the one of the EC130, the most sold Eurocopter helicopter. This is a light helicopter (maximal take off weight lower than 5tonnes) with hydraulic circuits working at low pressure (35bar).

This objective has been spread in three steps:

- modelling of servoactuator and in particular the power controller stage of the servoactuator: the hydraulic valve
- model-based design of the valve
- manufacturing of servoactuator prototypes and validation through experimental tests

These steps have been reached along the thesis and are described in different chapters. The first two chapters mainly present a general statement of the helicopter, the servoactuator and the valve. The last third chapters concern the studies realized to meet the objectives fixed by Eurocopter.

The first chapter is organised as a top-down approach from the helicopter to the servoactuator valve. It describes the main devices of the helicopter. Then a focus on the servoactuator behaviour permits to explain the functioning in the two operating modes (nominal and degraded). The critical component of the servoactuator is the valve which modulates the hydraulic power. Thus the operation of this device is a key point for the performances of the servoactuator. As the servoactuator, the valve is described for the two operating modes. In this chapter some technological solutions for the future design are selected for the servoactuator and the valve to meet the requirements of the application.

The second chapter presents the models and tools for the design and manufacturing of the servoactuator valve. It starts with a description of the servoactuator functional domain *i.e.*

the mechanical power plane characteristic. Then, the valve functional domain is described by three characteristic curves: the flow gain, the pressure gain and the leakages curve. These curves are analyzed in order to point out the links between the valve characteristics and the servoactuator performances. After that, the valve model equations are established for an orifice given as a function of the valve geometry and the fluid physical properties. These parameters are then analyzed and their range is defined. The last part of the chapter presents the simulation tools: the design of experiment, the implementation of the valve quasi-static model from the orifice valve model and the dynamic models of the servoactuator and of the valve.

The third chapter deals with the pre-design and the manufacturing of the first valves. To meet the requirements, specifications must be detailed and quantified. These specifications come from the existing servoactuators already in use and are completed by additional ones concerning the mixability with the existing servoactuator and the maximal flow consumed by the servoactuator. The chosen methodology for the valve pre-design is model-based. The model is a function of different parameters: some fixed parameters on the fluid, the valve and the servoactuator and some design parameters which influence the valve and servoactuator performances. The methodology consists in computing the design parameters using the model of the valve. This study allows defining an initial set of parameters. As it is known that the fixed parameters are defined with uncertainties *e.g.* manufacturing tolerances, some valves are manufactured around this initial set of parameters. The valves manufacturing is a difficult operation because of tolerances. Thus, a new low cost process is developed based on the asymptotic representation of the pressure gain characteristic curve. Finally, in order to test the manufactured valves and the servoactuator, two test benches are designed, manufactured and set up.

The fourth chapter presents the final design of the valve in the nominal mode. The experimental results are exploited thanks to a design of experiment in order to compute the design parameters from real valves. Moreover these tests are used to update the dynamic valve model and to assess the mixability over the full operating domain. The results of this evaluation point out that this requirement is not reached. In order to solve this problem, a new valve geometry is proposed. The design is updated using a model-based approach and validated by experimental tests on the new valve. Finally, the valve is mounted on a first servoactuator prototype which is tested on the servoactuator test bench. The obtained experimental results are used to update the servoactuator dynamic model and to check all the requirements. For only marketing reasons, some light modifications are proposed to increase the no-load speed.

Chapitre 1

From helicopter flight controls to actuator components

1.1 - French synthesis

Ce chapitre commence avec une description des principaux éléments de l'hélicoptère. Un de ceux-ci est la servocommande de vol. Ces servocommandes sont majoritairement hydrauliques et pilotées par un distributeur qui module la puissance hydraulique. Comme la thèse concerne la conception et la fabrication du distributeur vis-à-vis du comportement de la servocommande, les deux modes d'utilisation (nominal et dégradé) de la servocommande puis du distributeur sont décrits. Le chapitre se termine avec la sélection de solutions techniques pour la conception du nouveau distributeur afin de répondre aux spécifications.

Ca chapitre présente tout d'abord l'hélicoptère, avec ses spécificités. Les principaux éléments de l'hélicoptère sont:

- Un moteur qui fournit la puissance mécanique en particulier au rotor.
- Une boite de transmission principale qui adapte la vitesse de rotation du moteur à la vitesse de rotation du rotor
- Deux rotors. Le rotor principal assure la portance et la propulsion de l'appareil. Le couple moteur est transmis au rotor principal par la boite de transmission principale. Afin de compenser la réaction de ce couple sur l'appareil, un second rotor, plus petit, est généralement placé à l'extrémité de la poutre de queue.
- Un plateau cyclique constitué de deux parties, une stationnaire et l'autre rotative. Il est en charge de modifier l'incidence en s'inclinant dans toutes les directions et en bougeant verticalement.
- Un mélangeur qui transforme les ordres du pilote en demande de déplacement pour chaque servocommande.
- Les commandes de vol qui sont le lien entre le moteur (puissance), le rotor (vol) et le pilote (ordres). Le pilote utilise trois systèmes de contrôle : le cyclique, le collectif et le pédalier. Ainsi il peut changer l'altitude, l'attitude et la vitesse de l'appareil. Les servocommandes, généralement hydrauliques, sont placées sur la chaine cinématique afin de réduire l'effort au manche pour

garantir un pilotage possible et précis. Afin de correctement positionner le plateau cyclique, trois servocommandes le déplacent.

La seconde partie du chapitre concerne une servocommande principale. Il y a plusieurs sortes de servocommandes et deux sources potentielles d'énergie : électrique ou hydraulique. Les hélicoptères légers étant de petits appareils comparés aux aéroplanes, la densité de puissance est plus importante, ce qui explique que la puissance hydraulique ait été gardée. La servocommande relative à l'application est composée de :

- Un levier d'entrée, transmettant les ordres du pilote
- Un distributeur qui module la puissance en fonction de son ouverture
- Un piston qui transforme la puissance hydraulique en puissance mécanique
- Un corps et une tige pour transmettre les efforts mécaniques
- Des liaisons mécaniques qui assurent un asservissement en position de la servocommande

Afin de piloter avec facilité et précision, un vérin double effet est sélectionné. Dans ce cas, contrairement à un vérin simple effet, l'actionneur peut développer la puissance hydraulique dans les deux sens de fonctionnement.

Il y a deux manières d'intégrer une servocommande. Dans le premier cas, la tige est fixée au bâti de l'hélicoptère tandis que le corps est relié au plateau cyclique. Dans le second cas, c'est la tige qui se déplace tandis que le corps est fixé au bâti de l'appareil. Pour des questions de simplicité et de robustesse, la configuration à corps mobile a été retenue.

Il est intéressant pour une servocommande double effet d'avoir un comportement symétrique. Le moyen le plus simple d'y parvenir est d'avoir une tige symétrique. Cependant, une tige symétrique implique une longue tige avec deux portées au niveau du corps et donc deux joints dynamiques entre les corps pressurisés à l'environnement extérieur. Etant donné que la raison principale de dépose en maintenance des servocommandes concerne un problème d'étanchéité au niveau de ces joints, il est très important d'en limiter au maximum le nombre. Un actionneur dissymétrique nécessitant seulement un joint dynamique entre le circuit hydraulique et l'extérieur est donc sélectionné pour cette application.

La servocommande est un organe critique de l'hélicoptère. Il n'est pas acceptable que son fonctionnement soit interrompu en service même durant un très court moment. La perte du circuit hydraulique est un cas de panne n'étant pas extrêmement rare et le pilote ne peut contrôler un hélicoptère sans assistance mise à part pour les plus petits appareils. Pour cette raison, la fonction de transmission de puissance de l'actionneur a été doublé (deux corps). Chaque corps étant alimenté par un circuit indépendant. Si un circuit hydraulique est perdu, la servocommande peut fonctionner avec le second. Pour des raisons d'encombrement, les deux corps sont montés en tandem avec une ségrégation verticale.

L'interface permettant de transformer les ordres du pilote en puissance hydraulique est régie par le distributeur. Son fonctionnement est donc un point clé pour les performances de la servocommande.

Tout d'abord, étant donné que le vérin est dissymétrique, pour obtenir une réponse symétrique, il faudrait logiquement un fonctionnement dissymétrique du distributeur. Cependant, afin de réduire, les coûts, le distributeur est conservé symétrique, ce qui est une solution inhabituelle.

Le distributeur doit moduler la puissance hydraulique en fonction de son ouverture. Pour des raisons de coûts de fabrication, un distributeur cylindrique et linéaire a été retenu. Il est constitué d'une chemise fixe et d'un corps mobile.

Lorsque le distributeur est associé à un organe de transformation hydraulique, il réalise un pont de Wheatstone. Ceci permet avec un unique distributeur d'assurer les fonctions de direction du fluide vers le bon conduit et de modulation de la puissance.

En pratique, le distributeur est conçu sans joint dynamique afin d'éviter les non linéarités dues aux efforts de frottements. L'étanchéité entre les parties fixes et mobiles est donc assurée par des jeux de fabrication extrêmement faibles mais qui induisent néanmoins des fuites parasites. Le distributeur finalement sélectionné est un distributeur cylindrique, coulissant, dont les orifices sont taillés dans la chemise (Figure 13).

Comme le distributeur est la partie de pilotage de l'actionneur, afin de garantir la sécurité de l'hélicoptère, les différents cas de panne du distributeur doivent être pris en compte.

Tout d'abord en cas de perte d'un circuit hydraulique, un système de by-pass est utilisé pour éviter de conserver une pression résiduelle dans les chambres et de bloquer l'actionneur. Ensuite, le distributeur est constitué par un tiroir se déplaçant dans une chemise fixe. La conception du distributeur prend donc en compte un élément de secours permettant de piloter ou de créer un by-pass si jamais la tige se grippe dans la chemise et empêche donc de contrôler la servocommande. Une nouvelle pièce est donc ajoutée. Le tiroir principal bouge dans une tige de secours en fonctionnement normal. Le tiroir de secours, maintenu centré par une boite à ressort en fonctionnement normal, peut à son tour bouger dans la chemise si jamais la tige principale se grippe dans le tiroir secours. En cas de grippage, l'effort au manche devient donc plus important, mais l'hélicoptère est toujours pilotable.

Enfin, un limiteur de débit est ajouté en amont du distributeur de limiter la consommation d'une servocommande. Ainsi, même dans la configuration ou un maximum de débit est demandé (cas dégradé), le limiteur évite un désamorçage de la pompe donc la perte de tout un circuit hydraulique. Un débit minimal vers les autres servocommandes est donc garanti pour tous les cas de figure.

Le distributeur sélectionné est donc un distributeur linéaire avec deux portées, à tiroir circulaire. Deux tiroirs sont présents : le tiroir principal et le secondaire pour prendre en

compte les cas de panne. Un limiteur de débit est également ajouté pour garantir une consommation maximale de la pièce.

Les conceptions de la servocommande et du distributeur sont fortement liées à l'application. L'étude est basée sur un hélicoptère léger, ce qui implique le choix de certaines architectures. Le schéma de principe du fonctionnement de la servocommande est présenté à la Figure 15 avec ses corps mobiles en tandem, les deux tiroirs de distributeur (principal et de secours) et le levier d'entrée avec une commande de rétraction servocommande.

1.2 - Introduction

This chapter starts with a general description of the helicopter main devices. One of them is the flight control actuators. Theses actuators are hydraulic supplied and mechanically signalled piloted by a valve which modulates the hydraulic power. As the thesis concerns the valve design and manufacturing to ensure the servoactuator behaviour, the two operating modes (nominal and degraded) of the servoactuator and then of the valve are described. This chapter ends with a selection of some technological solutions for the future design of the servoactuator and of the valve to meet the requirements of the application.

1.3 - Helicopter flight controls

1.3.1 - A rotor aircraft: the helicopter

Before talking about helicopters, it seems interesting to present a more general class of aircrafts: the rotor aircrafts [18]. Indeed, the helicopter is only a particular case of rotor aircrafts (Figure 1).

In the rotor aircraft family are found aircrafts like:

- Autogyro. The rotor does not receive power; it is driven by aerodynamic forces that are created by the air flux through the rotor. The autogiro drag is balanced by a powered propeller. This type of aircraft is no more developed.
- Gyrodyne, combination between autogyro and helicopter. The rotor is powered by the gyrodyne engine for take-off, hovering and landing like a helicopter. At the others flight phases, the rotor operates as an autogyro.
- Hybrid aircrafts whose configuration can be changed during the flight. Various kinds of hybrids between fixed and rotary-wing have been created (tilt-rotor, tilt-wing …) and are still under development (e.g. Helicopter BA609).
- Helicopter which is the simplest configuration, dominates others, though its maximal translation speed is not the highest.

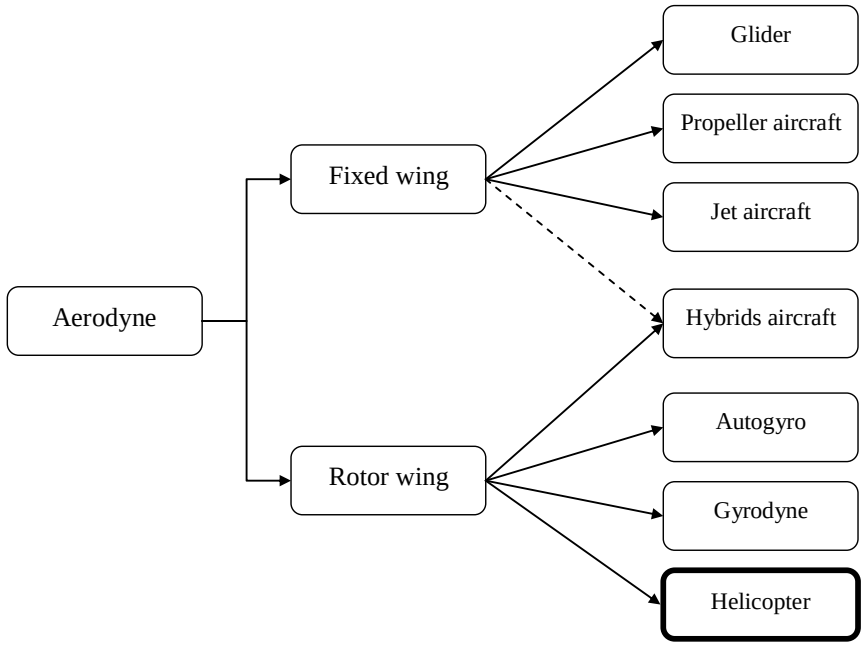

Figure 1: Which kind of aircraft is the helicopter?

1.3.2 - Helicopter architecture

The principle of a helicopter is explained in Figure 2:

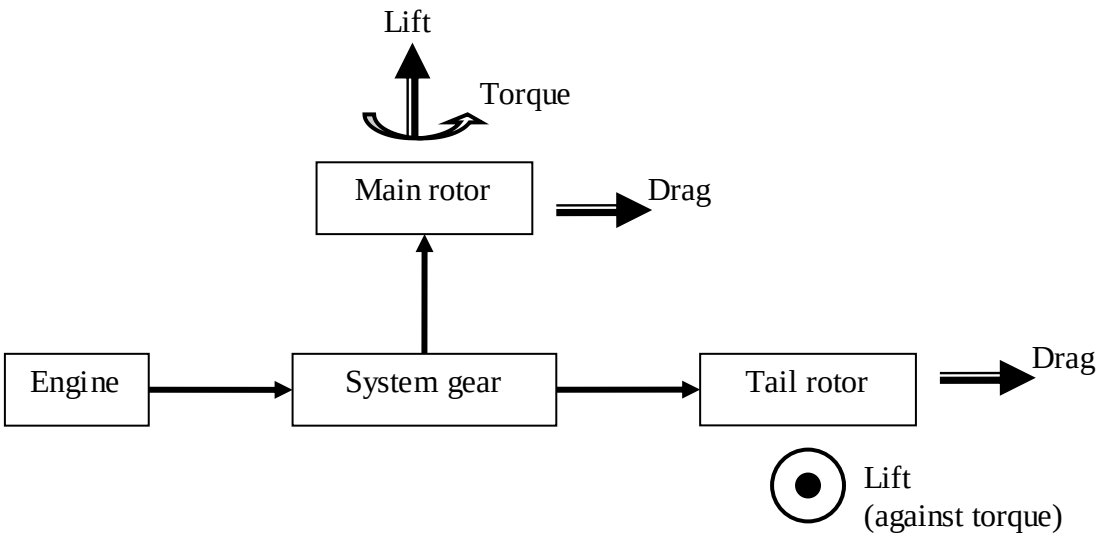

Figure 2: basic scheme of helicopter

In helicopters, lift is functionally created by the main rotor that rotates at a constant speed. The blades parasitic drag is compensated by the torque provided to drive the rotor by

the engine. In order to balance the helicopter around the yaw axis the reaction torque can be either provided by the tail rotor (conventional solution) or by directing the helicopter turbine flux properly (*e.g*. MD900 explorer).

1.3.2.1 - Engine

The engine provides mechanical power to rotors, as well as secondary power users (flight controls, rotor brakes, landing gear, hydraulic pomp, etc…). It can be made of one or more turbines engine, or pistons engine, that all drive the rotor at a constant rotation speed.

1.3.2.2 - Main gear box

The gear box is needed in order to transmit mechanical power since engine to rotor. It is in charge of adapting the speeds between the rotor (hundreds of revolutions per minute) and the engine (thousands of revolutions per minute) (Figure 3).

1.3.2.3 - Rotor

The main rotor, with a vertical axis and a large diameter, assumes (as said above) lift and propulsion. It is made by a given number of blades (minimum 2) which are attached to a central hub. The main gear box transmits mechanical power from engine to the rotor. In order to balance reaction induced by the torque on the helicopter, an additional and contrary torque is necessary. This one can be generated by different systems: for example, the NTR system (No Tail Rotor). In this case, the force is created by a tail air jet on the extremity of a beam. Another system is the presence of a second rotor which rotates in the opposite direction. Finally, the most common system is an auxiliary rotor placed at the extremity of a beam. It is the tail rotor, whose rotation plane is horizontal (Figure 3).

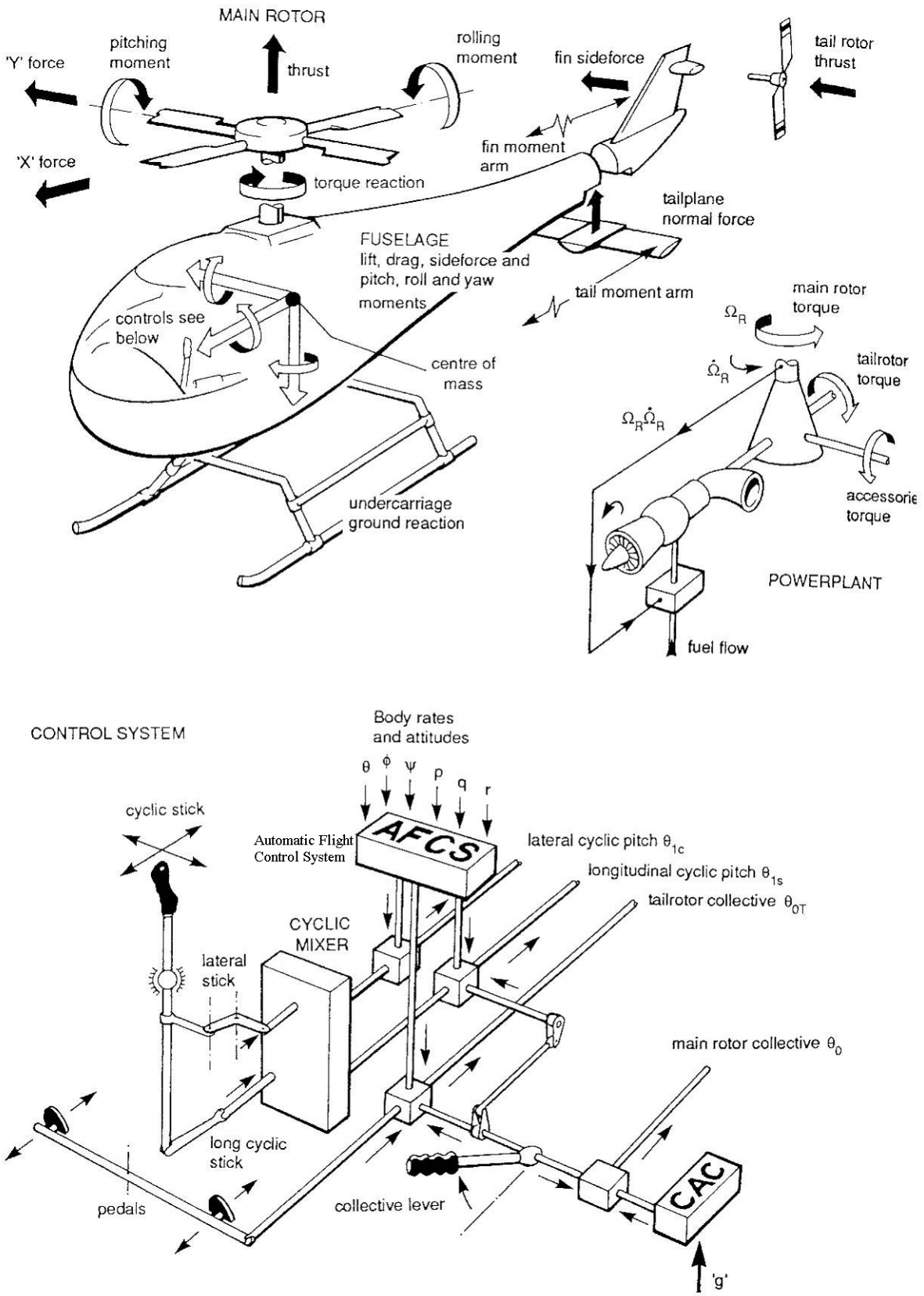

Figure 3: Complete scheme of helicopter [28]

1.3.2.4 - Swashplate

The swashplate is in charge of adjusting the collective and cyclic pitch of the main rotor blades. It consists of two parts: a stationary and a rotating swashplate. It is able to tilt in all directions and moves vertically (Figure 4).

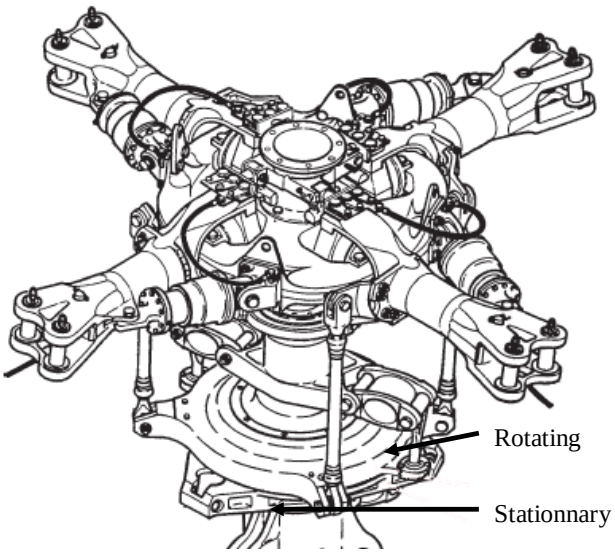

Figure 4: Scheme of a SuperPuma swashplate [33]

1.3.2.5 - Mixer

A mixer between pilot and flight controls is necessary. Indeed, one effect effectuated by the pilot (for instance, an action on the collective lever), creates one or more effects on the flight controls (in this example, all the main servoactuators have to move) [32]. Consequently, the mixer transforms pilot orders into servoactuator position demand (Figure 3).

1.3.2.6 - Flight controls

The flight control of a helicopter is a multiple input multiple output system. The pilot can modify the magnitude of the rotor lift vector by increasing the collective pitch of the main rotor blades. He can also overstate this vector (forward/backward, right/left) by modifying the blade pitch as a function on the blade angle in the rotation plane. The yaw axis is controlled by an action on the pedals that make the tail rotor blade pitch vary (Figure 5).

The autopilot operates in parallel with the pilot. So the pilot can act on the flight controls at anytime and the autopilot can correct the high frequency. Its authority is very low (3% of the blade defection). Consequently, it can be operative or cut off without moving the pilot commands.

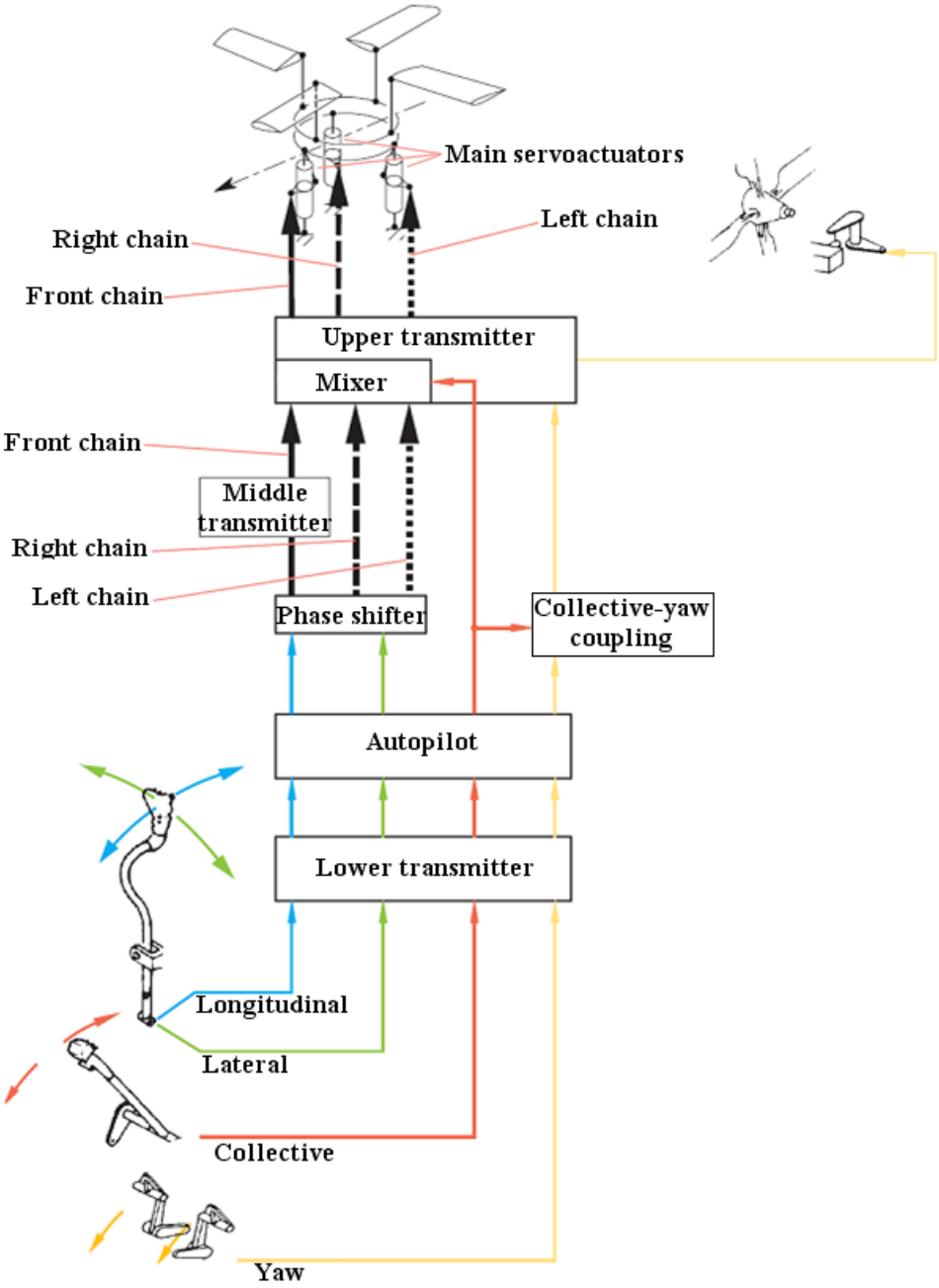

Figure 5: Helicopter command link [33]

Flight controls involve engine, rotor and pilot. Indeed, they use power engine to transmit the pilot orders in order to fly the vehicle.

A pilot uses three main controlling systems (cyclic control pitch (control stick), collective control stick and rudder bar (pedal)) to change the elevation, the velocity and the heading of the vehicle.

- The control stick controls the main rotor angle on tilting the rotor head on which blades are fixed with pitch link into the direction of the desired displacement. A swash plate assumes this inclination function.
- The collective stick controls the blades common angle that modifies lift generated by the rotor. A swash plate assumes this function too.
- The rudder bar increases or decreases the tail rotor lift which has to vary with the main rotor power, so collective position.

In order to reduce the amount of force required to the pilot, hydraulic actuators are placed in the flight controls path [18]. On small helicopters, the pilot force is amplified in normal mode and can be the only source of power in back-up mode. On larger helicopters, the pilot commands the hydraulic actuators as position demand signals. The collective and the cyclic sticks define the vertically position and the inclination of the swashplate (three degrees of freedom). As three points are needed to control the swashplate position, it is connected to the three main servoactuators (see Figure 6).

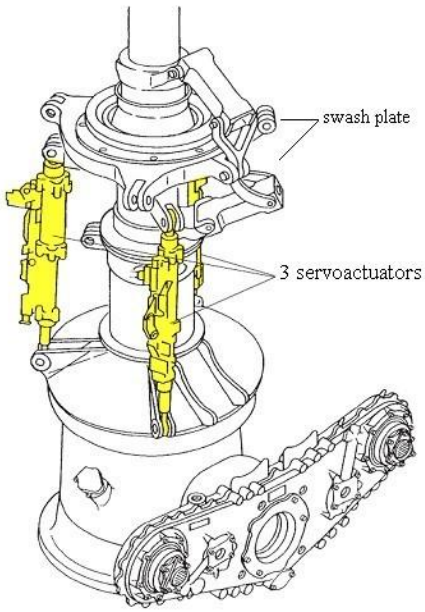

Figure 6: Scheme of a hydraulic actuator with the three main servoactuators connected to the swashplate

Note: in other fields of aerospace, servoactuators mean actuators using servovalves. In the present document, this word has to be understood as “actuator for servo control”.

They are different kinds of servoactuators and two power sources can be used: electrical power or hydraulic power. For helicopters that are small devices compared to airplanes, the power density of the hydraulic is very interesting. So the main servoactuators of helicopters are all hydraulically supplied. The mechanically signalling allows the pilot orders

to be directly transmitted to the servoactuator by rods in case of hydraulic failure (for small helicopters). Thus, the input signal of the servoactuator is mechanical. Electrically signaled helicopter flight controls have appeared at Eurocopter on the NH90 military transporter. However, the added complexity in the hard environment of the helicopter does not put a high pressure in helicopter manufacturing to switch to fly-by-wire as done for airplanes since two decades.

The main functions of a hydro-mechanical actuator are described in Figure 7. The engine is used to generate hydraulic power. The valve modulates the hydraulic power as a function of opening, and finally, the jack transforms the hydraulic power into mechanical power.

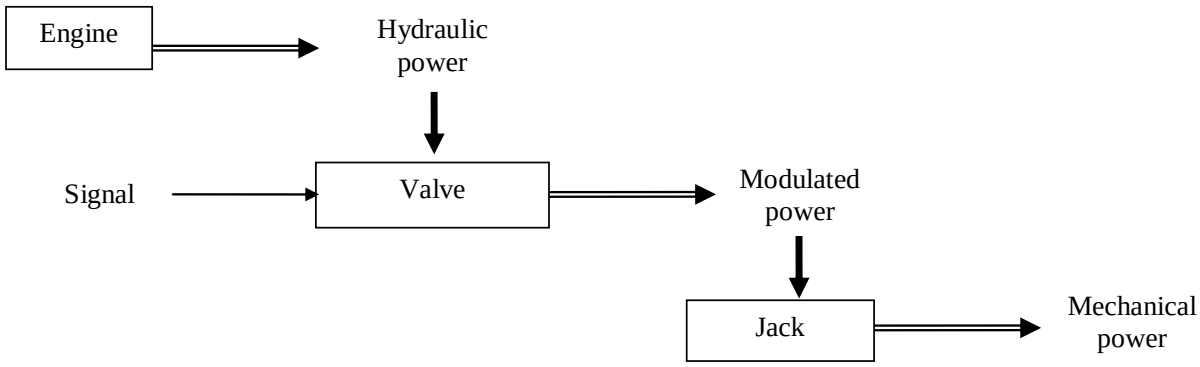

Figure 7: Scheme of a hydro-mechanical actuator

1.4 - Architecture of a main servoactuator for light helicopters

As this work concerns light helicopters, the architecture of a main rotor servoactuator is described for this particular application. Two modes of functioning are studied: nominal and degraded mode. The nominal mode corresponds to a normal operating of the device, whereas the degraded mode corresponds to the apparition of malfunction. The specifications are different for each case.

1.4.1 - Architecture in nominal mode

Helicopter hydro-mechanical actuators are constituted by (Figure 8):

- An input lever to transmit the pilot order
- A valve to modulate the power as function of its opening
- A piston to transform the hydraulic power in mechanical power
- A body and a rod to transmit the mechanical loads

- A mechanical linkage that performs a position closed loop by making the valve opening proportional to the difference between the pilot lever displacement position and the rod actual position.

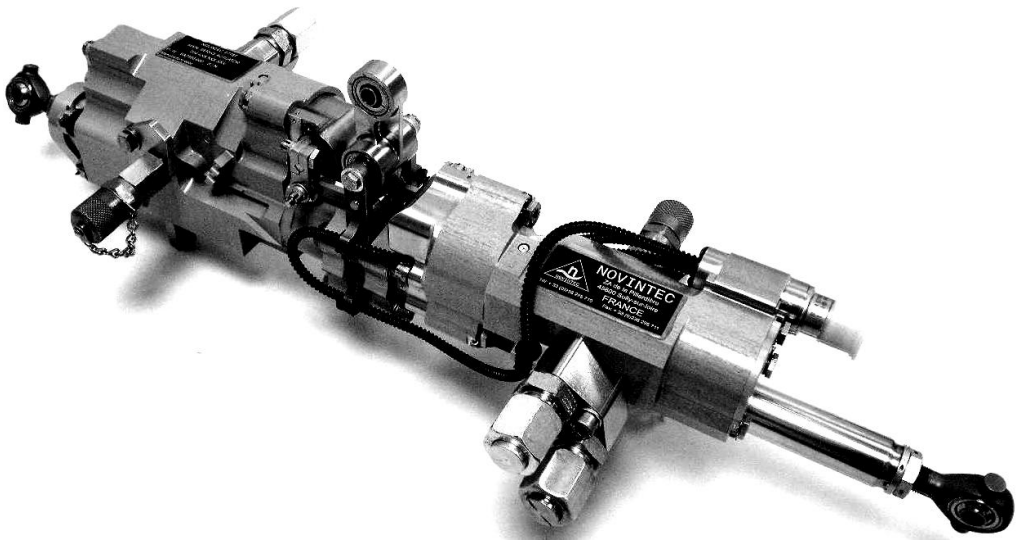

Figure 8: Example of servoactuator

In order to drive easily and with accuracy the motion of the actuators in the two sides, a double effect jack is selected (see Figure 9 (b) whereas Figure 9 (a) presents a single effect jack). It means that the hydraulic power can be used in the extension side as well as in the retraction side.

There are two ways to integrate the servoactuator. In the first case, the rod is fixed to the helicopter frame whereas the body is linked to the swashplate. In the second case, the rod moves with the swashplate whereas the body is fixed on the helicopter frame. A moving body configuration has been chosen for simplicity and robustness reasons.

The advantage of a moving body servoactuator is that it operates naturally in closed loop. Indeed, as the input lever is linked to the body, when the lever moves, the body follows the lever motion. On contrary, on a fixed body servoactuator, a motion of the input lever causes a motion of the rod, but there is no direct consequence on the lever. In this configuration a copy of the rod position is needed to link the rod and the lever. This configuration is so more complex and heavier.

The disadvantage of the moving body configuration is the requirement of flexible hydraulic pipes. So it cannot be used for very high pressures. For the case under study, operating at low supply pressure, the moving body configuration has been chosen.

It is interesting for a double effect servoactuator to have a symmetrical behavior. The easiest way to obtain it is to design a symmetrical jack. However, having a symmetrical jack implies to have a long rod and two seals to limit leakages between internal hydraulic circuit and exterior (Figure 9 (b)). Knowing that the main reason of the servoactuator maintenance is the external leakages of the servoactuator, it is very important to limit the number of seals between the high pressure domain and the ambiance of the servoactuator. A dissymmetrical actuator (Figure 9 (c)) that requires only one seal between internal hydraulic circuit and exterior is thus selected for our application.

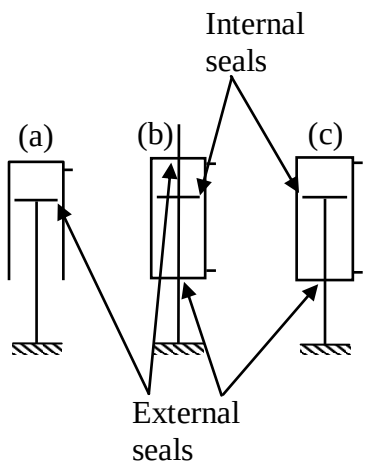

Figure 9: Motion body actuator. (a) Single effect actuator; (b) Symmetrical double effect actuator; (c) Dissymmetrical double effect actuator

1.4.2 - Architecture in degraded mode

The servoactuator is a critical device of the helicopter. It is not accepted that its operation is lost even during a short time.

The failure case is the loss of the hydraulic power. Such a failure is not extremely rare, and the pilot cannot control the helicopter without servoactuator excepted on very small helicopters with reversible servoactuators. For this reason, the actuator function is made redundant with two parallel power paths. If a hydraulic circuit is loss, the servoactuator can operate with the second one. For reasons of size, the two bodies are mounted in tandem with a vertical segregation (Figure 10) (it would be impossible to have the two bodies in parallel under the swashplate).

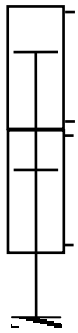

Figure 10: Moving body servoactuator in tandem with vertical segregation

The failure is monitored by dedicated lights at the flightdeck. A light is turned on to warn the pilot in case of hydraulic circuit loss, in case of the loss of control of one body and in case of excessive loads on the servoactuator. For security reasons (sensor requirements), the lights must be tested before each flight for the three cases.

1.5 - Architecture of the valve

The signal to power interface of the servoactuator is the valve. Thus the operation of this device is a key point for the performances of the servoactuator. As for the servoactuator, there are two operating modes: nominal and degraded.

In the section 1.4 - p23 it has been shown that the actuator is dissymmetrical for questions of space needs. In order to get a symmetrical response of the servoactuator, a dissymmetrical valve is needed. However for a cost point of view, the valve is kept symmetrical which is an unusual solution.

1.5.1 - Architecture in nominal mode

The valve has to modulate the power as a function of its opening. For reasons of manufacturing cost, a linear and cylindrical spool valve has been selected. It is constituted of a body, the external sleeve and a moving device, the spool.

When the valve is associated with the hydraulic transformer (motor or cylinder), the valve metering function is performed by combining four variable hydraulic resistances (metering orifices) that are associated in a full Wheatstone bridge (Figure 11a) [10]. This allows a four quadrant operation, the unique valve design ensuring both functions of directing the fluid to the right path and of modulating the orifices resistance to control the output flow to load. According to Figure 11c, when the valve opening X is positive, orifices c and a are functionally closed while orifices b and d are active. In the same manner, when the valve opening X is negative, Figure 11d, orifices b and d a functionally closed while orifices c and a are active. In absence of control input, all the orifices should be closed. However, the

manufacturing tolerances do not allow to meet exactly this objective and alters the valve performance due to defects (clearance, rounded edge radius).

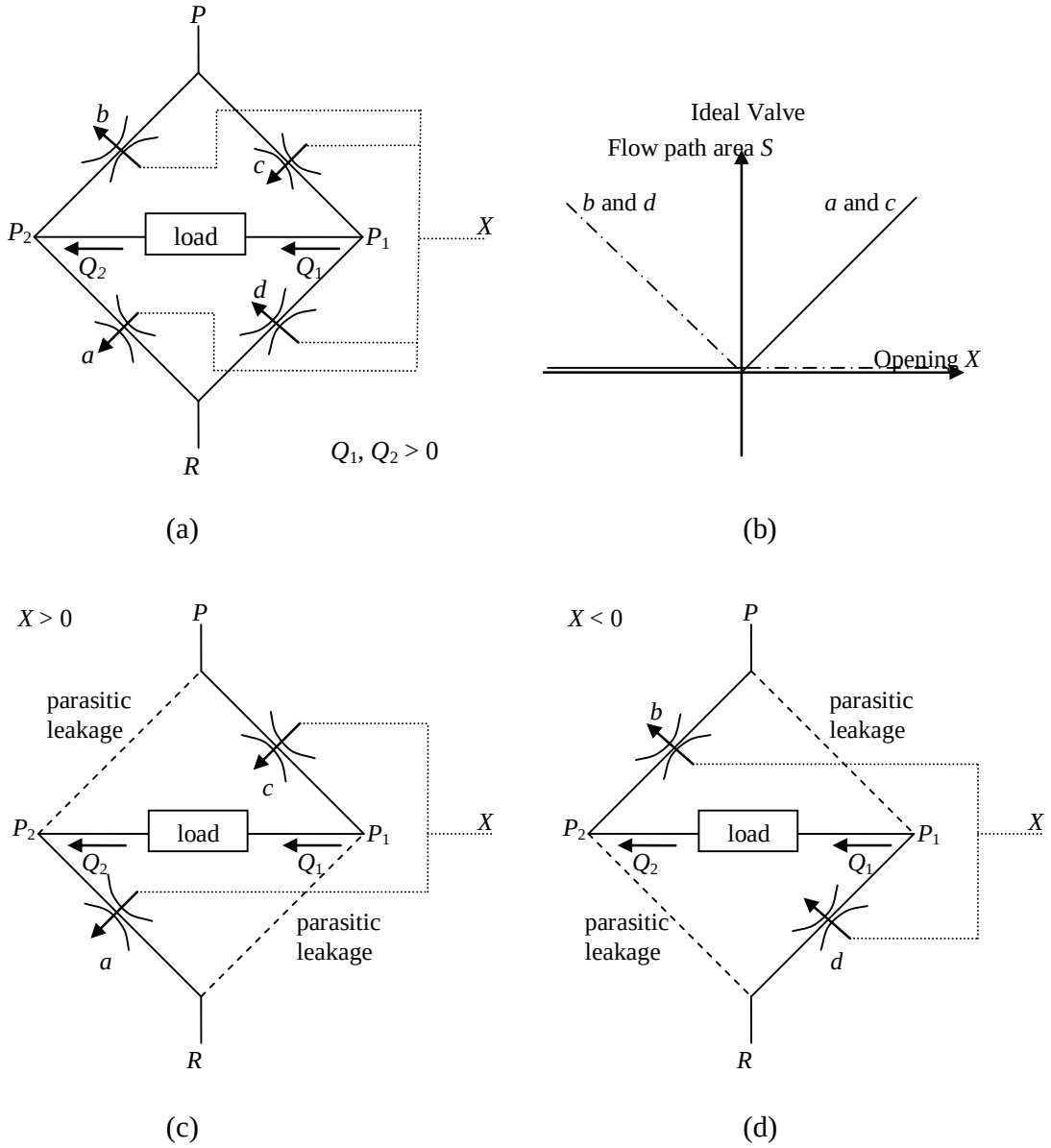

Figure 11: Valve seen as a full Wheatstone bridge

Where

P	Pressure supply (Pa)
R	Return pressure (Pa)
Q_1	Flow rate in jack chamber 1 (m^3/s)
Q_2	Flow rate in jack chamber 2 (m^3/s)
P_1	Pressure in jack chamber 1 (Pa)
P_2	Pressure in jack chamber 2 (Pa)
X	Valve opening (m)

S	Section of the valve (m²)
a, b, c, d	Names of the valve orifices (-)

In practice, the valve is designed without any dynamic seal to avoid friction non-linearities. Consequently, sealing between moving parts is only ensured by extremely low clearances that unfortunately induce parasitic leakages (dashed lines on Figure 11c and Figure 11d).

Moreover, the valve orifices operate mainly in turbulent conditions that make their hydraulic resistance strongly non linear.

As a consequence of all these technological defects, the flow rate Q delivered by a real valve depends non-linearly on its opening X and on the load pressure drop ΔP (Figure 12).

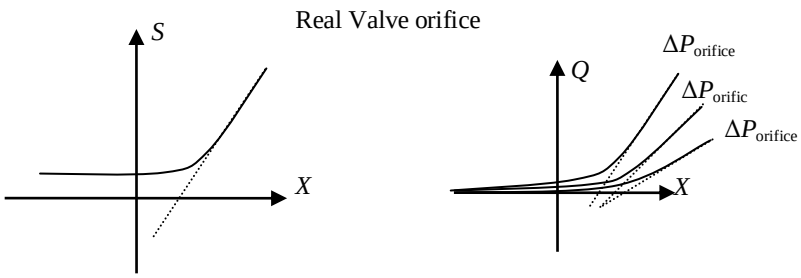

Figure 12: Non-linearities on the flow rate and pressure depending on the opening

Where

Q	Flow rate (m^3/s)
ΔP	Pressure drop (Pa)

The more common technological solution to produce hydraulic valves is the cylindrical, sliding spool valve of Figure 13 where the orifices a machined on the valve spool.

Finally, for a manufacturing point of view, the easiest technological solution to produce hydraulic valve is the cylindrical sliding spool valve with orifices machined on the spool (Figure 13)

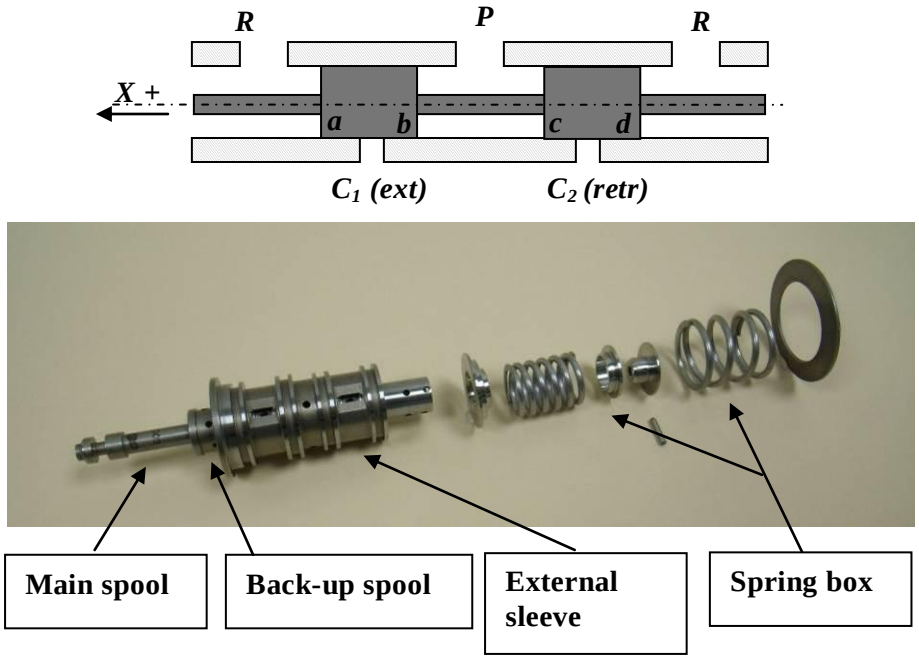

Figure 13: Cylindrical sliding spool valve

Where

C_1 Chamber 1 (-)

C_2 Chamber 2 (-)

1.5.2 - Architecture in degraded mode

The valve is the piloting part of the servoactuator. So in order to guaranty the helicopter safety, the different cases of failure are to be taken into account.

Firstly, in case of loss of hydraulic pressure, a by-pass system is used to avoid keeping pressure in the jack chambers and to lock (hydraulic lock) the servoactuator. The detection of the pressure loss is lead by a test piston and a spring. When the pressure in the supply line of the valve is too low, the test piston is moved by the spring connecting the jack chamber to the return line (by-pass). Moreover, the motion of the test piston turns on a light to warn the pilot. The light is checked before each flight. On the starting of the helicopter, the light must turn off when the pressure is supplied (when the test piston is moving).

Secondly, the valve is made by a spool, moving in a sleeve, without seals. The security specifications lay down a by-pass or a secondary control if the moving part is seized in the sleeve. The design of the valve is so modified:

- the main spool is moving in the back-up spool (primary stage, Figure 14)

- the back-up spool can move in the sleeve. It is maintained in the center position by a spring box. If the main spool is seized in the back-up spool, the load on the spool is increasing by the pilot until the back-up spool starts to move.

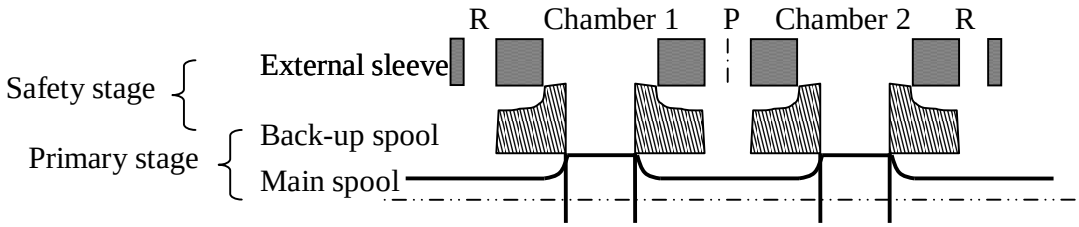

Figure 14: Architecture of the valve (main spool, back-up spool and external sleeve)

A third point of safety is the maximal consumption. The hydraulic pump supplies a constant pressure with a maximal flow limitation for the three servoactuator. In order to keep a minimal flow rate for the other servoactuator even if one is in degraded case (valve in by-pass mode), it will be shown is this thesis that a flow limiter (restriction) must be added on the supply line of the valve.

Without supply pressure, the test piston is moved by a spring. When the pressure increases in the hydraulic circuit, the test piston and the back-up spool move to come back in the nominal configuration. Hence in moving, the test piston checks before each flight that the back-up spool is not seized in the external sleeve. The detection of the main spool seizure is checked by the motion of the back-up spool. The same light that the one in case of hydraulic loss is turn on in case of seizure of the main spool. Consequently, the pilot cannot know if there is a hydraulic loss or a seizure but knows there is a problem and has to land or go back as soon as possible.

1.6 - Conclusion

The servoactuator and valve designs are very influenced by the application. The Figure 15 shows the functional scheme of the servoactuator with the technological choices adapted to the light helicopters studied in this thesis:

A tandem body motion servoactuator with its two valves (main and back-up spools) and its mechanical input lever in case of retraction. This architecture has to answer the problem of size, weight and particularly safety, which are imposed by aeronautical applications.

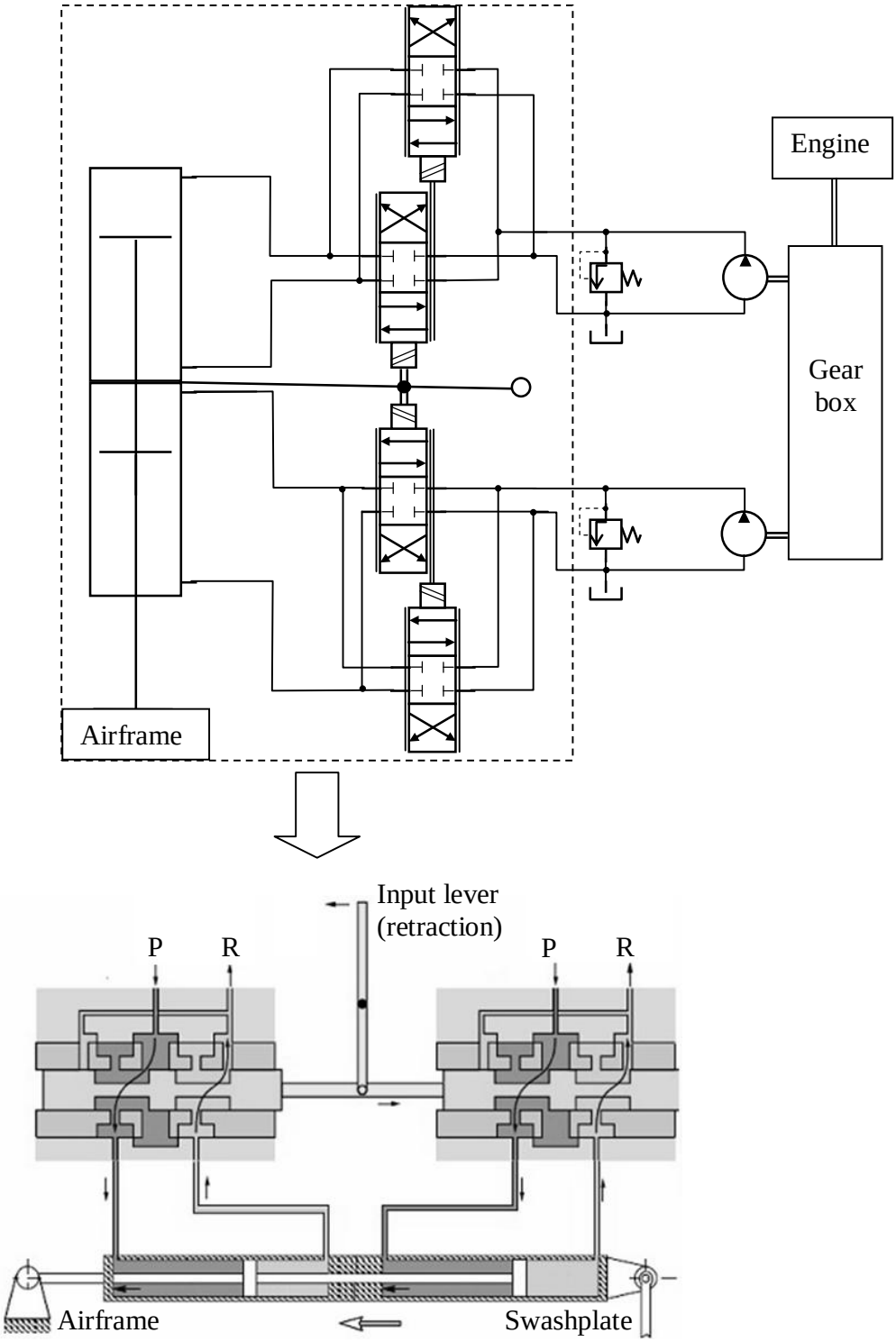

Figure 15: Scheme of the studied servoactuator

Chapitre 2

Models and tools for design and manufacturing

2.1 - French synthesis

Ce chapitre présente les modèles et outils pour le design et la fabrication du distributeur de servocommande. Il est composé de trois parties.

La première décrit le domaine de fonctionnement de la servocommande, c'est-à-dire le plan caractéristique de puissance mécanique.

La seconde partie concerne le distributeur. Son mode de fonctionnement est défini par trois courbes caractéristiques : le gain en débit, le gain en pression et la courbe de fuite. Ces courbes sont analysées afin de mettre en lumière les liens entre les caractéristiques du distributeur et les performances de la servocommande. Un orifice général de distributeur est mis en équation en fonction de sa géométrie et des paramètres de fluides. L'impact de ces paramètres sur le comportement du distributeur est finalement analysé et leur plage de fonctionnement défini pour l'application.

Les outils de simulation sont présentés dans la dernière partie du chapitre : les plans d'expériences, l'implémentation du modèle quasi-statique de distributeur et les modèles dynamique de servocommande et de distributeur.

Dans les systèmes hydrauliques aéronautiques, le fluide hydraulique est utilisé comme vecteur pour transformer l'énergie hydrostatique depuis un générateur de puissance hydraulique vers le besoin utilisateur. Idéalement, le déplacement de la partie mobile est proportionnel au volume transitant par le distributeur. La combinaison distributeur/transformateur apparait globalement comme un intégrateur pur avec une commande en position.

La puissance développée par l'actionneur est fixée par les pressions d'alimentation est retour, les sections effectives de piston du vérin et la capacité de débit du distributeur. Le distributeur et le vérin doivent être dimensionnés selon la puissance requise lors de l'utilisation. Généralement un domaine de fonctionnement (effort/vitesse) symétrique est requis autour d'un effort résistant permanent F_0. Au niveau du contrôle, le distributeur et le vérin doivent être conçus afin de fournir une caractéristique statique symétrique et proportionnelle en boucle ouverte. En présence d'un effort permanent, l'adaptation de l'actionneur à la charge est délicate sans concevoir un vérin spécifique. Concernant

l'application des hélicoptères légers, il ne serait pas indispensable d'avoir un vérin dissymétrique au vu du spectre d'effort. Cette configuration a été choisie pour d'autres raisons (voir Chapitre 1).

Ayant un vérin dissymétrique, les règles de conception voudraient qu'il y ait une adaptation du distributeur vers le vérin, ce qui signifie de concevoir le distributeur tel que l'actionneur est une capacité de vitesse symétrique. Pour cela il faudrait un distributeur dissymétrique. Cependant pour des raisons de coûts de fabrication, un distributeur symétrique est choisi.

Si la charge est supposée connue et que la servocommande opère dans le domaine spectral, il est possible d'évaluer, pour chaque fréquence, l'amplitude maximale de sortie que l'actionneur puisse produire. Les limites de ce domaine sont les suivantes :

- La limite de position qui est définie par les butées mécaniques de la tige de servocommande
- La limite de vitesse qui est définie par le débit maximal au travers de la servocommande
- La limite d'accélération qui est définie par la pression de l'huile
- La limite à faible amplitude qui est définie par la zone morte de la servocommande.

La seconde partie du chapitre présente le modèle non linéaire du distributeur, modèle qui sera utilisé pour les études ultérieures.

Généralement, l'actionneur hydromécanique est symétrique et requiert donc un distributeur symétrique. Ce cas est bien développé dans la littérature et défini par de nombreux standards. L'application qui nous concerne correspondant à un cas concret, les caractéristiques définies pour le cas dissymétrique ne sont pas directement applicables et doivent ainsi être adaptées.

La première courbe caractéristique est la courbe de gain en débit. Celle-ci correspond au débit mesuré à travers le distributeur pour une perte de charge constante. En pratique, il suffit de connecter les deux ports normalement reliés aux chambres de servocommande (ce qui équivaut à avoir un vérin symétrique et une charge nulle) et de maintenir une pression d'alimentation et de retour constante. Cette courbe permet d'indiquer la capacité du distributeur à contrôler la vitesse de la charge en fonction de l'ouverture sous un effort nul. Le gain en débit correspond à la pente de cette courbe. Pour les très faibles ouvertures, le gain en débit est altéré par les fuites dues aux imperfections du distributeur (rayons d'arrondi d'arête, jeux diamétraux). Aux grandes ouvertures, le gain en débit est généralement réduit à cause des pertes de charge parasites sous des vitesses de fluide importantes dans les conduites. Les défauts aux petites ouvertures n'influent que jusqu'à environ 5% d'ouverture mais jouent néanmoins au rôle majeur sur les performances de l'actionneur. La géométrie du distributeur modifie en particulier la forme du gain en débit aux très petites ouvertures comme présenté à la Figure 22. Les recouvrements peuvent à la fois être fonctionnels ou parasites. Dans le cas

des commandes de vol pour un hélicoptère, le recouvrement est préféré afin de garantir une zone morte, ceci afin d'éviter une transmission de puissance vers la charge provoquée par des vibrations au levier d'entrée.

La seconde courbe caractéristique est celle du gain en pression. Elle est donnée par une mesure de la pression en fonction du déplacement tiroir à débit nul. En pratique cette courbe est obtenue en obstruant les ports normalement reliés aux chambres de la servocommande et en y faisant un relevé de pression tout en maintenant la pression d'alimentation et de retour constante. Ceci correspond au cas où la tige et le corps de la servocommande sont figés. Cette courbe traduit donc la capacité du distributeur à délivrer de la puissance pour vaincre une charge statique. Le gain en pression correspond à la pente de la courbe pression/ouverture de tiroir autour du neutre. Une courbe idéale de gain en pression donnerait une transition instantanée de pression au voisinage du neutre hydraulique. En pratique ce n'est bien évidemment pas le cas, d'où l'intérêt de la mesure. Pour la suite on préféra représenter les courbes de pression de chaque port plutôt que le différentiel entre ceux-ci. En effet, plus d'informations sont ainsi fournies, par exemple la valeur d'ouverture de tiroir nécessaire pour égaler les pressions sur les deux ports qui correspond au point d'équilibre de la servocommande. Il indique le niveau de pression dans la servocommande sans sollicitation. Comme pour le gain en débit, les défauts affectent la courbe pour environ 5% d'ouverture. On considère comme valeur typique un différentiel de pression de 40% du différentiel maximal pour une ouverture de 1% du distributeur. Au final, les défauts permettent une transition progressive du différentiel de pression autour du neutre hydraulique ce qui contribue à limiter les problèmes de désynchronisation.

La troisième et dernière courbe est la courbe de fuites. Elle correspond au débit traversant le distributeur pour un débit délivré nul en fonction de l'ouverture distributeur. En pratique cette courbe est obtenue avec le même montage que pour la courbe de gain en pression en mesurant le débit quittant le distributeur. La fuite maximale est généralement observée autour du neutre hydraulique où tous les orifices opèrent entre ouverture et fermeture. De la même manière, les défauts jouent leur rôle autour de 5% d'ouverture distributeur. Il est important de contrôler le débit de fuite maximal afin de garantir que celles-ci seront compensées par l'alimentation hydraulique.

Le modèle d'orifice doit permettre de reproduire les effets dominants qui définissent les performances du distributeur. Dans un souci de précision il prend donc en compte les rayons d'arrondi d'arête, le jeu diamétral tiroir/chemise et les recouvrements de chaque arête. Chaque orifice est modélisé indépendamment en utilisant les équations (21) à (30). Les équations (21) à (24) ne sont pas applicables dans le cas d'un orifice non rectangulaire. Le modèle de distributeur est ensuite obtenu en associant les quatre orifices grâce aux équations de continuité dépendant de la configuration de l'essai (configuration d'essai de gain en débit ou de gain en pression). Douze paramètres définissent ainsi complètement le modèle de distributeur :

- Les propriétés physiques de l'huile. Les deux principales propriétés sont la densité (ρ) et la viscosité cinématique (ν). La viscosité dynamique est quant à elle déduite de ces deux paramètres.
- Les constantes du modèle d'écoulement. Il y a deux constantes qui sont le coefficient de débit limite ($C_{q\infty}$) et le nombre de débit de transition (λ_t). Ils dépendent complètement de la géométrie du distributeur et peuvent être estimés par une approche CFD (Computational Fluid Dynamic). Leurs valeurs ne peuvent pas être directement pilotées en changeant la conception du distributeur.
- Les paramètres géométriques. Les limites de ces paramètres dépendent de la géométrie de la servocommande. Il y a le nombre de fente (n_f), la largeur de fente (l_f), le jeu diamétral (c), le rayon d'arrondi d'arête (r) et les recouvrements de chaque arête (X_{i0}). Le domaine de variation possible de ces paramètres est récapitulé à la Table 1.

La troisième partie du chapitre concerne le choix et l'utilisation des outils de simulation nécessaire à l'étude.

Le premier outil est celui pour les plans d'expérience qui est utilisé pendant le processus de conception. Dans tout processus industriel, les essais représentent une phase critique du projet. En effet, ils peuvent être nécessaires pour comprendre des phénomènes, identifier, valider des paramètres de conception et/ ou les optimiser. La méthode par plan d'expérience (DOE) permet de réaliser et d'analyser les essais de façon optimale.

La méthode générale pas à pas d'un plan d'expérience est la suivante :

- Choisir le type de plan, c'es-à-dire les essais qui doivent être réalisés (factoriel complet, Taguchi, …)
- Choisir des facteurs (entrées)
- Choisir un niveau de plan afin de considérer les effets principaux et éventuellement les interactions de premier ordre puis de second ordre.
- Choisir des réponses (sorties)
- Générer le plan qui va indiquer les essais à réaliser parmi tous ceux possibles.
- Réaliser les essais
- Analyser les réponses avec le logiciel

Si une optimisation est requise, deux pas supplémentaires sont requis :

- Définir les critères sur les réponses
- Prédire l'optimum

Le second outil utilisé est un logiciel de simulation dynamique. Le logiciel AMESim (Advanced Modeling Environment for performing Simulations [5]) a été choisi pour

développer les modèles dynamiques de distributeur et servocommande. C'est un logiciel multiphysique réalisant des simulations de systèmes d'ingénierie.

Le modèle de servocommande est construit aussi près de la géométrie réelle que possible. Toutes les fonctions de la servocommande sont modélisées :

- Les deux corps mobiles avec leur valeur de longueur de chambre, de diamètre de tige et de diamètre de piston
- Les deux distributeurs : un pour chaque corps. Ils sont identiques et montés tête-bêche
- Le levier défini par son gain et son hystérésis
- Les charges appliquées sur la servocommande : poids, efforts extérieurs statique et dynamique, frottements de joints.
- Les générations hydrauliques avec les deux pompes, les régulations de pression et les bâches.
- De nombreux interrupteurs ont été ajoutés afin d'aisément simuler les différents cas de panne.

Comme la servocommande, un modèle dynamique de distributeur est construit. Le modèle a grandement évolué tout au long de l'étude puisque le distributeur est au centre de celle-ci. Le modèle se compose en particulier de :

- La section de restriction qui agit comme un limiteur de débit
- Le tiroir principal et le tiroir secours. De plus le déplacement du tiroir secours par le piston de test est simulé en cas de perte de pression
- Le diamètre hydraulique et la section de passage des distributeurs en fonction de l'ouverture sont calculés en tenant compte des différentes géométries de fente de tiroir (rectangulaire, trapézoïdale).

La première partie de ce chapitre a présenté le modèle utilisé pour définir l'écoulement à travers les orifices de distribution. Les paramètres de fluide et géométriques ont été extraits de ces équations, ce qui a permis de mettre en lumière les paramètres qui peuvent être optimisés. Du fait de sa grande influence sur les performances dynamiques de la servocommande et de sa possibilité d'être fabriqué avec précision, la largeur de fente a été le seul paramètre sélectionné pour l'optimisation. Etant donné l'approche faible coût de l'étude, un modèle statique de distributeur, puis des modèles dynamiques de distributeur et de servocommande ont été développés. Ils ont permis de gagner du temps et de l'argent durant la phase de développement de la servocommande.

2.2 - Introduction

This chapter presents the models and tools for the design and manufacturing of the servoactuator valve. It is composed of three parts.

The first one describes the servoactuator functional domain *i.e.* the mechanical power plane characteristic.

The second part concerns the valve. Its operating mode is defined by three characteristic curves: the flow gain, the pressure gain and the leakages curve. These curves are analyzed in order to point out the links between the valve characteristics and the servoactuator performances. A generic valve orifice is described by equations functions of the geometry and fluid parameters. The impact of these parameters on the valve behavior is finally analyzed and their range is defined for the application.

The simulation tools are presented in the last part of the chapter: the design of experiment, the implementation of the valve quasi-static model and the dynamic models of the servoactuator and of the valve.

2.3 - Servoactuator behavior

2.3.1 - Preliminary remarks on servohydraulic actuator

In aerospace hydraulic systems, the hydraulic fluid is used as a vector to convey hydrostatic energy from the hydraulic power generator to each end-user. As displayed by Figure 16, a modern aerospace actuation system involves typically four functions:

- a constant pressure and variable flow power generation,
- a power distribution network,
- for each end-user, a hydraulic closed centre valve metering the power delivered to the load from the hydraulic supply, according to its control input signal,
- for each end-user, a device transforming the hydrostatic power into mechanical power.

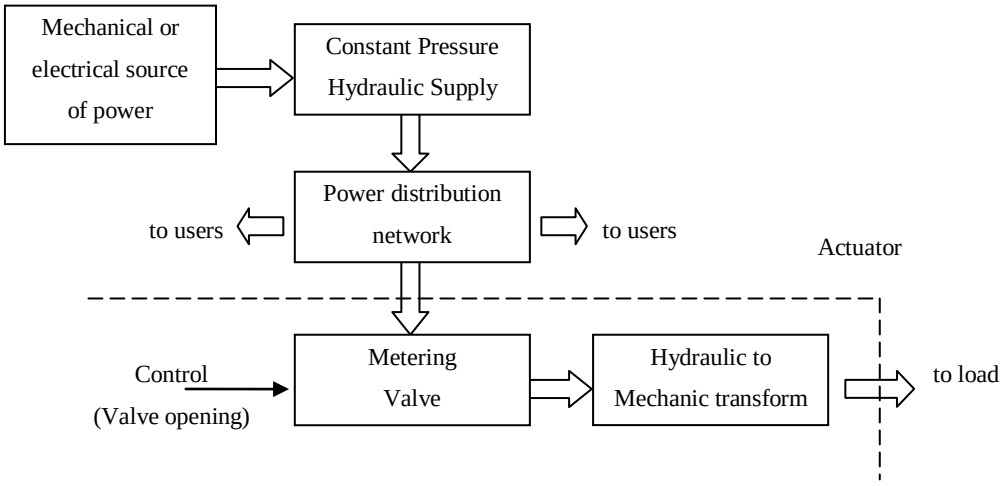

Figure 16: Actuation system

From a more control point of view (Figure 17), the valve is used as a power amplifier that functionally delivers flow proportionally to its opening. Ideally, the motion of the moving part of the hydromechanical transformer is proportional to the volume seek by the valve. Therefore, the valve/transformer combination appears globally for position control as a pure integrator.

For linear actuation $Y = \frac{K_v}{Ss} X$ (1)

For rotary actuation $\theta = \frac{K_v}{V_0 s} X$ (2)

with

K_v	Global valve to opening gain (m^2/s)
S	Unit displacement of the linear transformer (m^3/m)
s	Laplace transform (1/s)
V_0	Unit displacement of the rotary transformer (m^3/rd)
X	Valve opening (m)
Y	Output motion of the linear transformer (m)
θ	Output motion of the rotary transformer (rd)

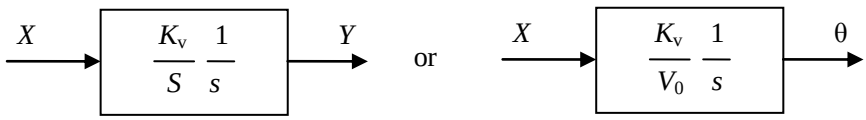

Figure 17: Control point of view actuator

Note: The following developments will only consider linear actuators with jack type hydromechanical transformers. However, there is no particular difficulty to extend these results to rotary actuators involving rotary jacks or hydraulic motors.

2.3.2 - Power requirements

Depending on the type of load to be actuated (and sometimes for geometrical integration constraints), the jack may be symmetrical of not. In the general - but not common - asymmetrical case, the hydrostatic force F_h applied to the load (Figure 18) is equal to

$$F_h = S_1 P_1 - S_2 P_2 \tag{3}$$

while the consumed flows under load velocity are equal to:

$$Q_1 = \dot{Y}\, S_1 \text{ and } Q_2 = \dot{Y}\, S_2 \tag{4}$$

where

S_1	Piston effective area of chamber 1 (m²)
S_2	Piston effective area of chamber 2 (m²)
$\dot{Y}$	Piston velocity (m/s)

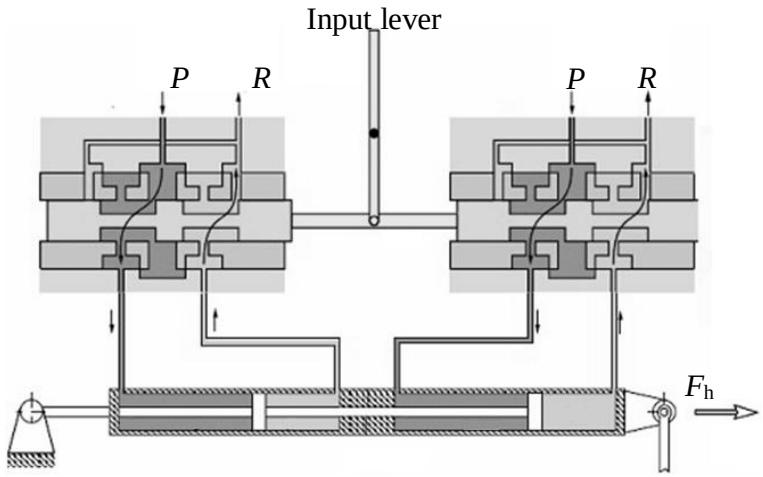

Figure 18: Load equilibrium on an asymmetrical jack

The power capability of the actuator is fixed by the supply and return pressures, the jack effective areas and the valve flow capability.

The valve and jack should be sized (or selected) according to the power required for actuation. Generally, a symmetrical operating domain (force/velocity) is also required. In the general case of a permanent external resistant load force F_0 and of an extra force to the load F_M, this is illustrated by Figure 19 in the mechanical power plane. At control level, the valve and jack should be matched in order to provide a symmetrical and proportional open-loop static characteristic (load velocity vs. valve opening).

where F_M (N) is the specified extra force to be delivered to the load.

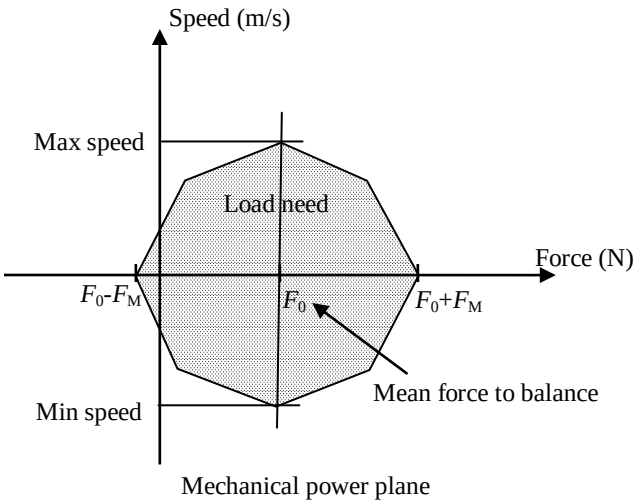

Figure 19: Typical servoactuator operating domain

2.3.3 - Jack-to-load adaptation

In order to meet the stall force requirements, the jack sizing should verify:

$$S_1 P_{10} - S_2 P_{20} = F_0 \tag{5}$$

where P_{10} and P_{20} are respectively the pressures in extension and retraction chamber at equilibrium and F_0 the load equilibrium at rest. For other operating points,

$$S_1 P - S_2 R = F_0 + F_M \tag{6}$$

$$S_1 R - S_2 P = F_0 - F_M \tag{7}$$

Equations (5) to (7) fixes the minimal jack effective areas as

$$S_1 = \frac{F_M}{P+R} + \frac{F_0}{P-R} \tag{8}$$

$$S_2 = \frac{F_M}{P-R} - \frac{F_0}{P+R} \tag{9}$$

and the asymmetry ratio α can be defined as

$$\alpha = S_1 / S_2 = \frac{1}{1 - \frac{F_0}{F_M}\frac{P-R}{P+R}} - \frac{1}{1 - \frac{F_M}{F_0}\frac{P+R}{P-R}} \tag{10}$$

In the presence of a permanent load, the adaptation is difficult to ensure without designing specific jacks as there is only a few set of α ratios for off-the-shelf jacks.

In case of null permanent load, the two areas are obviously equal, leading to a unit asymmetry ratio. However, even in the absence of permanent load, asymmetrical jacks may be designed to meet assembly requirements. This is particularly the case of tandem control actuators like those used in helicopters or fighters flight controls: two pistons are mounted on the same rod but with separated bodies to avoid any crick failure propagation between the two power paths.

Notes:

- In the following developments, it is assumed that the labeling of jack effective areas is such as α is greater than unity.
- Due to their negligible influence in the case of aerospace actuation, the hydrostatic force due to atmospheric pressure is not considered in equation (3).

2.3.4 - Valve-to-jack adaptation

The valve-to-jack adaptation consists in designing a valve that provides a symmetrical velocity capability while satisfying equations (4) and (5). An ideal "adapted" valve should so produce output flows according to the asymmetry ratio:

$$Q_1 = \alpha Q_2 \tag{11}$$

and pressures at null opening satisfying

$$P_1 - \tfrac{1}{\alpha} P_2 = \frac{1}{S_1} F_0 \tag{12}$$

2.3.5 - Frequency requirements

If the load is supposed known and the servoactuator operates in the spectral domain, it is possible to evaluate, for each frequency, the maximal output amplitude that the actuator can produce. Three asymptotic limits are defining the reachable frequency domain ([22], Figure 20):

- position limit: defined by the ends stroke (a)
- speed limit : defined by the flow rate through the actuator (b)
- acceleration limit: defined by the pressure (c)
- low amplitude limit and fluid compressibility (d)

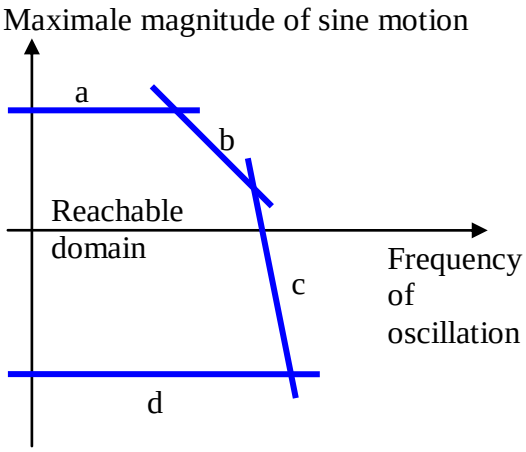

Figure 20: Limit frequency response [22]

2.4 - Non linear static valve model

2.4.1 - The valve characteristics

a) Common hydraulic characteristic

Only the common, but less general, case of symmetrical valves is well documented in the biography and in the standards. If the hydromechanical transformer is symmetrical (both areas equal to *S*), the well-known valve static hydraulic characteristic can be expressed assuming null valve leakages, no effect of the Reynolds number and perfectly synchronized orifices [21]:

$$Q = K_v X \tag{13}$$

where:

- $K_v = K_o \sqrt{\frac{2}{\rho}|P_v|} sign(P_v)$ is the valve flow gain (m^2/s) (14)
- $P_v = P_s - P_r - P_l sign(X)$ is the valve pressure drop (Pa) (15)
- $P_l = P_1 - P_2$ is the load pressure difference (Pa) (16)
- K_o is the equivalent orifice area/opening gain (m^2/m)

Note: The absolute and sign functions of equation (13) can be omitted if backflow is considered as not possible.

The hydrostatic force delivered by the jack to the load is directly related to the load pressure P_l :

$$F_h = (P_1 - P_2)S = P_l S \tag{17}$$

Consequently, the hydraulic characteristic can be translated into the mechanical domain, giving

$$S\dot{Y} = K_v X = K_o X \sqrt{\frac{2}{\rho}\left|P_s - P_r - \frac{F_h}{S} sign(X)\right|} sign(P_s - P_r - \frac{F_h}{S} sign(X)) \qquad (18)$$

As the valve opening is bounded ($\pm Y_M$), the power transfered from the supply to the load is limited by the valve. Then, the valve flow capability could be given by the values of K_v and Y_M, according to equation (13). However, this is not convenient in practice. For this reason, it is preferred to indicate the *valve nominal flow* Q_N that corresponds to the output flow at full opening, under a given valve pressure drop (*the nominal pressure drop* P_n, commonly 70 bars).

This simple and leakage-less model indicates clearly the dependence of the flow gain, (or the speed gain which is the transcription of the flow gain on the servoactuator):

- on the supply, return and load pressures,
- on the equivalent orifice gain that is sensitive to the effective orifices geometry and the amount of flow turbulence.

In the particular case of a valve with null output flow, the valve model of equation (18) yields to

$$P_1 - P_2 = (P - R) sign(X) \qquad (19)$$

that gives the hydrostatic force

$$F_h = (P - R) S\, sign(X) \qquad (20)$$

This equation represents an ideal view on the load. Indeed, the load/opening gain is infinity around the null opening. In reality, the defects of the valve induce a finite gain and so guaranty the continuity of the pressure around the null opening.

b) Means to quantify the valve characteristic

In practice, the real valve performance is defined through three different curves, as defined in [27] and [8].

- **The <u>flow/opening</u> curve,** Figure 21**.**

The curve is given as $Q_1 = Q_2 = f(X)$ at constant valve pressure drop. In practice, this characteristic is got connecting the two useports of the valve ($P_l = 0$) and maintaining constant the supply and return pressures. According to equations (4) and (13), this graph indicates the valve ability to control the load speed by its opening, under null load force

demand. The so called *valve flow gain* (K_{QY}) corresponds to the curve slope. At very low openings, the valve flow gain is altered by leakages due to the real geometry of the valve (rounded edges, clearance). At very high openings, the flow gain is generally reduced as a result of parasitic pressure drops (direct consequence of turbulent flow equation) under high fluid velocity within the flow path inside the valve.

Note: the de-synchronization is the fact that two orifices cannot be opened at the same time and reduced turbulence

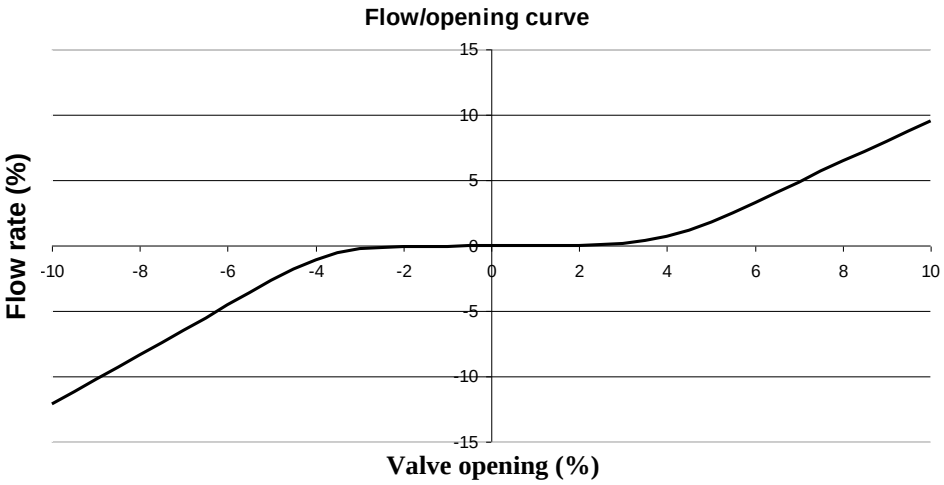

Figure 21: Typical flow gain curve

Analysis of the curve

Figure 21 shows a typical flow gain curve and is zoomed on +/-10% of the spool opening. The magnitude order of the real spool opening is around +/-1mm as observed. The defects of the spool affect only +/-5% of the opening. On a complete scale, the defects would be invisible although they play a major role in the actuator performance. The geometry of the valve modifies the shape of the curve at very low openings leading to the generic cases of Figure 22. Overlap or underlap can be either functional or parasitic.

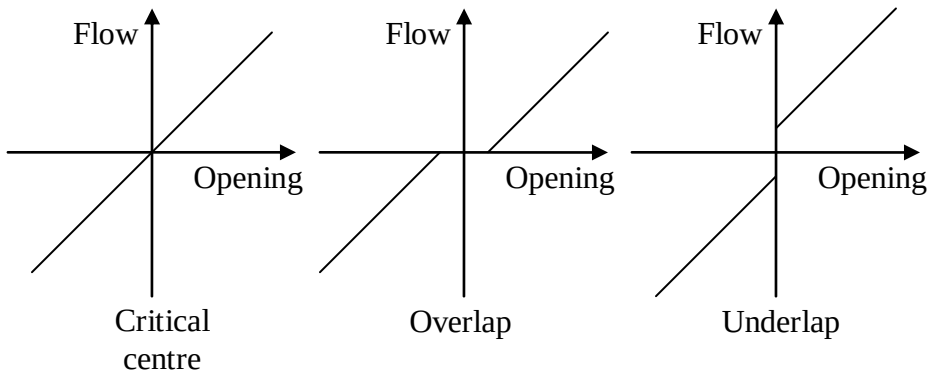

Figure 22: Defects of flow gain at very low openings

In the case of helicopter flight control actuators, overlap is preferred in order to produce a dead band effect. This avoids transmitting power to the load in the presence of noise (vibrations) on the valve input (spool displacement).

- **The <u>pressure/opening</u> curve,** Figure 23**.**

The curve is given as $P_l = g(X)$ at null output flow. In practice, this characteristic is obtained closing each useport of the valve ($Q_1 = Q_2 = 0$) and maintaining constant supply and return pressures conditions. According to equation (5), this graph illustrates the valve ability to deliver high force to drive a static load. The so-called *valve pressure gain* (K_{PY}) is the slope of the pressure/opening curve measured at hydraulic null ($P_1 = P_2$). In practice the pressure/opening graph significantly differs from the ideal one, equation (17), in the vicinity of the hydraulic null. Once again, this is the consequence of parasitic internal leakages, manufacturing tolerances and reduced flow turbulence.

More information is made available when plotting the individual pressure/opening curves ($P_1 = g_1(X)$ and $P_2 = g_2(X)$) instead of the differential pressure/opening one. In particular, the value at which the two useport pressures are identical may be of particular interest for quasi static actuator operation. Indeed, this point corresponds to the equilibrium (if α=1 and no load) of the servoactuator. It indicates the pressure level in the actuator without external force and around the hydraulic null (which corresponds to the main piloting domain).

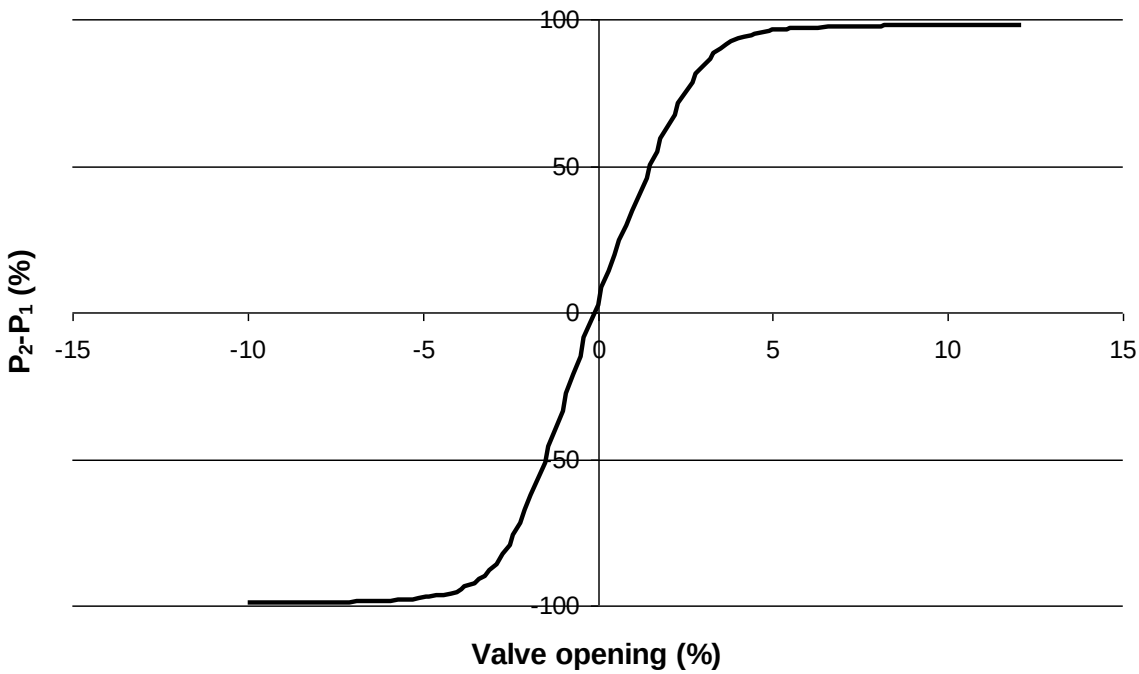

Figure 23: typical pressure gain curve

Analysis of the curve

Figure 23 shows a typical pressure gain curve and is zoomed on +/-10% of the spool opening. The magnitude order of the real spool curve is around +/-1mm, the defects of the spool affect only +/-5% of the opening. On a complete scale, the defects would be invisible. As a typical value, one can consider a differential pressure of 40% for an opening of 1%. Finally, defects contribute to obtain a progressive differential pressure around the null and to avoid problems of force-fighting due to a gap of synchronisation (see 3.3.1 - p71).

- **The internal leakage/opening curve,** Figure 24**.**

The curve is given as the consumed flow Q_c at null delivered flow, as a function of the valve opening $Q_c = h(X)$. The maximum valve leakage is generally observed in the surroundings of the null opening, where the orifices operate between closure and opening.

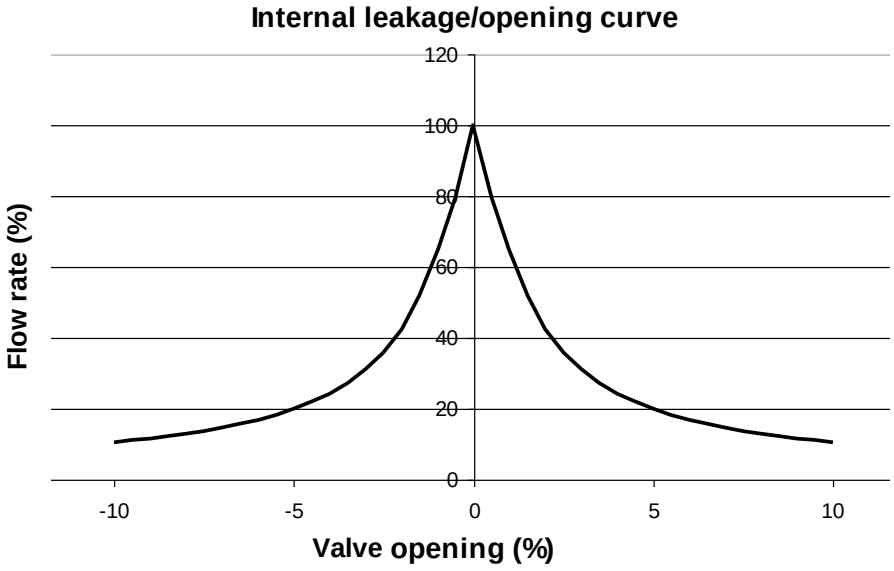

Figure 24: typical leakage curve [11]

Analysis of the curve

Figure 24 shows a typical leakage curve of the main spool and is zoomed on +/-10% of the spool opening. The magnitude order of the real spool curve is around +/-1mm, the defects of the spool affect only +/-5% of the opening. On a complete scale, the defects would be invisible. The valve operates around the null opening most of the functioning time. It is so very important to control the maximal leakage value to guaranty the permanent leakage flow to be compensated by the hydraulic supply.

2.4.2 - Orifice valve model

The orifice model must allow to reproduce the dominant effects that fix the valve performance. As illustrated by Figure 25, the more advanced model [6] takes into consideration rounded edge radius orifices (radius r), the spool-bushing radial clearance (c) and the individual orifice de-synchronization (X_{i0}).

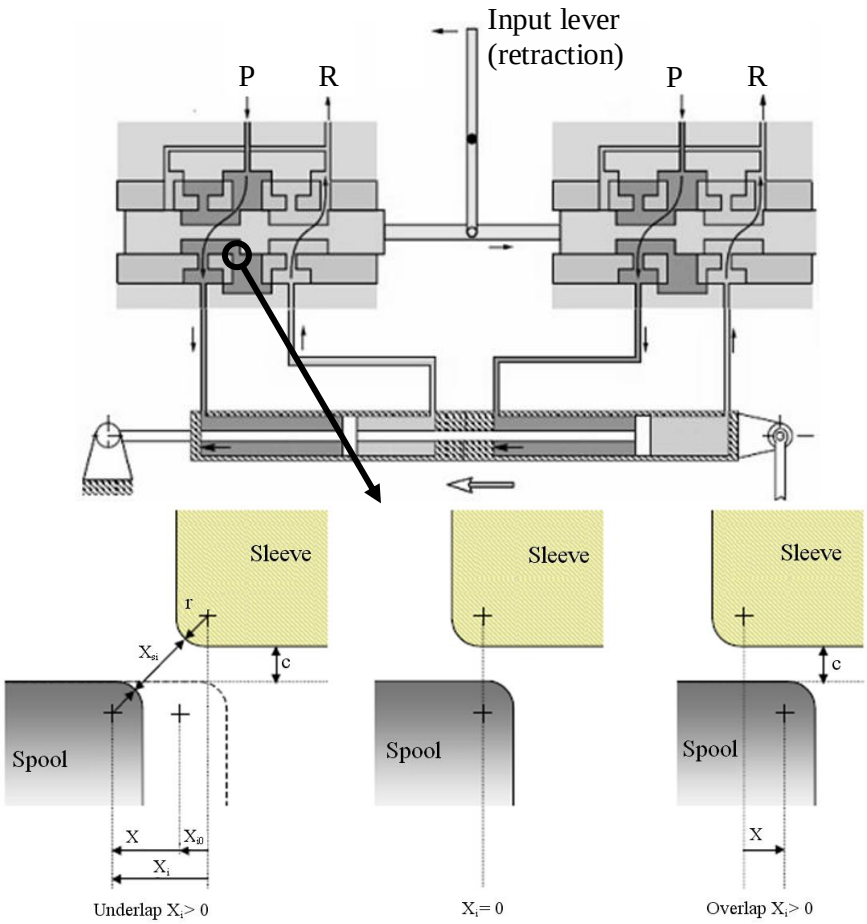

Figure 25: Real geometry of the valve edges [21]

Each orifice is modeled independently ($i = a$ to $i = d$), using the set of equations (21) to (30). Equations (21) to (24) are not applicable in case of non square orifices.

- *Orifice opening* X_i

$$X_i = X_{i0} + \varepsilon X \tag{21}$$

with

$\varepsilon_i = 1$	If orifice i tends to open as X increases (orifices a and c)
$\varepsilon_i = -1$	If orifice i tends to close as X increases (orifices b and d)
X_{i0}	Individual orifice underlap at null valve opening (m)

- *Cross-sectional length* X_{si} *(m)*

if $X_i > 0$ then orifice opened $X_{si} = \sqrt{X_i^2 + (2r + c)^2} - 2r$ (22)

else orifice closed $X_{si} = c$ (23)

with

r	Rounded edge radius (m)
c	Diametral clearance (m)

- *Cross sectional area* S_i *(m²)*

$$S_i = n_f l_f X_{si} \tag{24}$$

- *Orifice hydraulic diameter* D_{hi} *(m)*

$$D_{hi} = \frac{2 l_f X_{si}}{l_f + X_{si}} \tag{25}$$

with

l_f	Slot width (m)

- *Orifice pressure drop* ΔP_i *(Pa)*

$$\begin{aligned} \Delta P_a &= P_1 - R \\ \Delta P_b &= P - P_1 \\ \Delta P_c &= P - P_2 \\ \Delta P_d &= P_2 - R \end{aligned} \tag{26}$$

- *Orifice flow number* λ_i *(-)*

$$\lambda_i = \frac{D_{hi}}{\nu} \sqrt{\frac{2}{\rho} |\Delta P_i|} \tag{27}$$

with

ν	Fluid kinetic viscosity (St)
ρ	Fluid density (kg/m³)

- *Continuity constant* K_{gi} *(-)*

$$K_{gi} = \frac{64 C_{q\infty}}{D_{hi} \lambda_t} \tag{28}$$

With

$C_{q\infty}$	Limit flow coefficient (-)
λ_t	Transition flow number (-)

- *Orifice flow coefficient* C_{qi} *(-)*

$$C_{qi} = C_{q\infty} \tanh\left(\frac{\lambda_i}{\lambda_t} \frac{1}{1 + \frac{1}{2} K_{gi} (|X_i| - X_i)} \right) \tag{29}$$

- *Orifice flow rate* Q_i *(m^3/s)*

$$Q_i = C_{qi} S_i \sqrt{\frac{2}{\rho} |\Delta P_i|} \operatorname{sgn}(\Delta P_i) \tag{30}$$

a) Valve model

The valve model is obtained by associating the four orifices models according to the full bridge architecture. The fluid capacitance effect is neglected due to the small volumes of fluid at stake within the valve [23]. Hence, the continuity equation can be written as:

$$Q_b = Q_a + Q_1 \tag{31}$$

$$Q_d = Q_c + Q_2 \tag{32}$$

Previous orifice equations (21) to (30) involve 5 geometrical parameters (x_{i0} , r, c, l_f, n_f), 2 fluid physical properties (ν and ρ) and 2 flow model constants ($C_{q\infty}$ and λ_t). For cylindrical valves, it is generally assumed that r and c are identical for all orifices. Moreover, symmetrical valves are manufactured with same l_f and n_f for all orifices. Fluid properties and flow model coefficients are also assumed to be identical for all orifices. Only x_{i0} , that is affected by manufacturing tolerances, must be considered different for each orifice because it influences significantly the valve characteristic around the null opening.

Consequently the full valve model involves 12 parameters.

2.4.3 - Parameters of the four ways, sliding spool valve

A number of parameters have to be defined in order to understand the orifice model. Furthermore, an order of magnitude is given for each parameter to completely define the study domain.

a) Fluid physical properties

There are two major fluid physical properties: density (ρ) and kinematic viscosity (ν). These parameters are linked by the equation:

$$\mu = \rho \nu \tag{33}$$

where μ is the absolute viscosity that is mainly function of the temperature of the fluid. Note that the fluid physical properties are also function of pressure and temperature. The evolution of density and kinematic viscosity versus pressure and temperature are drawn at Figure 26 in the case of MIL-H-83282.

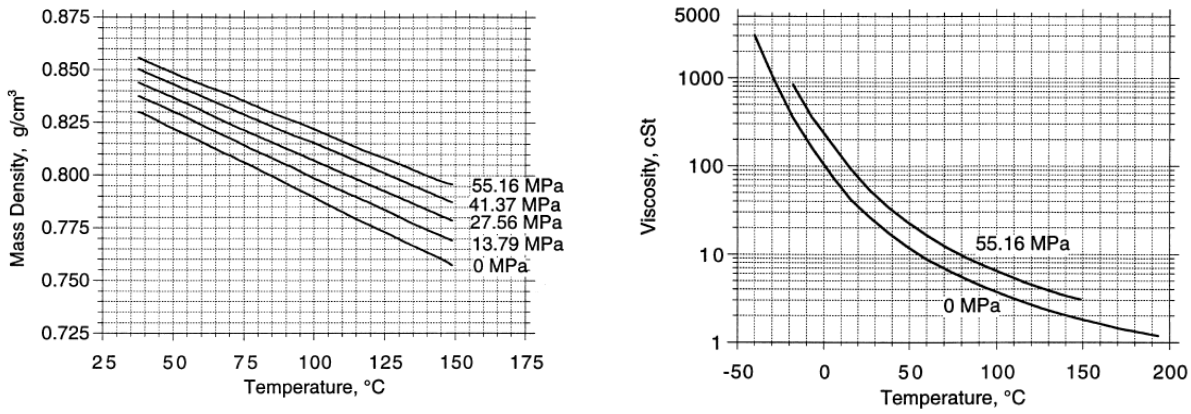

Figure 26: Density and kinematic viscosity for the MIL-H-83282 oil [2])

b) Flow model constants

As it has been defined above, there are two flow model constants: $C_{q\infty}$ and λ_t. These parameters are totally under the influence of the valve geometry. To strictly deduce them, CFD (Computational Fluid Dynamic) would be an efficient support. Simulation of the real flow rate across orifice would be a good manner to get $C_{q\infty}$ and λ_t values. It is important to keep in mind that modifying one or two of them can generate consistent charges in the valve and servoactuator performance. The values cannot be directly varied by design.

- Limit flow coefficient $C_{q\infty}$

Von Mises had shown that for a generic configuration, the minimal value of flow coefficient is π/(π+2) = 0.611 [12]. Experiments give a limit flow coefficient varying between 0.6 and 1.

- Transition flow number λ_t

In case of singularity, the transition laminar flow/turbulent flow is related to the value of the Reynolds number value between: $100 < Re_t < 400$ [12]. Moreover, the flow number can be linked to Reynolds number by equation:

$$\mathrm{Re} = \frac{C_q D_h}{\nu}\sqrt{\frac{2}{\rho}\left|\Delta P\right|} = C_d \lambda \tag{34}$$

with

C_d Discharge coefficient (-)

The discharge coefficient and flow coefficient are really near. So the transition flow number is in a same order of magnitude than the transition Reynolds number. With a security coefficient, the range of transition for the flow number is taken as below:

$$20 < \lambda_t < 500$$

c) Geometrical parameters

The limits of these parameters are dependent on the geometry of the servoactuator. Thus, numerical results given thereafter are valid only in our case of study.

- Number of slots (n_f)

Naturally, there is one slot at least. However, one slot for the valve creates radial efforts by dissymmetry. In this case, it has to be noticed that sticking of the main spool is increasing. A priori, the number of slots will be lower or equal to four to limit the machining. So, the slot number is bounded as below:

$$1 < n_f < 4$$

- Slot width (l_f)

The width of slots is not a free parameter. Indeed, it is fixed by the nominal flow of the valve if other parameters are fixed, so the system is losing one degree of freedom. The first constraint is geometrical:

$$n_f\, l_f < \text{main spool external perimeter}$$

Secondly, the slot width is one of the main design parameters of the valve if the nominal opening is given (equations (21) to (30)). To obtain upper and lower limits of the parameter, it is necessary to solve the set of equations in the worst case (T = -40°C; ΔP = 35 bar).

With these constraints and a security factor, this range of the parameter is:

$$0.1\text{mm} < l_f < 2\text{mm}$$

Slot width is a parameter which directly acts on the nominal flow and so on the servoactuator dynamic behaviour. Furthermore it can be adjusted easily on the definition range. Hence it is a geometrical parameter selected for the valve optimisation.

Note: the internal diameter of the main spool must large enough to avoid pressure losses.

- Radial clearance (c)

Internal leakage of the valve is directly influenced by the clearance between the main spool and the sleeve [7]. It is naturally strictly upper than null and must be kept as low as possible to reduce the leakages.

- Rounded edge radius (r)

In case of ideal valve, the rounded edge radius is null, so the lower limit is: $r > 0$. To find an upper limit for this parameter, the rod velocity curve versus spool opening is under interest (Figure 27). This curve is limited by the specification of the servoactuator: 90 mm/s < V < 150mm/s. If consider one limit as a perfect valve behaviour ($r = 0$), the distance between the two limits corresponds approximately to two maximal rounded edge radii. This gives: r_{max} = 25µm (see Figure 27). This value is majored using a safety coefficient. The range below is kept for the study:

$$0\mu m < r < 100\mu m$$

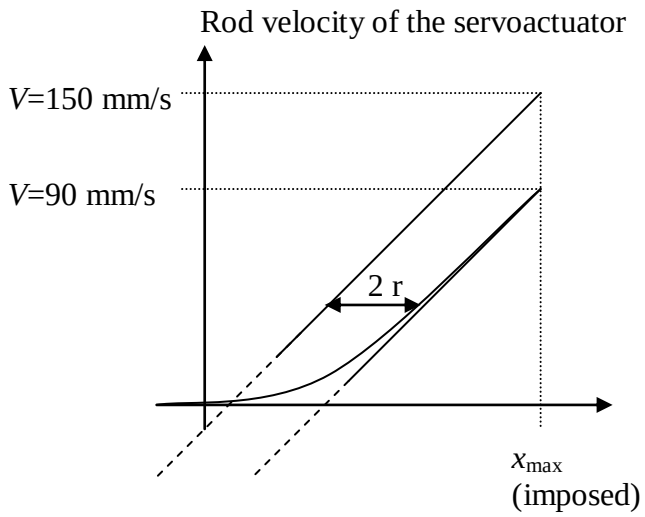

Figure 27: Effect of the rounded edge radius on the actuator speed in function of its opening

- Overlap (X_{i0})

The range of overlap is the same for all orifices. To get an idea of this range, the rod velocity curve is used like above. The valve is supposed perfect, so r is taken null. For X positive and X negative, the curve corresponding to the lower limit of specification (V_{rod} = 90mm/s) is drawn. The maximum overlap supposed is half distance between the two curves at

null flow rate. The obtained overlap is: X_0 = 30µm. An underlap is unacceptable with respect to input lever noise reinjection. So:

$$0\mu m < X_{i0} < 50\mu m$$

d) Synthesis

All previous data are summarized in the Table 1.

	parameters	***Label (unit)***	***Lower limit***	***Higher limit***
Fluid parameters	*Temperature*	*T (°C)*	*-40*	*100*
	=> density	*ρ (kg/m³)*	*894*	*810*
	=> kinematic viscosity	*ν (cSt)*	*2000*	*3.7*
	Limit flow coefficient	$C_{q\infty}$ *(-)*	*0.5*	*1*
	Transition flow number	λ_t *(-)*	*20*	*500*
Geometrical parameters	*Number of slots*	n_f *(-)*	*1*	*4*
	Width of slots	l_f *(mm)*	*0.1*	*2*
	Radial clearance	*c (µm)*	*0*	*10*
	Rounded edge radius	*r (µm)*	*0*	*100*
	Overlap	X_{i0} *(µm)*	*0*	*50*

Table 1: Summary of the model parameters range

2.5 - Simulation tools

Several simulation devices will be used during the development of the new servoactuator. This section aims at presenting these tools and mainly why and how they are used.

The first tool is a design of experiment tool (DOE) which has been involved in the design process with two objectives:

- Optimization: it permits to select and define a minimal number of tests to be performed on a test bench, to analyze the results with the best accuracy and to extract the optimum configuration for the valve design.
- Sensitivity analysis: the analysis will be performed making a top level calculation sheet in the MS Excel environment that permits developing a static model of the valve.

The last tool that has been used in this thesis is software for dynamic simulation. The software AMESim (Advanced Modeling Environment for performing Simulations [5]) has been chosen to develop dynamic models of the servoactuator and the valve.

2.5.1 - Design of experiments

In all industrial projects, the tests represent a critical phase of the project. Indeed they can be needed to understand some phenomenon, to identity, to validate the design parameters and/or to optimize them. But the method to select, perform and analyze the tests must also be optimized, that tests being real or virtual (simulation). It can be done with a DOE approach. A lot of DOE softwares exist. The software Design expert ([30]) has been chosen for its simplicity and its capacity to generate the tests needed, to analyze the responses and to compute an optimum.

<u>Design of experiment: the general method [16]</u>

The step-by-step procedure of the DOE method is:

- Choose the type of design, *i.e.* which tests must be performed (complete factorial, fractional factorial, Taguchi, …)
- Choose the factors (inputs)
- Choose the level of the design to consider the main effects of the factors and eventually the interactions of first order and also of second order of the factors
- Choose the responses (outputs)
- Generate of the design which gives the tests selected among all the possible tests.
- Perform the tests
- Analyze the response with the software

If optimization is required, two more steps are needed:

- Define the criteria on the responses
- Predict the optimum design

Note: From a mathematical point of view, an optimization is often associated to maximization or minimization. A lot of methods have been developed to extract a maximum on a topographic profile. But the response surface is needed. The design of experiment

permits to obtain an approximation of this response surface with the lowest possible incertitude in choosing the most relevant tests and with the adequate mathematical treatment.

Design of experiment: terminology [20]

Experiment: An investigation that can be real or virtual (simulation) and that establishes a particular set of circumstances under a specified protocol to observe and evaluate the implications of the resulting observations

Experimental Unit A physical entity or subject exposed to the treatment independently of the other units (the valve here for example).

Response: A characteristic of an experimental unit measured after treatment and analyzed to address the objectives of the experiment.

Experimental Error: Error due to the fact that experimental units treated independently and identically will not have identical responses.

Observational Study: An investigation in which the investigator observes experimental units and measures one or more response variables without imposing treatments on the individuals

Factor (or parameter): Input of the investigation that can take two or more values

Levels: The different values of a factor

Full Factorial Treatment Design: The treatment consists of all possible combinations of the levels of the factors of interest.

Design of experiment applied to the valve design

The DOE will be used on the valve tests in order to optimize its geometry with a minimum of manufactured valves.

In the case of the valve optimization, only two input factors are considered, one with three levels and the other with two levels. So, a complete factorial design will be used because of the few tests needed. The DOE advantage for the present study is the capacity to interpolate behaviour in the experimental domain with only few data (because of few tested valves). For each response, the DOE will suppose a priori a polynomial approximation of the response surface. The coefficients of the polynomial are computed from the performed tests with a method based on the variance analysis (ANOVA [9]).

Finally the optimization tool is used. A criterion is defined for each response from the specifications. One or many solutions which satisfy the criteria are so extracted and permit to compute a desirability curve. This curve gives information on the robustness of the optimum.

This method permits to find an optimum in the experimental domain. A last experiment is nevertheless necessary to check the DOE predictions.

Design of experiment applied to the valve manufacturing

Another application of the DOE in this study is to perform a sensibility analysis on the parameters of the valve in order to develop a methodology to grind its flanks. The DOE is applied not on real tests but on simulation results extracted from a quasi-static model implemented in the MS Excel [31]. This study is developed in section 3.5 - p84 while the implementation of the model is explained in the next section.

2.5.2 - Implementation of the valve quasi-static model

2.5.2.1 - Implementation of the equations of each edge

The equations that describe the flow rate for one edge can be summarized in the diagram of Figure 28 (*i* represents the edge orifice).

The starting point is the main spool displacement vector X. Knowing X and with the data of Table 1, it is possible to compute X_i, X_{si}, S_i, D_{hi} and K_{gi}. Then a second input is necessary: the pressure vector ΔP_i that permits to compute the parameters λ_i ans C_{qi} and finally the flow rate Q_i. The pressure vector will be generated as explained in the following section.

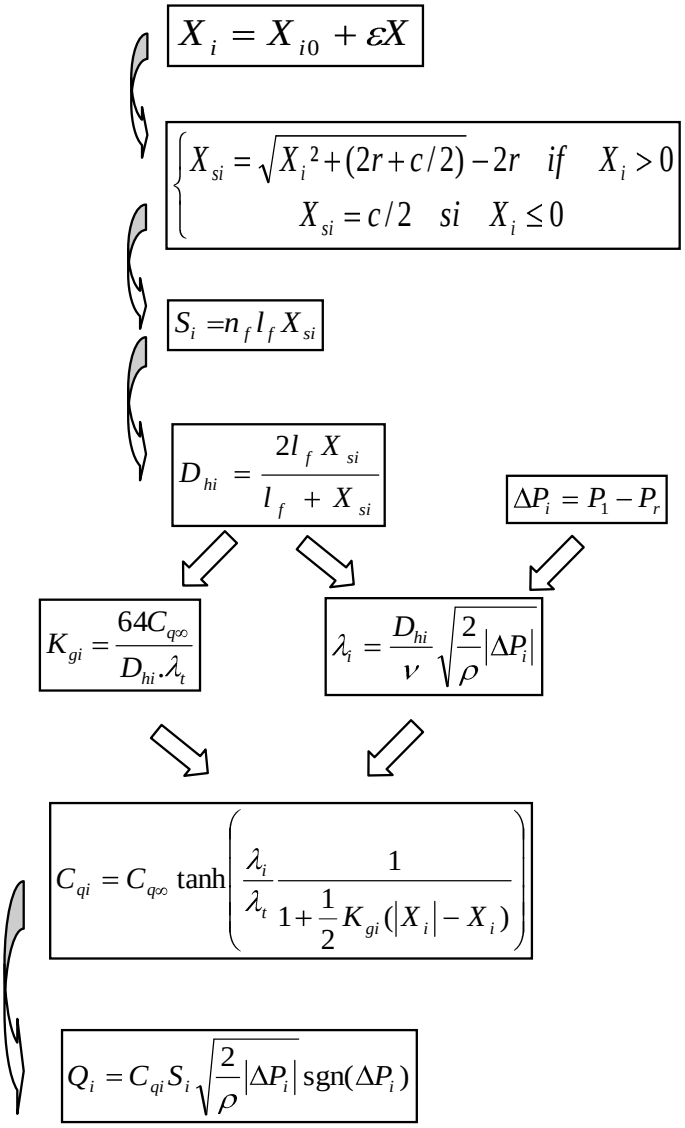

Figure 28: Diagram of the valve orifices model defined by the equations (21) to (30)

2.5.2.2 - Computation of the flow gain and of the pressure gain

The computation of these gains requires the equations of the edges and the continuity equations that link the pressures in each chamber and the flow rate of each edge.

a) Flow gain

For the flow gain, the continuity equations are:

$$Q_a - Q_b = Q_c - Q_d \quad \text{and} \quad P_1 = P_2$$

The solver modifies the pressures P_1 and P_2 and computes the flow rate Q_a, Q_b, Q_c and Q_d so that the cost function J_Q is minimized:

$$J_Q = \sqrt{\frac{1}{n}\sum_{j=1}^{n}\left((\mathrm{Q_{aj}} - \mathrm{Q_{bj}}) - (\mathrm{Q_{cj}} - \mathrm{Q_{dj}})\right)^2} \tag{35}$$

with j the index of the vector and n the length of the vector.

The flow gain curve $Q_a - Q_b = f(X)$ can then be plotted.

b) Pressure gain

For the pressure gain, the continuity equations are:

$$Q_a = Q_b \text{ and } Q_c = Q_d$$

The solver is used twice:

- firstly the pressure P_1 is modified to compute the flow rate Q_a and Q_b so that the cost function J_{P1} is minimized:

$$J_{P1} = \sqrt{\frac{1}{n}\sum_{j=1}^{n}\left(\mathrm{Q_{aj}} - \mathrm{Q_{bj}}\right)^2} \tag{36}$$

- secondly the pressure P_2 is modified to compute the flow rate Q_c and Q_d so that the cost function J_{P2} is minimized:

$$J_{P2} = \sqrt{\frac{1}{n}\sum_{j=1}^{n}\left(\mathrm{Q_{cj}} - \mathrm{Q_{dj}}\right)^2} \tag{37}$$

The pressure gain curves $P_1 = f(X)$ and $P_2 = f(X)$ can then be plotted.

2.5.2.3 - Linking the quasi static model and the design of experiment

When the DOE is used for sensibility analysis, it uses the results got from the simulation of the quasi static model. The procedure for this analysis is:

- the parameters of the valve equations are the factors for the DOE: $\theta = [f, C_{q\infty}, \lambda_t, n_f, l_f, c, r, X_{i0}]^T$
- the DOE software generates the design (it gives tests which have to be performed)
- the pressure gain and flow gain curves are computed
- The responses of the DOE are extracted from these curves
- These responses are implemented in the DOE software for the sensibility analysis.

2.5.3 - Dynamic models of the servoactuator and of the valve

The development of a servoactuator is a complex system which cannot be performed at the first time. A dynamic model is thus built to obtain a predictive tool which can help to save time and money. The tool used to create this model is AMESim.

AMESim is a multiphysics software performing simulations of engineering systems. One of the advantages of AMESim is to perform dynamic analysis of systems. It has been used to develop a model of the servoactuator involving a detailed model of the valve.

2.5.3.1 - Servoactuator model

The servoactuator model has been built as close as possible to the real geometry of the servoactuator (Figure 29). All the functional parts of the servoactuator are modelled:

- The two moving bodies with the values of the chambers length, of the rod diameter and of the piston diameter.
- The two valves: one for each body. They are identical and mounted top-to-tail.
- The lever defined by its gain and hysteresis.
- The loads applied to the servoactuator: weight, external static and dynamic loads, seal loads.
- The hydraulic generation made of the two hydraulic pumps, the valves pressure relief to limit the supply pressure and the tanks.

Lots of switches are added to easily simulate the different degraded cases and the servoactuator behaviour in closed loop or open loop.

The valve is modelled by a customized component that has been developed in the frame of the present work. It is described in the following section.

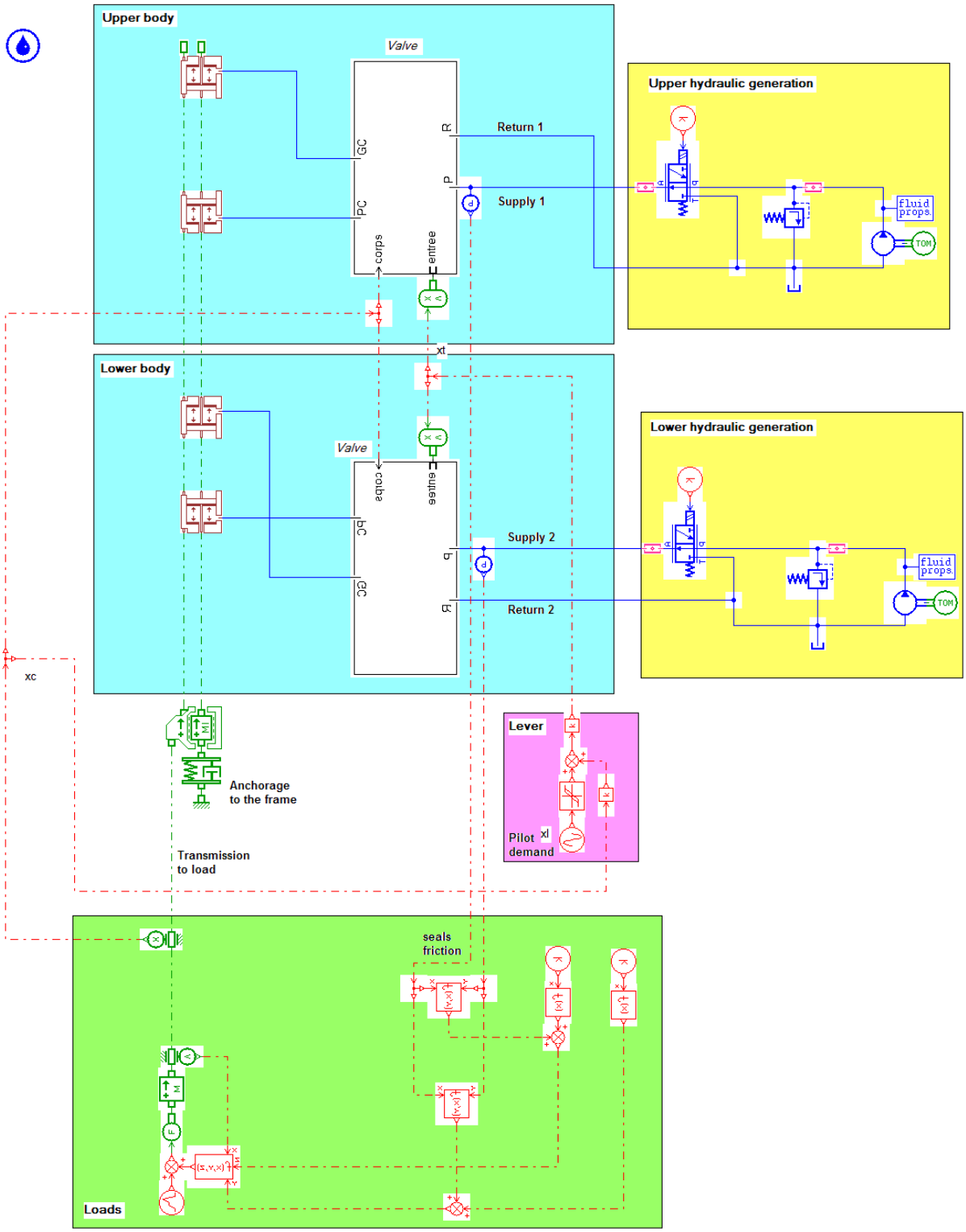

Figure 29: AMESim servoactuator dynamic model

2.5.3.2 - Valve model

Like the servoactuator, a dynamic valve model has been developed, as shown in Figure 30. The model parameters have first been fixed from the valve design and then updated with the tests realized throughout the study. Some functional parts are worthwhile to notice:

- the restriction section which acts as a flow limiter.
- the main spool and the back-up spool. Furthermore, the displacement of the back-up spool pushed by the test piston is simulated in case of loss of supply pressure.
- The hydraulic diameter and flow section functions of opening are computed to take into account different geometries of valves.

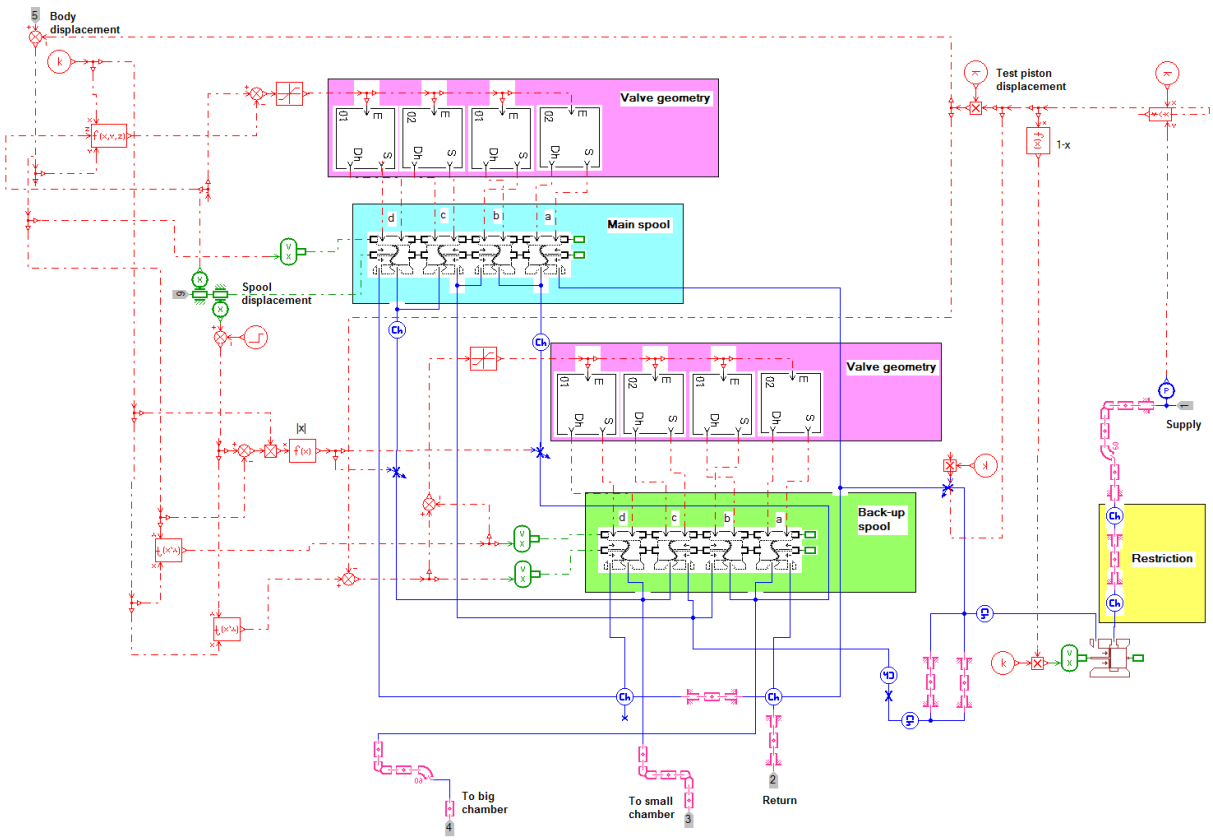

Figure 30: AMESim dynamic valve model

The main spool is a very important part of the valve described by the following parameters:

- The spool diameter and the rod diameter
- The hydraulic diameter and flow section functions of opening

- The diametral clearance
- The rounded edge radius of each edge
- The overlap of each edge
- Hydraulic constants: maximum flow coefficient and critical flow number

Concerning the overlap, there is a big difference between the overlap implemented in AMESim (effective overlap) and the measured overlap (apparent overlap). The Figure 31 shows the difference:

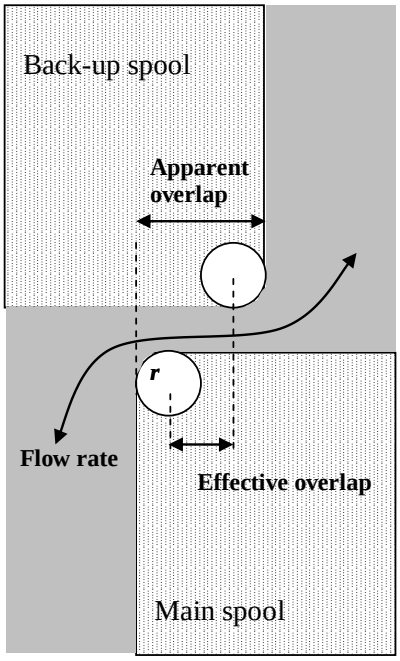

Figure 31: Definition of the effective and apparent overlaps

The apparent overlap corresponds to the flak to flank length from the main spool to the back-up spool (or external sleeve). The effective overlap corresponds to apparent overlap only if the rounded edge radius is null. It's the overlap defining in the models. The relation between the two overlaps is:

$$\text{Apparent overlap} = \text{effective overlap} + 2r \tag{38}$$

This detailed model has permitted to obtain a predictive model of the valve and consequently of the servoactuator.

2.6 - Conclusion

The first part of this chapter was to present the model used to define the flow through the valve orifices. The fluid and geometrical parameters were extracted from these equations and hence it has permitted to point out the parameters which can be optimized. Because it mainly influences the servoactuator dynamic and can be manufactured with accuracy, the slot

width was the only parameter selected for the optimization. As the method is oriented with a low-cost view, the valve static model and then the dynamic models of the valve and the servoactuator has been developed. They have to save time and money during the servoactuator development.

Chapitre 3

Pre-design and manufacturing of the valve

3.1 - French Synthesis

Ce chapitre présente le pré-design et la fabrication des premiers distributeurs de servocommande. Pour cela, les spécifications concernant la servocommande sont définies, puis les paramètres de design du distributeur sont calculés à partir d'un modèle quasi-statique de distributeur. Enfin un premier jeu de distributeur a été fabriqué avec une nouvelle méthode orientée vers une réduction des coûts de fabrication.

La première partie du travail a été de récupérer et d'expliciter les exigences existantes concernant les servocommandes principales d'hélicoptère :

- le diagramme effort/vitesse qui correspond au domaine de fonctionnement de la servocommande. Il est construit à partir de la vitesse maximale à vide et de l'effort de réversibilité. Eurocopter a fixé un effort de réversibilité de 220daN en rétraction, 350daN en extension et une vitesse maximale à vide V_{max}:

$$90\text{mm/s} < V_{max} < 130\text{mm/s}$$

- la course morte qui garantit un bon confort de pilotage tout en filtrant les excitations parasites. Le standardAIR8520 donne une valeur de course morte de 0,2mm
- la synchronisation des corps qui permet d'assurer un fonctionnement de concert des deux corps de la servocommande. Cela correspond à la distance entre les neutres de chaque corps. Si cet écart est trop important, pour certaines zones de fonctionnement, les deux corps peuvent travailler en opposition, endommageant prématurément l'actionneur. Eurocopter spécifie une désynchronisation maximale de 100µm.
- l'effort maximal d'entrée qui influence le confort et la précision de pilotage. L'expérience montre que pour des efforts supérieurs à 5N des problèmes peuvent apparaitre. Il a donc été spécifié un effort de maximal de 3N.
- les efforts statiques sur le levier. Ces efforts sont spécifiés par les standards FAR et JAR.

- la réponse en fréquence pour différentes amplitudes afin de garantir le bon comportement dynamique de la servocommande. Pour de petits déplacements, la réponse de la servocommande doit se trouver entre 80% et 100% du déplacement d'entrée. Pour des déplacements plus importants, des gabarits issus de l'expérience sont définis en fonction de la fréquence.
- la tenue mécanique en température, en fréquence et sous charge pour assurer l'intégrité de l'appareil
- les fuites internes et externes maximales. Les fuites externes sont définies par le département qualité d'Eurocopter. Elles sont d'une goutte pour 100 manœuvre butée à butée pour un actionneur neuf. Les fuites internes doivent être limitées vis-à-vis de la consommation. Elles sont spécifiées à un maximum de 0,4l/min.
- l'exigence sur l'huile utilisée. L'huile sélectionnée au vu de l'application est la MIL-H-83282.

A ces exigences sont ajoutées deux exigences :

- l'exigence de mixabilité qui permet de pouvoir remplacer n'importe quelle servocommande existante par la nouvelle développée sans avoir besoin de changer les autres servocommandes déjà en place sur l'hélicoptère. C'est un critère important d'un point de vue de la maintenance.
- l'exigence de consommation maximale qui garantit un débit maximal consommé par la servocommande dans tous les cas de figures.

La seconde partie de ce chapitre concerne les paramètres à définir pour que la servocommande réponde à ces exigences. Plusieurs paramètres sont fixés rapidement:

L'huile

L'huile utilisée n'est pas un paramètre sur lequel on peut jouer. L'huile brassée dans les circuits hydrauliques des hélicoptères est une huile minérale : MIL-H-83282. La densité et la viscosité sont donc fixées ainsi que les pressions d'admission et de retour.

Le distributeur

Le recouvrement sur les arêtes du distributeur est choisi d'environ 20µm. Un recouvrement positif est indispensable pour éviter que les vibrations de l'appareil n'engendrent une réponse de la servocommande. Il provient de l'exigence d'une course morte. Le recouvrement au niveau du tiroir secondaire peut quant à lui être plus important étant donné qu'il n'intervient qu'en mode dégradé. Il est donc choisi de 250µm afin de limiter les fuites provoquées par celui-ci.

Les jeux diamétraux au niveau du distributeur sont choisis aussi faibles que possible sans prendre le risque de coincement d'un tiroir dans sa chemise. En conséquence, des jeux diamétraux d'environ 6µm sont choisis.

La course du tiroir principal est choisie de +/-1mm ce qui correspond à la course du distributeur existant avec un gain de levier de 3 (course levier de +/-3mm), pour répondre au critère de mixabilité.

Le vérin

Les spécifications imposent les charges maximales que doivent développer la servocommande en extension (350daN) et en rétraction (220daN) avec une vitesse nulle. La pression d'alimentation étant imposée, les sections de piston sont automatiquement déduites.

Concernant les joints, ils seront choisis avec des frottements aussi faibles que possible (environ 10daN).

Il reste donc un seul paramètre de design concernant le distributeur sur lequel on puisse jouer pour satisfaire les spécifications : la largeur de fente. A cette architecture est ajouté un composant original : une restriction en amont du distributeur, utilisé comme limiteur de débit afin de garantir l'exigence de consommation maximale.

La troisième partie sur la conception consiste à définir ces deux paramètres à partir d'un modèle quasi-statique de distributeur. Tout d'abord, une méthode originale permettant de transformer un débit traversant un orifice de distribution plein ouvert en vitesse maximale d'une servocommande dissymétrique ayant des frictions dues aux joints est développée afin de vérifier les exigences de vitesse maximales à vide. Ensuite la méthode suivante est mise en place :

- Une largeur de fente est fixée
- Le diamètre maximal de restriction est calculé à partir d'un solveur afin d'obtenir le débit de fuite permanent
- Les vitesses maximales à vide de la servocommande sont calculées en extension et en rétraction.
- Ces vitesses calculées sont comparées avec les spécifications. Si les vitesses ne sont pas acceptables, une autre largeur de fente est sélectionnée et la méthode est réitérée. Le pas minimal défini de largeur de fente est de 1/100 de millimètre. Si les vitesses sont acceptables, le couple diamètre de restriction/largeur de fente est conservé. La vitesse cible correspond au centre de la zone de spécification de vitesse.

Un jeu de paramètres de 1.38mm de largeur de fente et 1.15mm de diamètre de restriction est sélectionné puisque les résultats prédits par le modèle quasi-statique assurent

les tenues aux exigences de vitesse maximales à vide en extension et en rétraction et à la consommation maximale.

Les paramètres de conception ayant été fixés par l'étude menée avec le modèle quasi-statique de distributeur, les distributeurs doivent ensuite être fabriqués. Une nouvelle approche est développée pour la fabrication de distributeur en cas de petites séries. Les performances du distributeur sont directement liées à la géométrie du tiroir et de la chemise. La largeur de fente, leur nombre et la course maximale du tiroir sont fixés par les spécifications. Le jeu entre le tiroir et la chemise est défini le plus faible possible et nécessite un apérage afin de limiter les fuites sans coincement (chaque chemise possède son propre tiroir). Les rayons d'arrondi au niveau des arêtes tiroir sont taillés aussi aigus que possible puisque il serait trop difficile d'en spécifier un. Enfin les recouvrements au niveau de chaque arête jouent un rôle important puisqu'ils définissent la course morte et la pression d'équilibre dans les chambres de la servocommande. Ils doivent être fabriqués avec une grande précision (<5µm). Contrairement aux autres paramètres, ils peuvent être ajustés par un procédé de rectification. La nouvelle méthode consiste à déterminer le recouvrement de chaque arête grâce à l'analyse de la seule courbe de mesure de gain en pression (il faut habituellement mesurer le gain en débit également dont l'essai est relativement long et apporte des informations redondantes, voir Figure 40). A partir de la mesure du gain en pression, une tendance asymptotique de la courbe est extraite, puis analysée. Le recouvrement au niveau de chaque arête est ainsi calculé avec un indice de confiance sur la pertinence du résultat obtenu. Plus qu'un seul essai est donc nécessaire pour retoucher les flancs distributeur.

Ces essais ont pu être réalisés grâce à la fabrication d'un banc d'essai distributeur spécifique. Celui-ci a été rapidement suivi par un banc d'essai servocommande afin de pouvoir effectuer les tests sur la future servocommande.

Le pré-design, fonction de la largeur de fente et du diamètre de restriction, a donc été effectué grâce à une méthode fondée sur le modèle quasi-statique de distributeur. Le diamètre de restriction a été ajouté à la largeur de fente comme paramètre de conception afin de vérifier la nouvelle spécification de consommation maximale. Après la définition de ces deux paramètres, le distributeur a été fabriqué avec un procédé original de rectification des flancs de tiroir afin de réduire les coûts. La méthode a été développée en partie avec une approche par plan d'expérience sur la courbe de gain en pression. Durant la thèse, deux bancs d'essai (un pour le distributeur et un pour la servocommande) ont été développés, fabriqués, et configurés pour obtenir les données expérimentales sur le distributeur et la servocommande.

3.2 - Introduction

This chapter deals with the pre-design and the manufacturing of the first valves. These ones will be designed to meet the requirements of the servoactuator whose specifications are detailed and quantified in the first section of the chapter. Then the valves are pre-designed using a model-based methodology. The model involves fixed and design parameters. The methodology consists in computing the design parameters which influence the valve and servoactuator performances. This study allows defining an initial set of parameters that permits manufacturing the first valves. As the valves manufacturing is a difficult operation because of tolerances, a new low cost methodology is developed. Finally, in order to test the manufactured valves and the servoactuator, two test benches are designed, manufactured and set up.

3.3 - Specification of the servoactuator

3.3.1 - Specification from the existing servoactuator [17]

3.3.1.1 - Velocity and reversibility load

A good velocity of the flight controls is required in order to execute all possible handlings in all flight domains. Consequently, the helicopter manufacturer specifies its servoactuators with the rules below:

- For a single body servoactuator, pilot should be informed of the flight domain limit with a feedback on the control. For instance, the specification is:

  Reversibility load: 2000 N (load to obtain a null speed with a full opening valve)

  Velocity at null load: 110 mm/s

- For a double body servoactuator, the pilot has to be able to move the servoactuator at the required maximal velocity when static loads are extreme and a body is failed. A ratio of 3 or 4 between velocity at null load and velocity under maximal load is chosen in order to obtain a reversibility load not too high, with a good load reserve.

For the new servoactuator, Eurocopter has fixed:

- the maximal velocity at null load in the range:

$$90\text{mm/s} < V_{max} < 130\text{mm/s}$$

- the reversibility load to 220daN in retraction and to 350daN in extension.

3.3.1.2 - Dead stroke

It is the maximal input lever displacement that does not induce any load motion. A dead stroke is needed for a pleasant flying, but an important dead stroke reduces the flight accuracy. The standard AIR8520 ([1]) gives a value of 0.2mm for the dead stroke.

3.3.1.3 - Synchronization between power paths

It exists only for double bodies servoactuators. The desynchronization is the difference between the neutral's settings of the two valves (Figure 32). If the difference is too important, the dead stroke can be degraded, and contrary loads between the two bodies can appear. It is the force fighting phenomenon. To test the synchronisation, each body is tested independently with a sinusoidal input at low frequency and amplitude and the output is measured accurately. In case of perfect system, the two operating are identical. The gap between the two operating is the desynchronization of the servoactuator.

Eurocopter requires a maximal desynchronization of 100µm.

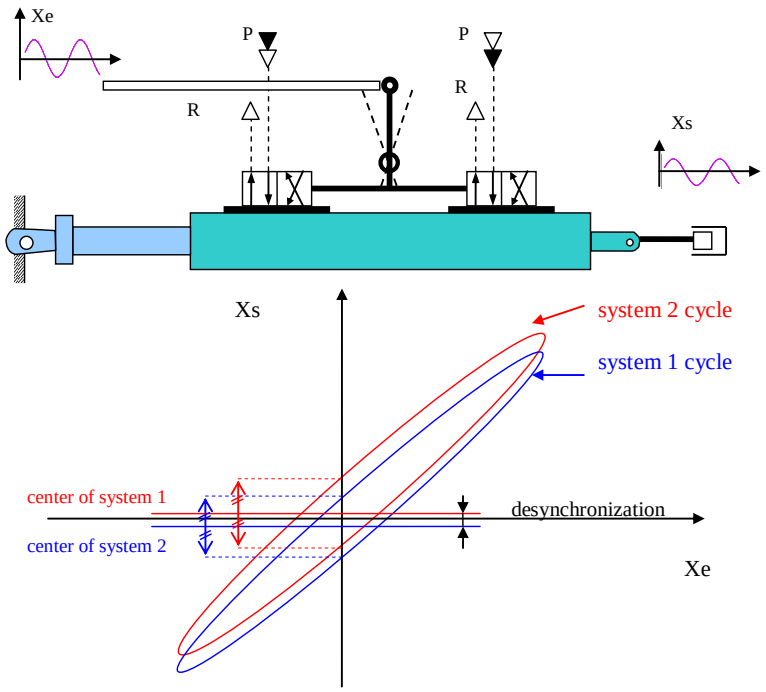

Figure 32: Cycle of each body of the servoactuator is plotted. Desynchronization is the difference between the two centres along Xs-axis.

3.3.1.4 - Input load

If the input load is high, pilot loads are important. Consequently, the accuracy of control and the comfort are degraded. A right value of the maximal force to move the input lever is 3N. According to Eurocopter experience, some real problems can appear for loads higher than 5N. The input load must not exceed this value, even in case of a hydraulic failure of one body for double bodies' servoactuator.

3.3.1.5 - Static constraints

Loads which are applied on the input lever are defined by FAR or JAR standards. They are assumed by the lever and the stops of the lever.

The limit of the loads on the end-stroke of the jack has to be 1.2 times the load developed by the servoactuator at nominal pressure and by the pilot.

3.3.1.6 - Closed-loop performance

a) Response of the servoactuator to low input displacement

The response of the servoactuator to low input displacement is a very important characteristic to guaranty the quality of the servoactuator. It is essential and has not to suffer of a deviation. Eurocopter experience is that the response of the servoactuator must meet the following criterion:

Input lever peak to peak magnitude: 0.35mm which implies that the servoactuator displacement is between 80% and 100% of the input lever

b) Frequency response

The gain and the phase have to be included in the frequency domain defined by:

- a low limit given by the frequency response of the existing servoactuator
- a high limit given by the frequency response of a servoactuator whose behaviour is known to present risks of instability for high frequencies.

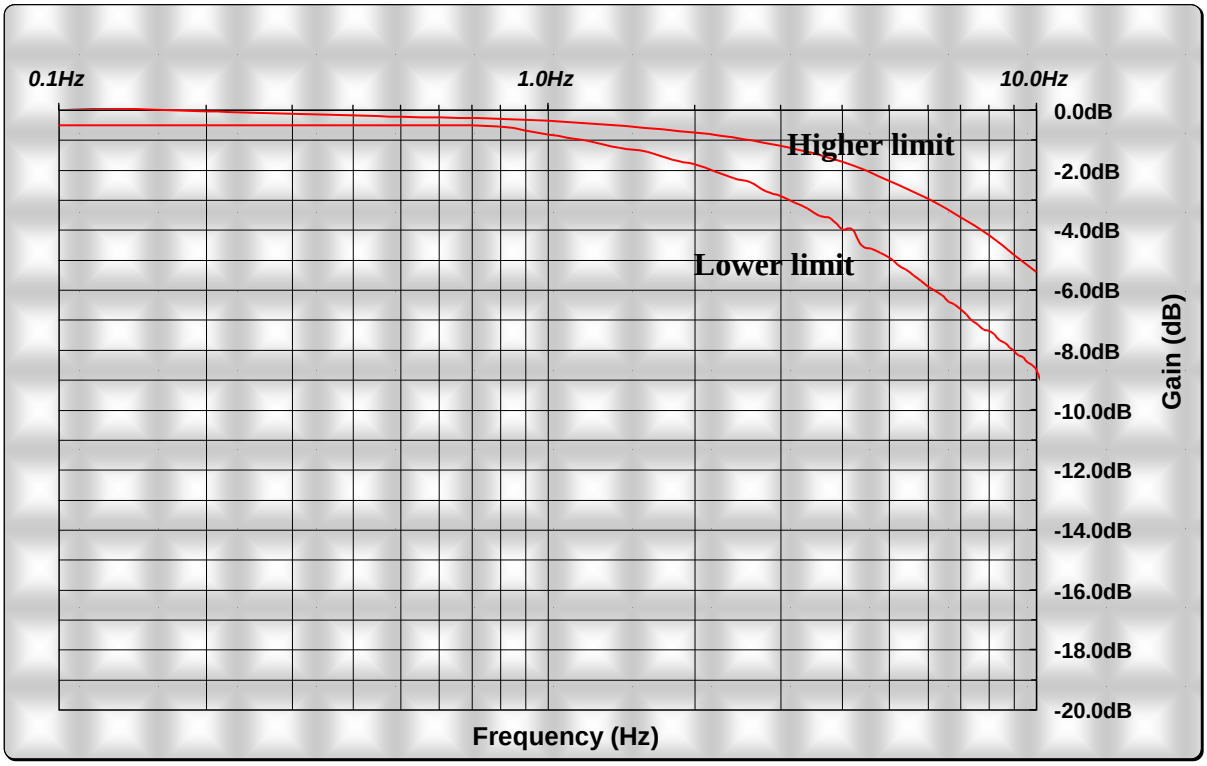

Figure 33: gabarit of the servoactuator magnitude. Lever input +/-1mm

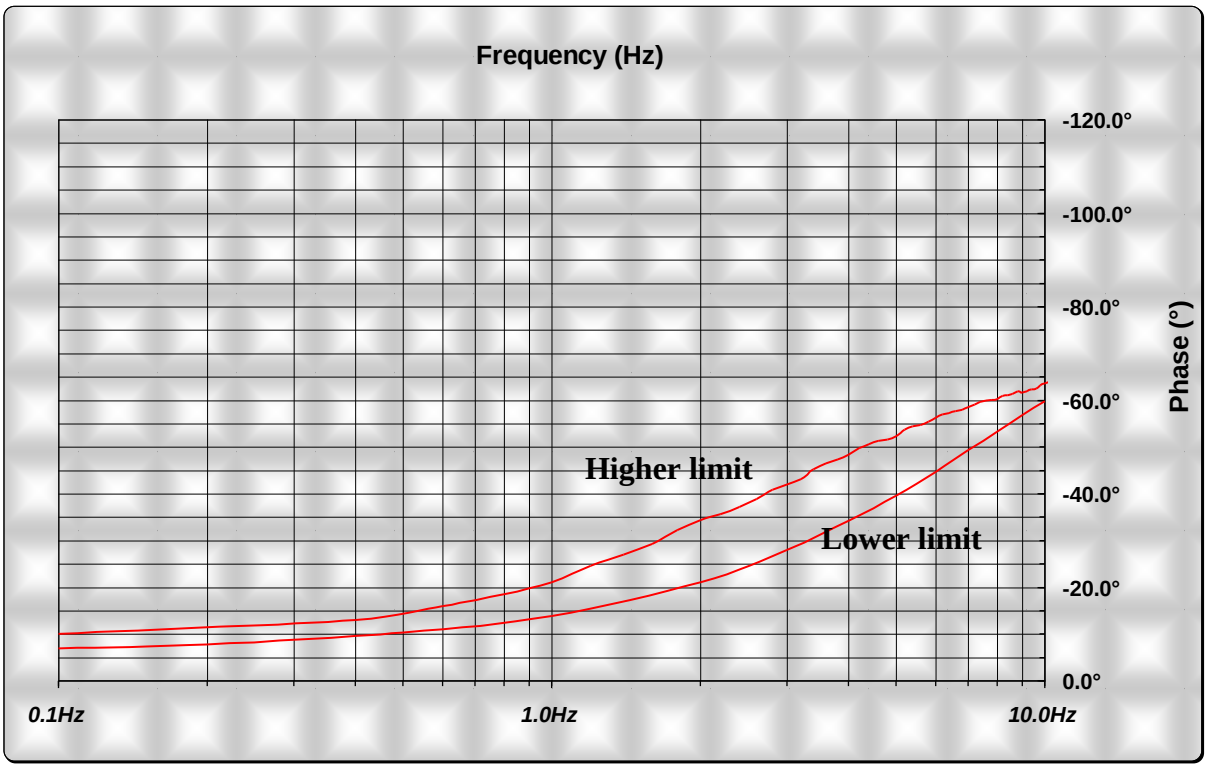

Figure 34: gabarit of the servoactuator phase. Lever input +/-1mm

c) Stability

No phenomenon of chatter or vibration, auto-maintained or maintained has to appear during the following tests:

- Large magnitude and rapid alternating movements
- Large magnitude and slow alternating movements
- small-amplitude rapid alternating movements
- small-amplitude slow alternating movements
- rapid movements, stopping on the mechanical stops

These tests are realized for the following conditions (AIR 8520):

- without load and with a nominal lock stiffness and two equivalent mass
- without load and with a third lock stiffness and a nominal equivalent mass
- with half of the maximal load and with a nominal lock stiffness and two equivalent mass
- with half of the maximal load and with a third lock stiffness and a nominal equivalent mass

3.3.1.7 - Mechanical aspect

a) Temperature range

The temperature range defined below is generally taken during the endurance test of the servoactuator:

- A time of 2% of the servoactuator life corresponding to a cold weather (-55°C)
- A time of 10% of the servoactuator life corresponding to a weather relatively cold (-45°C)
- A time of 78% of the servoactuator life for ambient temperature (25°C)
- A time of 10% of the servoactuator life corresponding to a weather relatively warm (90°C)

b) Load spectrum

Aerodynamic department provides the time percentage during which one the servoactuator is solicited by static loads and dynamic loads. Unfortunately, no values have been obtained.

c) Movements solicitation

The movements solicitation is defined by Eurocopter experience:

- 95 movements of the input lever of +/-15mm at 0.3Hz
- 260 movements of the input lever of +/-5mm at 0.5Hz
- 2000 movements of the input lever of +/-35mm at 1Hz

3.3.1.8 - Security/reliability

a) Protection filter

A hydraulic filter is needed to protect the servoactuator against particles' penetration. It has to be thin enough to guaranty a good protection and not too thin to avoid its clogging. Eurocopter found a good compromise with a filter at 100µm.

b) Leakages

i) External leakages

External leakages are inevitably present. Indeed, even if static seals may be oiltight, dynamic seals present a leakage. Criteria of the external leakages of the servoactuator are given by the quality department:

- 1 drop for 100 movements (full stroke) for a new device
- 1 drop for 25 movements (full stroke) for a device in use

In a security approach, these criteria are available because a seal leakage cannot increase rapidly in some hours and the leakage is weak enough not to have an influence on the hydraulic level in the tank.

ii) Internal leakages

Internal leakages are the leakages existing between supply line and return and caused by mechanisms which do not have seals. These leakages depend on the supply pressure and have to be minimised to avoid a too high flow consumption. For the servoactuator with two bodies under study, Eurocopter requires internal leakages to be less than 0.4l/min for a supply pressure of 35bar.

c) Input stroke

The input stroke is the displacement of the input lever in the two extreme cases where the valve slots are completely opened and where the velocity of the servoactuator is maximal. The displacement is limited by two stops. The velocity gain of the servoactuator is directly linked to the gain of the lever (ratio input motion/valve opening). The higher the gain is, the better dynamic performances of the servoactuator will be, but the less stability margin will be. The input stroke is chosen between +/- 3 or 4mm as for the existing servoactuator.

d) Locking mechanism

Blocking of a moving component has not to cause a lost of control. Three manners can meet this requirement:

- If the risk of blocking is judged extremely weak from statistics computation based on experience, definition and manufacturing quality, nothing to do is needed.

- If the risk of blocking is judged catastrophic (it means that it is superposed to another failure), each failure has to be detected during the flight or between two flights.
- There must be some means to survive this blocking and these means have to be testable (during the flight or between two flights) or the probability of double failure must be extremely weak.

3.3.1.9 - Fluid specifications

The mineral oil selected by Eurocopter for its qualities in temperature is the MIL-H-83282 oil. At 25°C, its viscous characteristics are: ρ=850kg/m^3 and υ=25cSt.

3.3.2 - New specifications

3.3.2.1 - Interchangeability/mixability

There are three main servoactuators on a helicopter. New servoactuators will be mounted on new and old helicopters and can replace one or more of the existing servoactuators. So, existing and new servoactuators can be mixed on the same helicopter. That is why the behaviour of the servoactuators must be sufficiently close.

It has been decided that the difference of speed between two servoactuators must be lower than 10mm/s for all the valve openings.

3.3.2.2 - Maximal flow rate

For the application, the supply pump has a constant flow rate of 6l/min. This flow provides the three main servoactuators. So, a security approach imposes that in all cases – and in particular in degraded cases (seizure) – the flow consumption of a servoactuator must be lower than 4l/min. Thus, the two others servoactuators still have 2l/min to move. If this criterion is not met, the required flow can be too high, the pump can be drained and so a hydraulic circuit can be lost.

3.3.3 - Summary of the specifications

The main specifications are summarized on Table 2.

Maximal speed	*$90<V_{max}<130mm/s$*
Maximal death stroke	*0.2mm*
Input load	*3N*
Interchangeability/mixability	*ΔV(existing/new)<10mm/s; for all valve openings*
Servoactuator load	*350daN in extension; 220daN in retraction*
Dynamic	*Input=0.35mm ; 80% of 0.35mm<ouptut<0.35mm*
desynchronization	*100µm*
Oil temperature	*-40°C to 110°C*
Protection filter	*100µm*
External leakages	*1drop/100movements*
Internal leakages	*0.4l/min*
Maximal flow rate	*4l/min*

Table 2: Summary of the main points of the specification

3.4 - Model based methodology for the valve pre-design

The valve must be designed to verify the servoactuator specification described previously. The valve behaviour is influenced by the slot width and the restriction diameter. The objective here is to compute some preliminary values of these two parameters. This pre-design requires the data of the fluid and of the servoactuator already fixed by the specifications and the implementation of some equations of the valve and of the servoactuator. Final results are given by a method developed as design sheets in the MS-Excel environment.

3.4.1 - Fixed parameters for the pre-design

a) Fluid

Fluid used is the MIL-H-83282 and for a pre-design, temperature is taken at 25°C. So, ρ=850kg/m^3 and υ=25cSt. Supply pressure is P=35bar and return R=0bar.

b) Valve

The overlap chosen for the main spool is 20µm. A positive overlap is described in the specification in order to filter the vibrations of the helicopter. The maximal dead stroke on the lever is specified at 0.1mm. The gain of the lever is 3, so with 20µm, the dead stroke due to the overlap is 60µm, which is lower than 100µm (see 2.4.3 - p51).

The overlap on the back-up spool is chosen bigger. Indeed, the limitation of the dead stroke is not applicable in this case because it is a degraded case. Furthermore, the diameter of the back-up spool is bigger than the one of the main spool. So, to limit the leakages, the overlap on the back-up spool is taken at 250µm (see 2.4.3 - p51).

The clearances on the main spool and the back-up spool are chosen as small as possible in order to decrease the leakages across the valve (no seals). The clearance on the main spool diameter is taken at 6µm. The one of the back-up spool is chosen a little bigger to decrease the cost and because of the associated big overlap. It is taken at 8µm.

The stroke of the main spool is chosen at +/-1mm which corresponds to the stroke of the existing valve. With a lever gain of 3 this makes a lever stroke is +/-3mm.

c) Jack

The supply pressure of the servoactuator is given by the pomp and is 35bar.

The specification of the servoactuator gives developed loads of 350daN in the extension side and of 220daN in the retraction side for two bodies operation. So, for one body only, the obtained loads are 175daN in extension and 110daN in retraction. With a pressure of 35bar, the area of the piston necessary is 500mm² for the big chamber and 317mm² for the small chamber.

	Big area piston (mm²)	*Small area piston (mm²)*
Upper body	*497.57*	*317*
Lower body	*506.53*	*317.06*

Table 3: Sections of the piston in each chamber

The seal loads in the jack are estimated on the existing servoactuator and supposed identical:

	Seal loads (daN)
Extension	*3*
Retraction	*6*

Table 4: Seal loads in the jack in extension and retraction.

3.4.2 - Equations for the pre-design

The two main parameters which have to be determined to meet the specifications, the valve slot width (l_f) and the restriction diameter (σ), influence the maximal speed and the maximal flow rate. Their computation is shown below.

a) Equation of the valve leakage flow rate

The leakage flow rate is the maximal flow rate when the valve main spool is seized at extreme opening and when the system is in the initial neutral position (Figure 35).

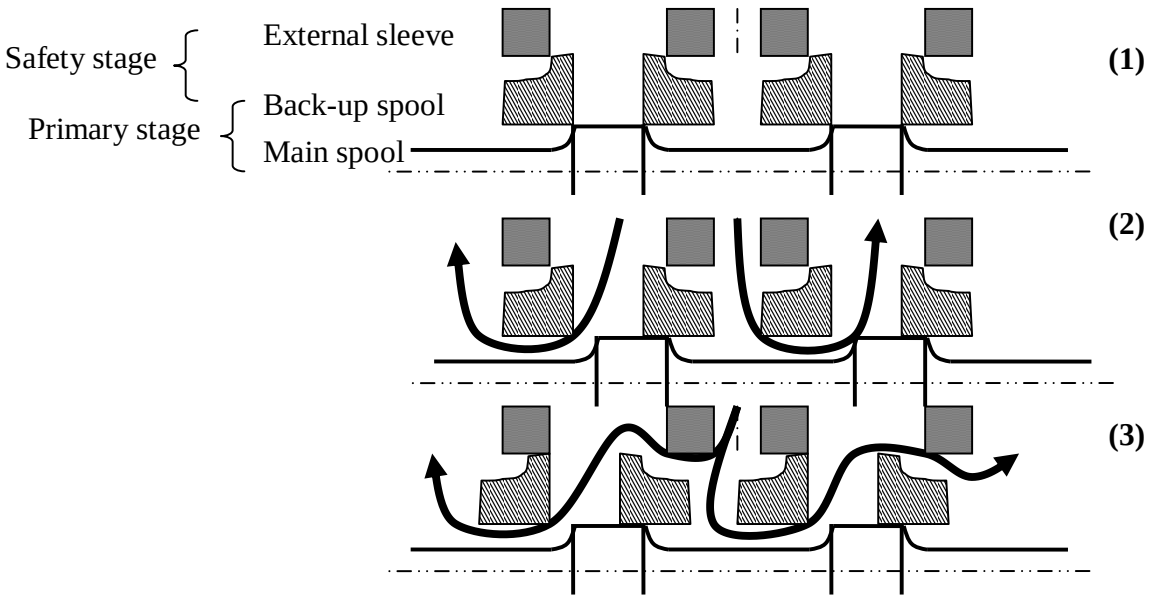

(1) lever at neutral position
(2) main spool at extreme opening
(3) lever at neutral position and main spool seized at extreme opening

Figure 35: Scheme of the valve spools for different operating modes

In order to compute the flow rate, an equivalent area is needed and obtained from the valve cross-flow areas defined in Figure 36, assuming flow coefficient are identical because of the large opening areas (turbulent flow, so C_q=$C_{q\infty}$) [6]):

- when the two sections S and S' are in series (for example in the Figure 36, S_1 is in series with S_2 and S_3 is in series with S_4), the equivalent area S_{eq} is such that:

$$\frac{1}{S_{eq}^2} = \frac{1}{S^2} + \frac{1}{S'^2} \tag{39}$$

- when the two sections S and S' are in parallel (for example in the Figure 36, S_1 and S_2 are in parallel with S_3 and S_4), the equivalent area S_{eq} is:

$$S_{eq} = S + S' \tag{40}$$

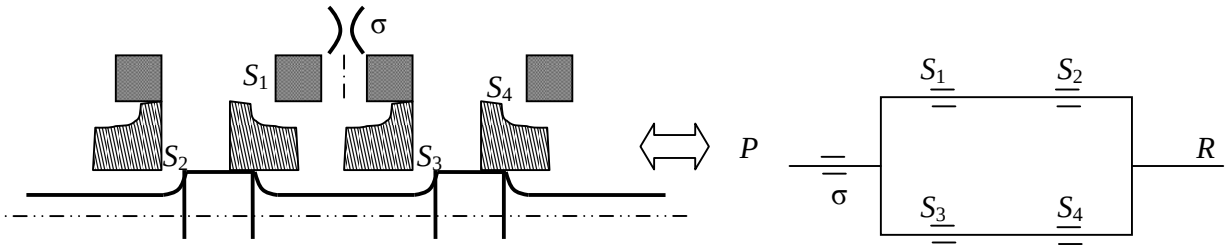

Figure 36: Valve sections in the seized case at extreme opening

The maximal flow rate in the seized case at extreme opening is given by:

$$Q_{\max-seized\ case} = n_f C_q S_{eq} \sqrt{\frac{2}{\rho}|P-R|} sign(P-R) \tag{41}$$

with:

S_{eq} Equivalent section of the system described in Figure 36

b) Equation of the servoactuator speeds

The speed must be computed in extension and in retraction. The scheme of the servoactuator in extension is given in Figure 37.

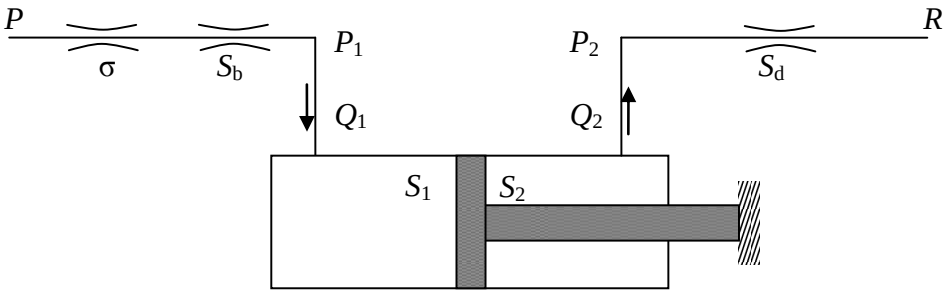

Figure 37: Functional diagram of a servoactuator bodies in extension

The flow rates for the edges b and d are computed with the following equations:

$$Q_1 = C_q \frac{1}{\sqrt{\frac{1}{\sigma^2} + \frac{1}{S_b^2}}} \sqrt{\frac{2}{\rho}(P - P_1)} \tag{42}$$

$$Q_2 = C_q S_d \sqrt{\frac{2}{\rho}(P_2 - R)} \tag{43}$$

where S_b and S_d are the valve opening sections associated to the edges b and d respectively.

The servoactuator speed equation is given by:

$$\dot{X}_{extension} = \frac{Q_1}{S_1} = \frac{Q_2}{S_2} \tag{44}$$

It is also possible to write the equilibrium equation:

$$P_1 S_1 = P_2 S_2 + 2F_{seal} \tag{45}$$

where

F_{seal} Seal load (N)

Then, there are 3 equations and 3 unknown parameters ($\dot{X}_{extension}$, Q_1 and Q_2). While resolving the system of equations, the servoactuator speed in extension $\dot{X}_{extension}$ is thus computed.

The computation of the speed in retraction is based on the same methodology. The scheme of the servoactuator in retraction is given in Figure 38. The flow rates for the edges a and c are computed as for the extension case while taking into account the valve opening sections associated to the edges a and c (S_a and S_c). The equilibrium equation for the retraction case is given by:

$$P_1 S_1 + 2F_{seal} = P_2 S_2 \tag{46}$$

The servoactuator speed in retraction $\dot{X}_{retraction}$ can thus be computed.

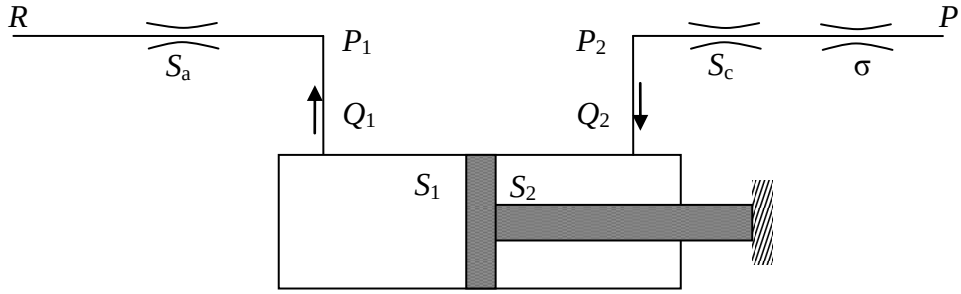

Figure 38: Functional diagram of a servoactuator in retraction

3.4.3 - Methodology and computation of the design parameters

The aim is to compute the slot width and the restriction diameter. These two parameters influence both the valve maximal flow rate and the servoactuator speed in the different configurations of use. It is not possible to compute the two parameters by solving a system of equations that describe all the configurations and that meet all the required specifications (because of an algebraic loop). An iterative method is proposed to solve the problem and is described in Figure 39:

- the slot width is fixed.
- the restriction diameter is computed by a solver to get a maximal flow rate of Q_{max} in seizure case at extreme opening.
- the servoactuator speeds are computed in extension and in retraction phases.
- The computed speeds are compared with the specifications. If the results are not correct, another slot width is selected and the computations are re-run. The minimal step on the width slot is 1/100 of millimeter. Otherwise, the desired pair of slot width and restriction diameter is kept as the solution. The speed targeted is the mean of the speed specification more or less 10% (the convergence criteria).

The computation gives for the pre-design an optimal operating point defined by a slot width ws_{init} and a restriction diameter $Ø_{init}$.

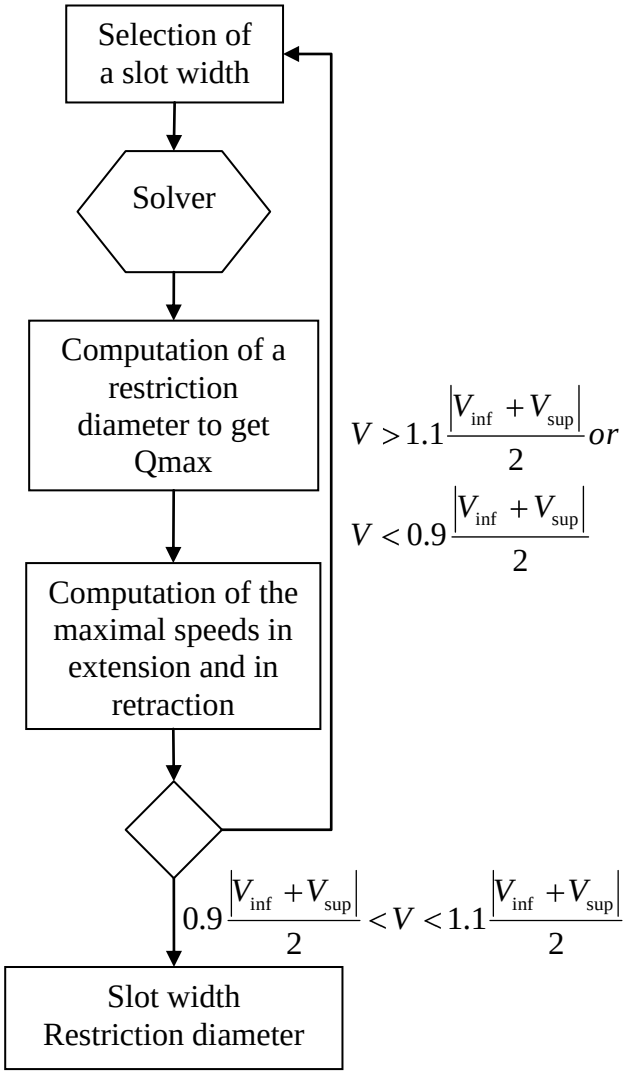

Figure 39: Functional diagram of the computation of the slot width and of the diameter restriction

3.5 - Asymptotic method for valve manufacturing

This section presents an approach to support valves manufacturing in the particular cases of production in few series. The performances of hydraulic valves are directly linked to the spool and sleeve geometry. The valve supply pressure is generally fixed by the application. The width (l_f) and the number (n_f) of the sleeve slots and the maximal spool stroke (X) are set by the required dynamics of the valve. The spool and the sleeve diameters are accuracy manufactured to guaranty a radial clearance in the specification (between 4 and 8µm). That is why each spool has its sleeve designed. The rounded edges of the spool are grind as sharp as possible since their manufacturing is difficult to manage. The orifices individual overlaps that define the dead stroke and the equilibrium pressure of the valve and that play an important role in the stabilization of the servoactuator must be defined with high

accuracy. Unlike the other parameters, they can be adjusted by an appropriate machining of the valve with resort to an adequate grinding of the spool flanks.

3.5.1 - Using the valve model to define the machining process

In order to determine the individual orifice overlaps, usual method consists mainly in the following steps:

- The three characteristics curves (pressure gain, flow gain and leakages, see 2.4.1 - b) are to be measured and constitute the starting point.
- An inverse method is computed in order to identify the unknown model parameters of the valve model from these experiments.
- The apparent overlap is extracted from the model and used to define the required spool flanks (Figure 25) grinding.

This method is efficient but gives redundant information and needs the three characteristic curves (top of the Figure 40). For this reason, a method that only uses the pressure gain curve is proposed. With one curve, less information will be obtained but only the equilibrium pressure and the dead stroke are looked for. The equilibrium pressure is obtained straight on the pressure gain curve. The problem is to compute the dead stroke. A method based on the asymptotic representation of the pressure gain curve is proposed at this aim (bottom of the Figure 40). The following sections will define the asymptotic pressure curve and show that this curve allows computing the dead stroke.

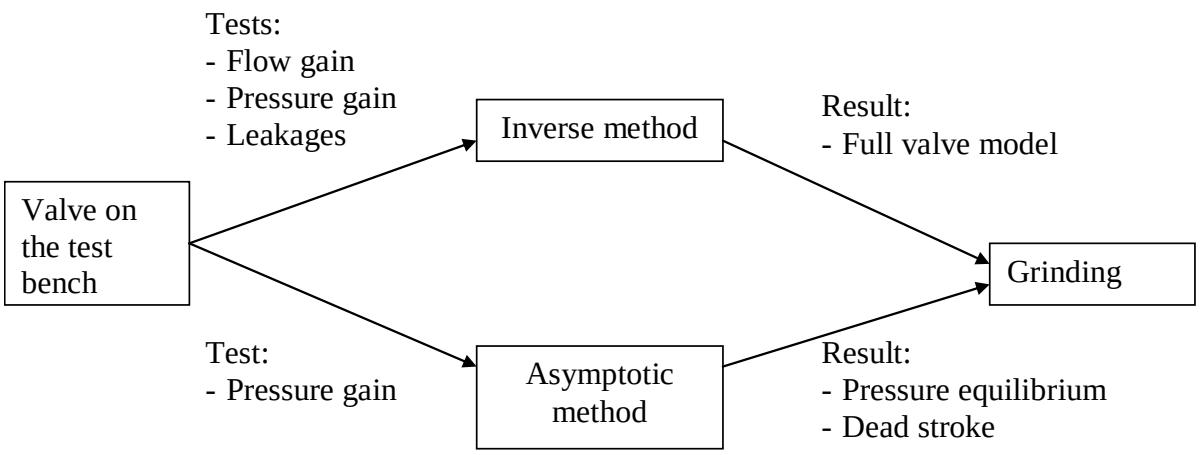

Figure 40: simulation methods of grinding

3.5.2 - Asymptotic pressure gain

The interest of the asymptotic treatment is to define a curve with few and well-defined points.

The pressures in each chamber are measured during the test. The asymptotic behaviour is clearly defined at high openings: pressures in chambers are given by the supply and return pressures. The transition between these two states can be approximated by a straight line for each chamber (Figure 41), each line being defined by two points. Consequently, only four parameters are needed to define an asymptotic representation of the pressure gain curve.

These parameters needed to define the asymptotic curves constitute a vector (equation 47) that is identified from the measured pressure gain curve using a curve-fitting approach.

$$X_{asym}^{t} = \begin{pmatrix} x_{11} & x_{21} & x_{12} & x_{22} \end{pmatrix} \tag{47}$$

The pressure equilibrium is taken from the cross point of the two asymptotic curves and is directly linked to the parameters vector. The abscissa corresponding to the pressure equilibrium is the hydraulic null which is the reference opening of the valve:

$$\begin{aligned} x_{eq} &= \frac{x_{22}x_{12} - x_{11}x_{21}}{x_{22} - x_{21} + x_{12} - x_{11}} \\ P_{eq} &= \frac{P}{x_{11} - x_{12}}(x_{eq} - x_{12}) \end{aligned} \tag{48}$$

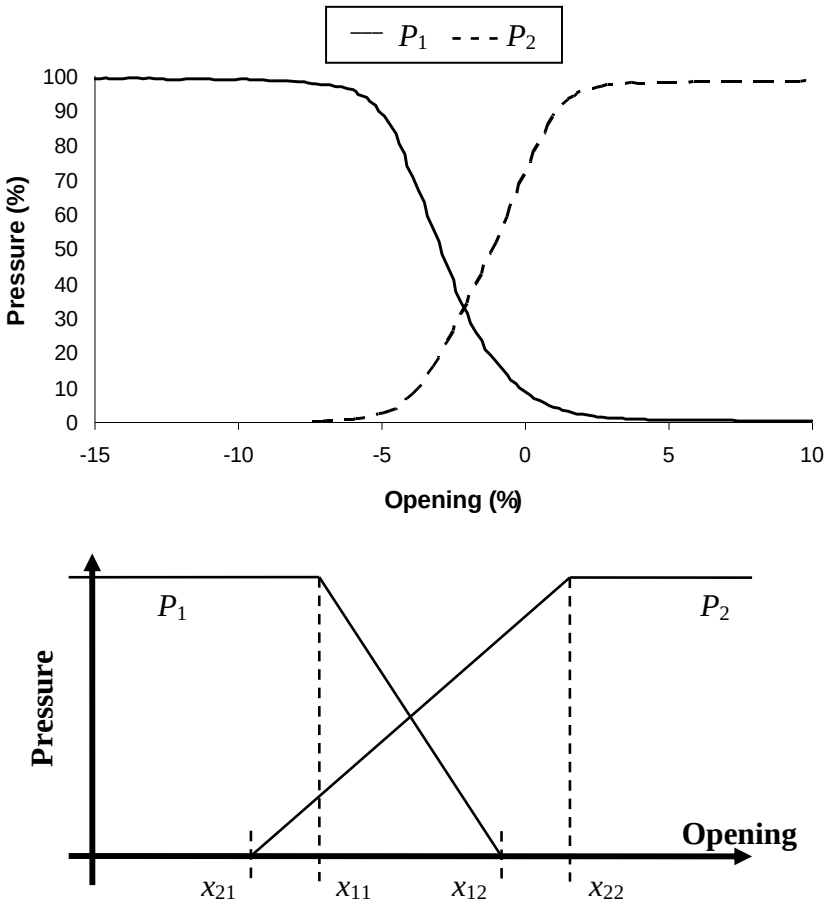

Figure 41: Asymptotic behaviour

A relation must now be found between the dead stroke and the parameters vector. The dead stroke results from the non linear combination of the apparent overlap of each edge. The problem thus consists in computing the apparent overlap from the parameters vector.

The scheme of the Figure 41 allows defining the position of one edge by one parameter of the X_{asym} vector:

- edge a is associated to x_{21}
- edge b is associated to x_{22}
- edge c is associated to x_{11}
- edge d is associated to x_{12}

This leads to the system of equations (49):

$$\begin{aligned} X_{a0app} + X_{b0app} &= f(x_{21} - x_{22}) \\ X_{c0app} + X_{d0app} &= f(x_{11} - x_{12}) \\ X_{c0app} + X_{b0app} &= f(x_{11} - x_{22}) \\ X_{a0app} + X_{d0app} &= f(x_{21} - x_{12}) \end{aligned} \tag{49}$$

where f represents the link between apparent overlaps of two edges and the distance between the two associated parameters of the X_{asym} vector. The function f is supposed identical for all the equations. A mathematic function cannot be established to describe this link because of the non-linearities and of the algebraic loop in the model (equations (21) to (30)). However, it is possible to analyse this link while studying the sensitivity of the overlap to the valve parameters.

3.5.3 - Link between the valve overlap and the valve parameters

To study the link, all the parameters are initially taken into account. The demonstration is achieved for the first equation of the system (49) and thus requires working only with a half-valve. It is proposed to look for:

$$x_{21} - x_{22} = f^{-1}(X_{a0app} + X_{b0app}) \tag{50}$$

with $X_{a0app} + X_{b0app} = X_{a0} + X_{b0} + 4r$ (relation 38)

Introducing the complete valve model yields:

$$x_{21} - x_{22} = f^{-1}(P, T, Cq, \lambda_t, n_f, l_f, c, r, X_{a0}, X_{b0}) \tag{51}$$

For given values of $X_{a0app} + X_{b0app}$, it is particularly important to evaluate the sensitivity of $x_{21} - x_{22}$ to the parameters $P, T, Cq, \lambda_t, n_f, l_f$ and c. For two test cases (test1 and test2), $x_{21} - x_{22}$ are computed with the model of Figure 28 for different sets of $P, T, Cq, \lambda_t, n_f, l_f$ and c. The influence of the parameters is measured by the maximal variation of $x_{21} - x_{22}$ (Table 5).

	Variation of parameters		$\Delta(x_{21}-x_{22})$
	Test 1	Test 2	Max (µm)
T (°C)	40	0	0.2
l_f (mm)	2	1	0.01
n_f (-)	1	4	0.001
P (bar)	35	100	0.1
Cq (-)	0.7	0.8	3.3
λ_t (-)	100	150	12
c (µm)	4	8	16

Table 5: Influence of the parameters on the asymptotic vector

It clearly appears that P, T, n_f and l_f have a very little influence on this maximal variation and that they can be removed from equation (51) that becomes:

$$x_{21} - x_{22} = f^{-1}(Cq, \lambda_t, c, r, X_{a0}, X_{b0}) \tag{52}$$

Moreover, the previous study also indicates that the influence of the three parameters c, C_q and λ_t is constant whatever $X_{a0app} + X_{b0app}$. Indeed, Figure 42 shows that the slopes of the curves $x_{21} - x_{22}$ versus $X_{a0app} + X_{b0app}$ are identical for any individual parameter change.

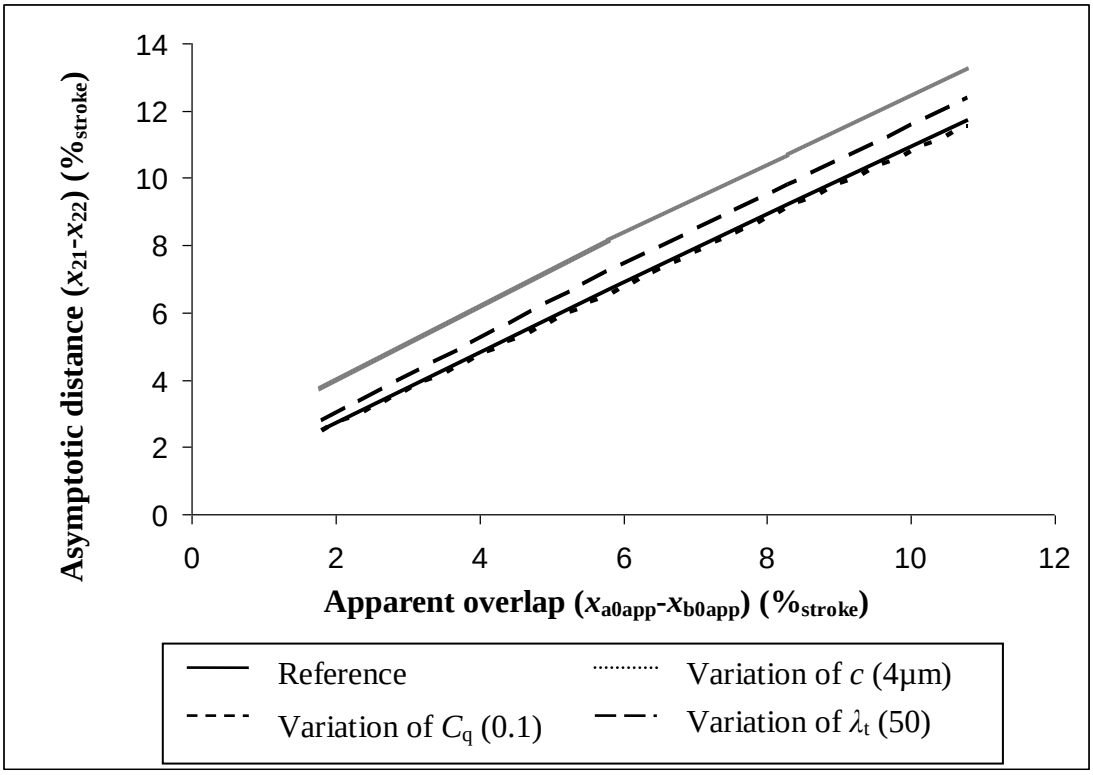

Figure 42: Asymptotic distance versus apparent overlap

Consequently, in order to remove the influence of c, C_q and λ_t from equation (52) and to obtain relation (50), it is suggested to introduce an offset. This offset is deduced from a pressure gain test combined with a single metrology. The metrology gives the real value of $X_{a0app} + X_{b0app}$. The test gives a pressure gain curve from which the asymptotic behaviour and consequently $x_{21} - x_{22}$ are computed. The offset is equal to the difference between these two values and finally:

$$x_{21} - x_{22} = f^{-1}(r, X_{a0}, X_{b0}) + offset \tag{53}$$

Then a model reduction is achieved by selecting only the influencing parameters to find a relation between $x_{21} - x_{22}$ and $X_{a0app} + X_{b0app}$.

3.5.4 - Parasitic influence of the rounded edge

The proposed method is tested on a case where the offset was computed for an effective overlap before grinding of 100µm and a rounded edge radius of 3µm. The Figure 43 shows the apparent overlap computed with the asymptotic method versus the apparent overlap during the grinding process (so for different values of effective overlaps). Moreover, as the rounded edges may vary during the grinding, the process has been assessed for different rounded edges radius (1 to 5µm) as also displayed by Figure 43.

Results obtained with the offset are not as good as expected since they are sensitive to the variation of the rounded edges radius. For a constant value of r = 3µm, the computed overlap is very close to the apparent overlap and the error is lower than 2µm. The error reaches 7µm for a variation of 2µm of the rounded edge radius.

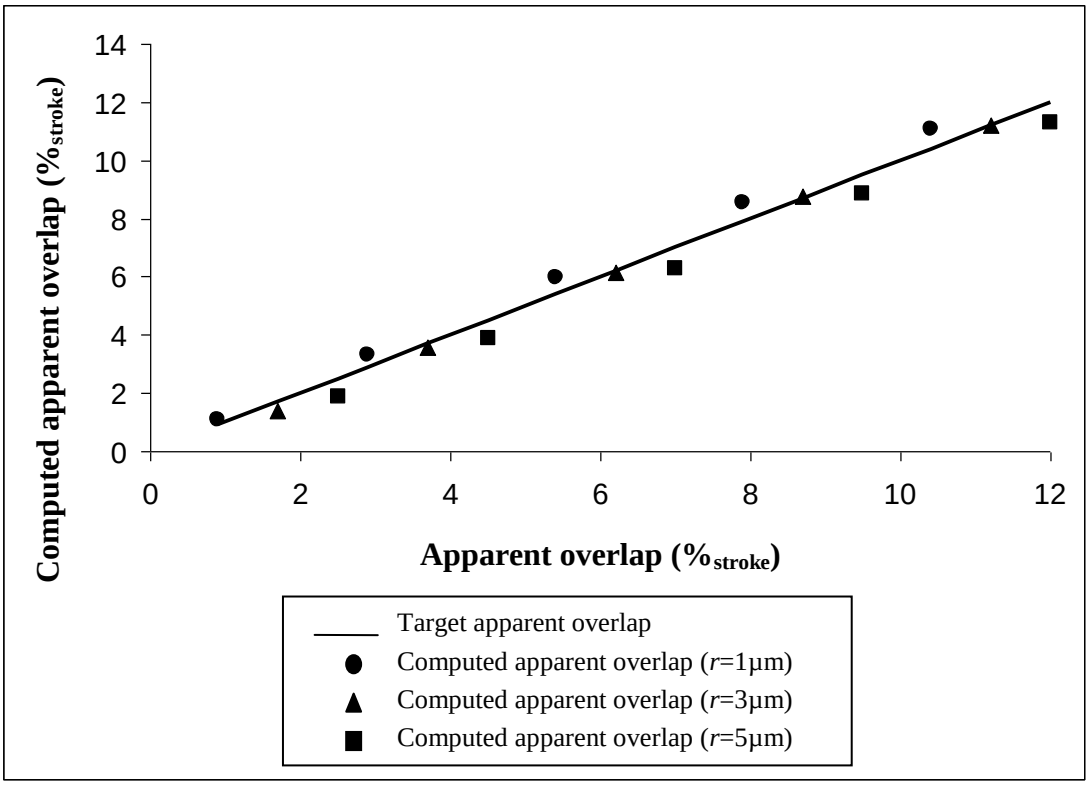

Figure 43: Computed overlap versus apparent overlap

Usually the specification of the valve grinding imposes sharp edges (eventually controlled with a microscope). The effect of rounded edge can so be assumed as negligible and the apparent overlap is identical to the effective overlap (equation 38). The asymptotic method with an initial offset becomes a very accurate tool to estimate the overlap of the valve (Figure 44).

On the Figure 44, the offset has been computed for a null rounded edge radius and an overlap of 100µm. Estimation of the computed overlap from the effective overlap is very accurate (error lower than 3µm).

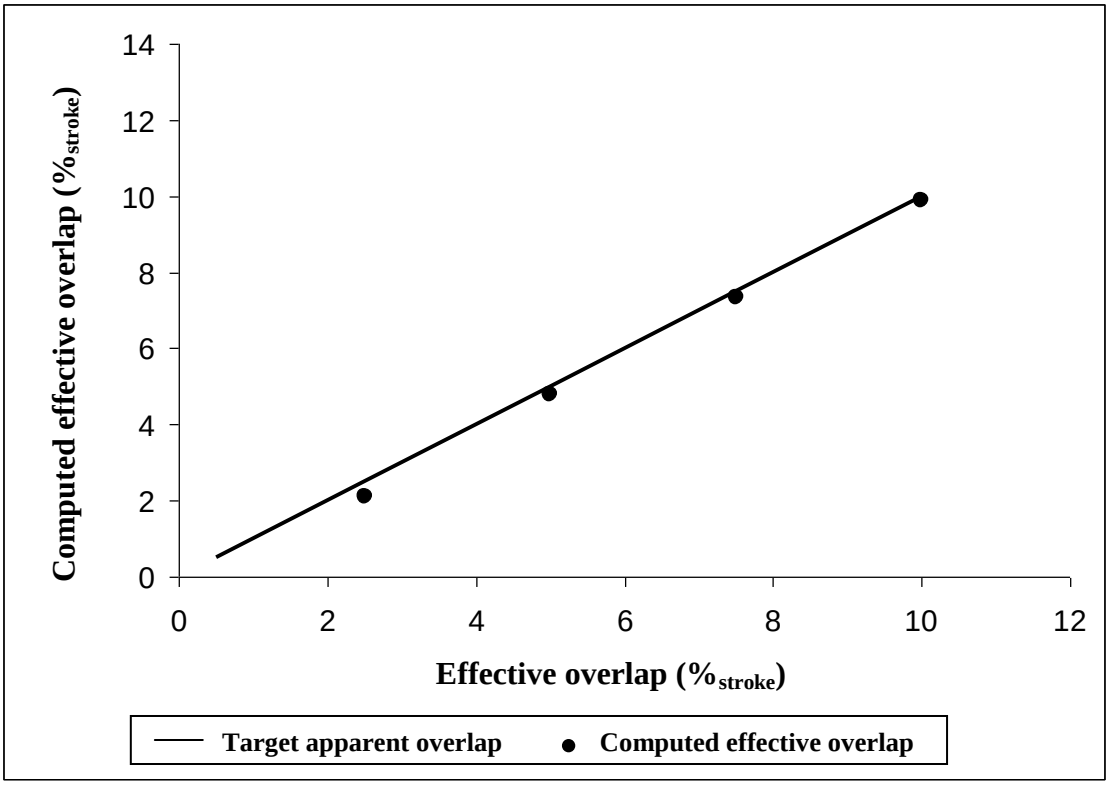

Figure 44: Computed overlap versus effective overlap

The proposed asymptotic method has been preliminary validated through a model based approach and under two assumptions: the maximal allowable error between estimated and effective overlaps is 5µm and the rounded edge radius is considered as null. The next section will deal with the experimental validation.

3.5.5 - Experimental validation

The proposed method has been tested on two valves sized for a typical nominal flow of 9l/min. The difference between the two valves consists in their width of slots. After each grinding, the valves overlaps have been measured by metrology and compared with overlaps computed by the asymptotic method. Results for the two valves called “100” and “200” are summarized respectively in the Table 6 and the Table 7. The first line (init) of these tables gives the offset required for the asymptotic method.

	Asymptotic method			Metrology	error
	Overlap ($\%_{stroke}$)	Overlap with offset ($\%_{stroke}$)	Quality (%)	($\%_{stroke}$)	($\%_{stroke}$)
0	13.2	13.2	93	11.8	Offset = 1.4
1	14.5	13.1	**89**	10.5	2.6
2	6.9	5.5	95	5.3	0.2

0: initial step (without grinding), 1: after grinding 1, 2: after grinding 2

Table 6: grinding of the valve 100

	Asymptotic method			Metrology	error
	Overlap ($\%_{stroke}$)	Overlap with offset ($\%_{stroke}$)	Quality (%)	($\%_{stroke}$)	($\%_{stroke}$)
0	11.6	11.6	95	11.7	Offset = 0.1
1	7.8	7.9	96	7.9	0
2	5.6	5.7	94	5.4	0.3

0: initial step (without grinding), 1: after grinding 1, 2: after grinding 2

Table 7: Grinding of the valve 200

Each line presents the results after one step of grinding. The columns two and three indicate the computed overlap without and with offset corrections. The quality of approximation given in the fourth column represents the relative root mean square error between the test pressure gain curve and the computed asymptote. Any value lower than 90% points out a problem in the process of the pressure gain curve. The fifth column is the overlap measured from metrology with a 3µm accuracy. Finally, the error of the asymptotic method is provided in column six.

$$Q = 1 - \sqrt{\frac{1}{n}\sum_{i=1}^{n}\left(f(x_i) - y_i\right)^2} \tag{54}$$

After the grinding step 1 of valve “100”, the error is important. However, the criterion of quality of approximation indicates clearly if the asymptote correctly represents the pressure gain measure (as confirmed by Figure 45). Oppositely, the results associated with the second grinding step are excellent. This also applies to the results relative to the valve “200” (Table 7).

Finally, these tests confirm the efficiency and accuracy of the asymptotic method developed above.

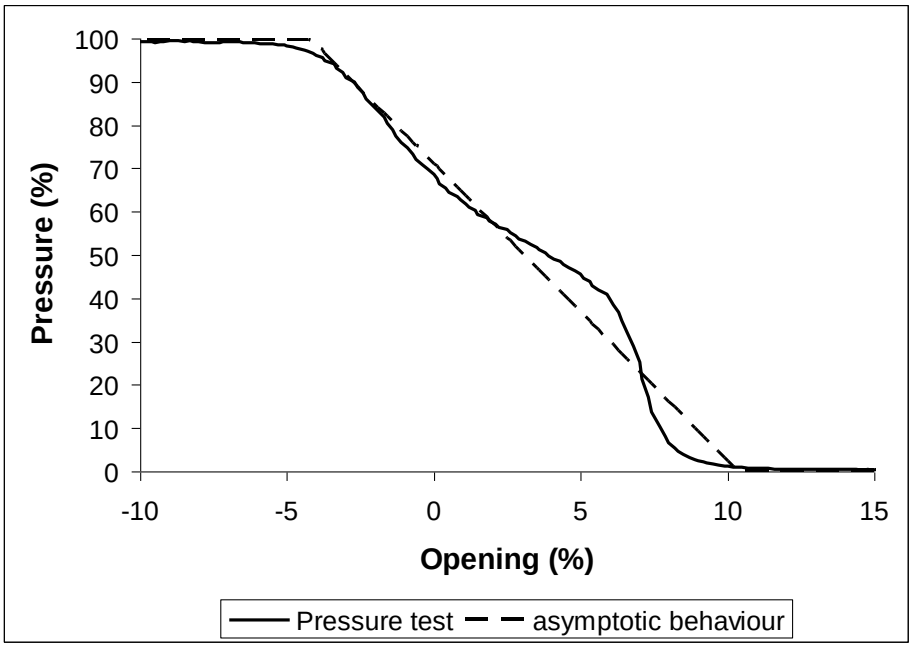

Figure 45: Computed compared with measured pressure on valve 100 (grinding 1)

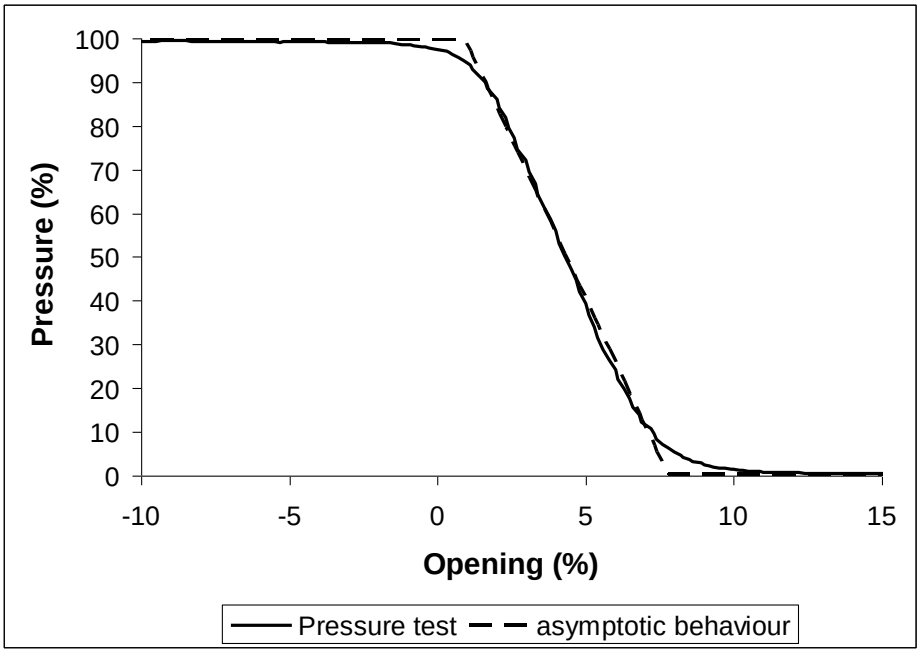

Figure 46: Computed compared with measured pressure on valve 200 (grinding 2)

This section aimed at defining a low-cost manufacturing process for hydraulic spool valves in the case of very low production rate. An original method has been proposed to manage the spool flanks grinding from the single measurement of the pressure gain curve in order to get the specified hydraulic characteristics. Identifying an asymptotic pressure gain curve allows extracting the effective geometry of the spool with accuracy. This provides directly the amount of spool valve grinding. After a model-based preliminary validation, the method has been fully validated for two different valves.

If the quality criterion is not meet, the dead stroke cannot be deduced from the asymptotic pressure gain. If this case happens, the solution is to perform a flow gain and to extract the dead stroke from the asymptotic flow gain.

3.6 - Design of the test bench

Two test benches are developed in order to test the valves and the servoactuator. The valve test bench has to perform the static response tests of the valve and the servoactuator test bench has to perform the performance and endurance tests.

Valve test bench

Static responses of the valve are the pressure gain, the flow gain and the leakages. The hydraulic schematic principle is presented in Figure 47 [31]. The test bench has been designed for the valve under study but also for valves of bigger servoactuators. The test environment is:

- fluid MIL-H-83282 [2]
- cleanliness class: 5 (standard NAS1638 [3])
- Fluid temperature: 20-40°C
- Air temperature : 15-35°C
- Atmospheric pressure: 860-1060hPa
- Relative humidity: 45-75%
- Nominal pressure: 200bar
- Nominal flow: 20l/min

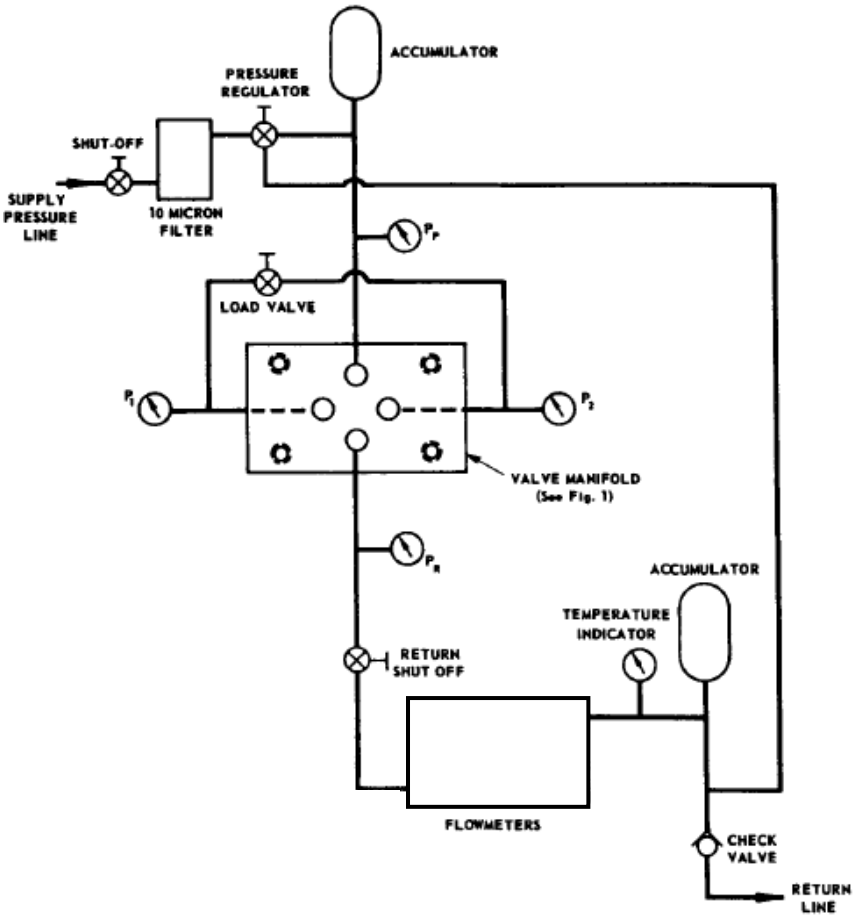

Figure 47: Static test hydraulic schematic [31]

The test bench can be controlled by the input lever at different speeds, different starting and end points and in the two ways.

Specification on the sensors is very important because of the accuracy required on the valve dimensions. A synthesis is shown on Table 8 and the test bench is shown in Figure 48.

- Pressure: 4 measurements are needed but 2 sensors are necessary since only 2 measurements are realised in the same time
- Flow: The range of measurement is too large to find one sensor that covers all the range with enough accuracy. That is why two flowmeters are necessary: one for the small flow rate and the other for higher flow rate. The selection of the flowmeter must be automatic and the small flowmeter must be protected against an accidental important flow.
- Load: the load sensor is vertical to avoid the parasite radial loads.
- Displacement: a high accuracy is necessary on the displacement. It is a difficult key point of the test bench.
- Temperature: The difference of temperature between fluid and test bench has to be controlled. So two sensors are needed but can be identical.

Pressure	*Supply pressure*	*Return pressure*	*Chamber 1*	*Chamber 2*
Accuracy (%)	*<0.3*	*<0.3*	*<0.3*	*<0.3*
Range of measurement (bar)	*0-250*	*0-250*	*0-250*	*0-250*
Flow	*Small flowmeter*		*Big flowmeter*	
Accuracy (%)	*<0.3*		*<0.3*	
Minimal flow rate (l/min)	*0.002*		*0.2*	
Maximal flow rate (l/min)	*0.2*		*40*	
Load	*Spool*			
Accuracy (N)	*<0.05*			
Minimal load (N)	*10*			
Displacement	*Spool*			
Accuracy (µm)	*<5*			
Maximal stroke (mm)	*>5*			
Temperature	*Temperature*			
Accuracy (°C)	*0.1*			
Range of measurement (°C)	*0-100*			

Table 8: Synthesis of the sensors specification

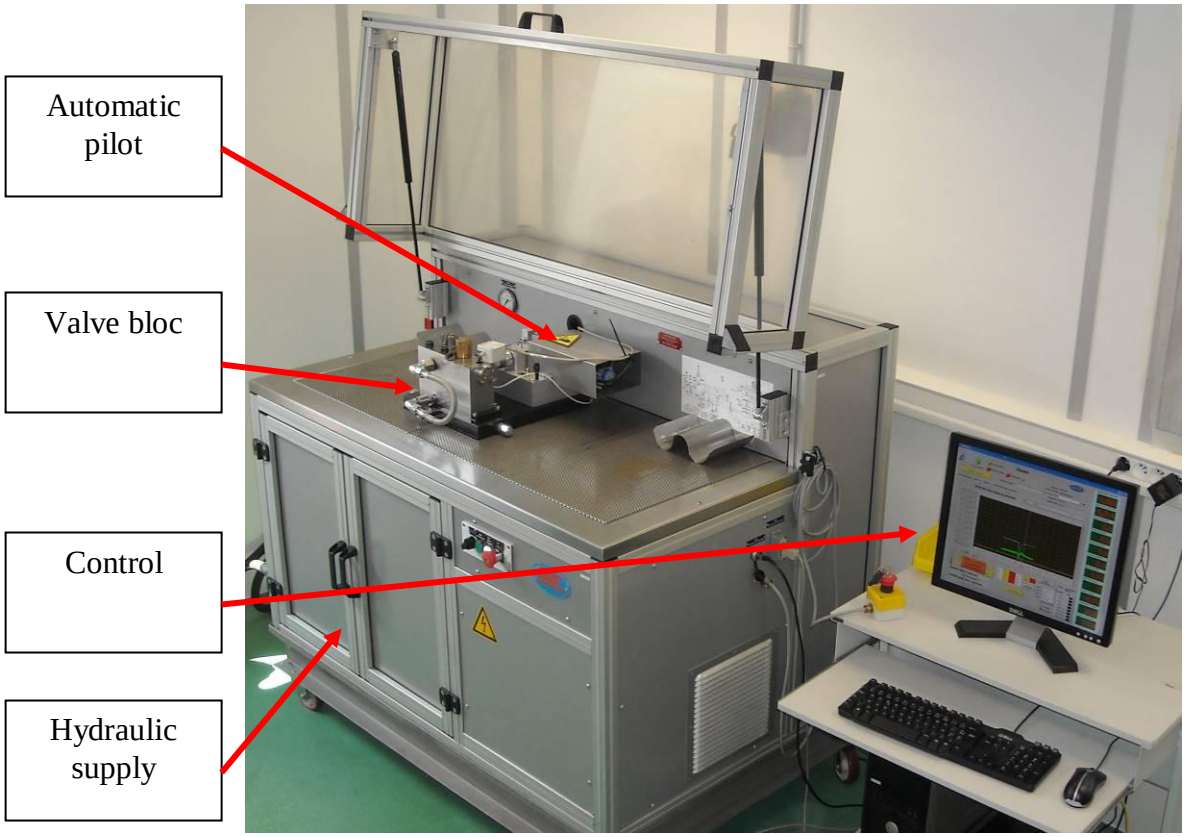

Figure 48: Valve test bench

Servoactuator test bench

The servoactuator test bench is shown in the Figure 49. Some parts can be seen:

- the load jack which has to reproduce the loads applied on the servoactuator (1)
- the lever jack which has to reproduce the displacement of the lever generated by the pilot and the automatic pilot (3)
- the servoactuator (2)
- the electric bay to control the test bench
- the pump
- the climate enclosure to reproduce the extreme temperatures that could be withstood by the servoactuator

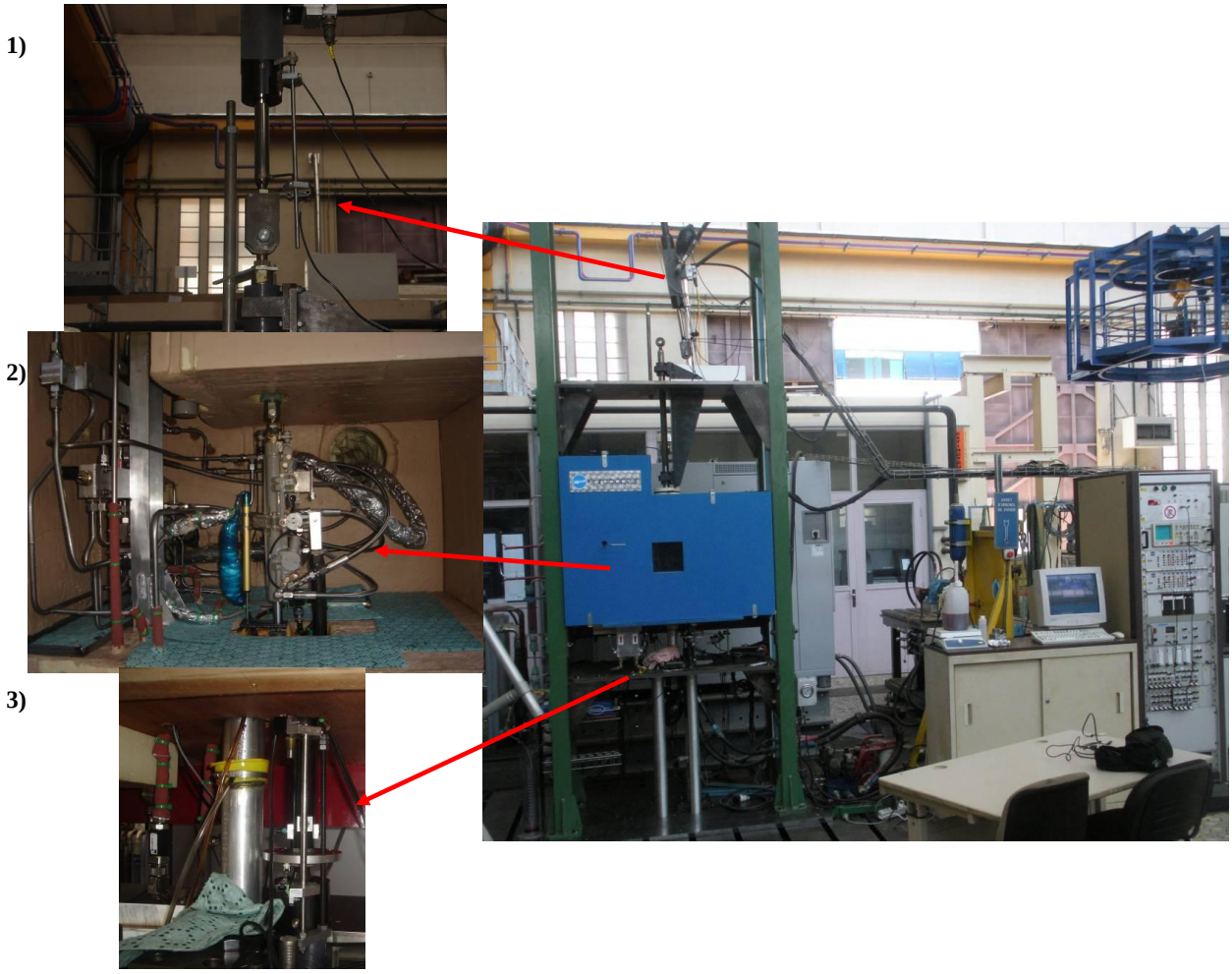

Figure 49: Servoactuator test bench; 1) Load jack; 2) Servoactuator to be tested; 3) Lever jack

3.7 - Conclusion

The pre-design of the valve as a function of the slot width and of the restriction diameter has been performed with a method based on the valve static model in this chapter. The restriction diameter has been added to the slot width as a design parameter to guaranty the new specification of maximal flow rate. These two parameters were defined by the pre-design and then the valve has been manufactured with an original process for grinding the spool flank to meet the requirements of manufacturing cost. The method has been developed using DOE treatment on the only pressure gain curve. During the thesis, two test benches: one for the valve and one for the servoactuator, have been developed, manufactured and set up to obtain experimental data for the valve and for the servoactuator.

Chapitre 4

Final design of the valve in the nominal mode

4.1 - French synthesis

Ce chapitre présente la conception finale du distributeur pour le mode nominal. Un premier jeu de paramètres est calculé à partir de l'analyse par plan d'expérience des tests sur des distributeurs fabriqués après le pré-design. De plus, ces essais sont utilisés pour recaler le modèle dynamique de distributeur et pour évaluer la mixabilité de la servocommande sur tout le domaine de fonctionnement. Il sera montré que cette exigence n'est pas atteinte et qu'une nouvelle géométrie de distributeur est nécessaire. Enfin, une approche à partir de modèles de simulation permet de définir le design final qui est validé par des essais expérimentaux sur le nouveau distributeur.

La première partie concerne le design du distributeur et le recalage du modèle de distributeur à partir des résultats expérimentaux.

L'étude préliminaire avec un modèle quasi-statique de distributeur a permis d'estimer les valeurs optimales des paramètres de design de distributeur : largeur de fente (l_f = 1,38mm) et diamètre de restriction (Ø 1.25mm). Ces résultats doivent maintenant être confirmés par des mesures. Des essais vont être effectués autour de ce point afin d'obtenir l'optimum réel (distributeur ayant les performances les plus proches du distributeur existant). Un domaine d'étude défini par différentes largeurs de fente et différents diamètres de restriction incluant le point optimal calculé est défini. Etant donné qu'un des objectifs concerne la réduction des coûts, le nombre de point dans le domaine d'étude sera limité. Une approche par plan d'expérience est donc utilisée.

Pour le plan d'expérience, la largeur de fente et le diamètre de restriction sont considérés comme des entrées. Les sorties sont quant à elles déterminées par les spécifications :

- Débit de fuite maximal. Le critère de sécurité donne un débit de fuite maximal de 4L/min. Le débit de fuite sera mesuré dans la configuration la plus pénalisante afin de bien obtenir un maximum.
- Vitesse maximale à vide en extension. La spécification donne une vitesse maximale à vide devant se trouver dans la zone [90 – 130mm/s] avec une préférence pour une vitesse de 106mm/s (vitesse la plus courante sur les servocommandes en utilisation). Cependant, les essais sont réalisés sur le banc

de test distributeur et mesure un débit et non une vitesse de servocommande. Une méthode réalisée sur tableur pour transformer la courbe de gain en débit en courbe de gain en vitesse d'une servocommande dissymétrique possédant le même distributeur symétrique a été développée (voir annexe1). La vitesse maximale est donc extraite de la courbe de gain en vitesse.

- Vitesse maximale à vide en rétraction. Identique à la configuration extension.
- Zone d'influence du distributeur. Il correspond au pourcentage de déplacement du tiroir nécessaire afin d'égaler la section d'ouverture du distributeur et la section de restriction. Le pourcentage minimal choisi est de 70%.

Afin de limiter le nombre de distributeurs à fabriquer et à tester, des largeurs de fente de 1mm et 2mm sont choisies, la largeur de 1,38mm étant bien inclue entre ces deux valeurs.

Trois valeurs de diamètres de restriction sont ensuite sélectionnées : 1,25, 1,2 et 1,15mm. Il est inutile de chercher des diamètres inférieurs à 1,15 mm. En effet, si l'on applique une différence de pression de 35bar entre les deux ports d'une restriction de diamètre 1,15mm, le débit mesuré est de 4L/min. Les pertes de charge dans le distributeur étant forcément plus importantes, 1,15mm représentent donc la limite basse. Seules trois restrictions ont donc été fabriquées au vu de l'approche faible coûts. Si jamais une restriction ayant un diamètre plus important parait intéressante au cours de l'étude, celle-ci sera fabriquée.

Etant donné le peu de facteurs (entrées), un plan factoriel complet a été choisi. Les résultats d'essais obtenus sont résumés dans la Table 10. L'outil d'analyse et d'optimisation du logiciel de plan d'expérience est ensuite utilisé pour déterminer les entrées qui seraient nécessaires afin de vérifier les spécifications sur toutes les sorties. Une courbe de désirabilité est ainsi obtenue en fonction des entrées. Le maximum de la courbe correspond à la configuration dite optimale.

En parallèle des essais et pour tenter de gagner du temps, un troisième distributeur correspondant à l'optimal du pré-design (c'est-à-dire une largeur de fente de 1,38mm) a été fabriqué. Les plans d'expériences donnent un optimal pour une largeur de fente de 1,34mm. De plus, la courbe de désirabilité est très plate autour de l'optimum. La réponse est donc robuste (vis-à-vis de la largeur de fente) et l'écart de réponses entre un distributeur ayant une largeur de fente de 1,38mm sera très peu différent d'un distributeur de largeur de fente de 1,34mm. Le troisième distributeur est donc utilisé pour valider le plan d'expérience. Les erreurs entre la prédiction et la mesure restant dans le bruit de mesure, le résultat est validé. Il a été jugé inutile de refaire un distributeur de largeur de fente 1,34mm. La configuration optimale conservée est donc un diamètre de restriction de 1,15mm et une largeur de fente de 1,38mm.

Cependant le critère de mixabilité n'a pas encore été vérifié. En effet, au début de l'étude, il a été supposé qu'il était suffisant de répondre aux spécifications de vitesses

maximales à vide en extension et en rétraction. Malheureusement, l'important critère de mixabilité n'est pas vérifié avec cette configuration. En effet, la Figure 53 montre que les deux vitesses pour la servocommande existante et celle développée ne correspondent que pour les pleines ouvertures (un écart supérieur à 10% entre les vitesses apparait pour des ouvertures moyennes). Il apparait qu'un orifice rectangulaire ne permet pas de satisfaire le critère de mixabilité sur toute la plage d'ouverture. En conséquence une largeur de fente variant avec l'ouverture sera donc essayée.

Un modèle dynamique de distributeur a été développé avec le logiciel AMESim en parallèle du pré-design. Le modèle a été construit à partir des plans du distributeur. Lorsque cela fut possible, les paramètres géométriques ont été contrôlés par métrologie. Le modèle ainsi obtenu est simulé afin d'obtenir une courbe de gain en débit qui est ensuite comparé aux résultats d'essai. Ceci a permis de reproduire la course morte simulée en jouant sur les rayons d'arrondi d'arête et les recouvrements (tout en restant dans les marges définies par les plans ou la métrologie). Le second recalage concerne la pente de la courbe et donc l'ajustement du coefficient de débit C_q. Le recalage est réalisé sur la courbe de gain en débit lors de l'essai avec le diamètre de restriction 1,15mm, puis il est vérifié en comparant les courbes de gain en débit avec le diamètre de restriction 1,25m. Ceci a permis de valider le modèle de distributeur. Un coefficient de débit général de 0,7 est approprié pour les orifices du distributeur.

La seconde partie concerne donc la définition et la validation de la nouvelle géométrie de distributeur.

Pour la nouvelle conception, le diamètre de restriction de 1,15mm est conservé puisqu'il garantit que quoiqu'il arrive, le débit de fuite sera inférieur à 4L/min. La première partie du chapitre a montré qu'une fente à largeur constante ne pouvait satisfaire le critère de mixabilité. Une fente à largeur variant avec l'ouverture est donc maintenant à l'étude pour satisfaire toutes les exigences. Au vu de la forme du gain en vitesse de la servocommande existante et du besoin de coût faible de fabrication, une fente de forme trapézoïdale est choisie.

Le modèle recalé de distributeur est maintenant utilisé comme point de départ. Il est tout d'abord modifié afin de prendre en compte la nouvelle géométrie de fente. Pour cela la section de passage de l'huile est calculé en fonction de :

- L'ouverture du tiroir. C'est la valeur d'entrée du modèle, donc la valeur n'est bien évidemment pas fixe.
- De la section maximale d'ouverture. Elle a été calculée de sorte qu'avec cette ouverture et le diamètre de restriction de 1,15mm, la vitesse de la servocommande voisine de 106mm/s en extension et en rétraction.
- De la petite base du trapèze (Figure 58). C'est le paramètre à définir par l'étude pour obtenir la bonne forme de gain en débit.

- De la course totale du tiroir. Elle est conservée par rapport à la configuration précédente.

Les résultats obtenus précédemment avec le modèle de distributeur étaient excellents (erreur entre la prédiction et les essais inférieure à 5% en tous points de fonctionnement). Le modèle sera donc un outil central pour la définition de la nouvelle géométrie. Les différentes étapes pour la sélection de la fente sont les suivantes :

- Implémentation de la nouvelle géométrie de fente dans le modèle.
- Simulation du gain en débit pour différentes bases de trapèze et obtention d'une réponse en fréquence de la servocommande prédite en intégrant le modèle de distributeur dans le modèle de servocommande.
- Sélection de la fente optimale avec un diamètre de restriction de 1,15mm.
- Fabrication du distributeur avec les fentes sélectionnées.
- Vérification et validation de la nouvelle conception grâce aux résultats d'essai sur banc.

L'outil de simulation dynamique permet de trouver aisément la petite base de trapèze optimale afin d'obtenir un comportement de la servocommande le plus proche possible du comportement existant. Les réponses en fréquence étant un critère prépondérant pour la mixabilité des servocommandes, celles-ci ont également été prédites avec la fente obtenue. Un seul distributeur est donc fabriqué puis passé sur banc d'essai. La Figure 64 montre la comparaison entre le gain en débit simulé et celui issu de mesures. L'écart entre les deux courbes étant extrêmement faible (erreur inférieure à 5%), la nouvelle fente est donc définitivement sélectionnée puisqu'elle satisfait également au critère de mixabilité.

La dernière partie du chapitre étend l'étude au comportement de la servocommande. Un premier prototype de servocommande a été fabriqué et est maintenant testé sur banc d'essai. Le premier critère à vérifier est la vitesse maximale à vide de la servocommande. Les résultats de vitesse étant quelque peu différents des vitesses prédites par le modèle de servocommande, il est nécessaire de le recaler (pressions réelles mesurées, course réelle du tiroir, poids réel de la servocommande).

Le modèle dynamique de servocommande était basé sur le modèle de distributeur, les plans de la servocommande et quelques données supposées. Une analyse métrologique sur le prototype a permis de connaître les dimensions exactes des pièces, ce qui a entrainé la modification de certaines valeurs du modèle. Après recalage, les vitesses maximales à vide entre le modèle et les mesures sont très proches.

La seconde chose à vérifier est la réponse harmonique de la servocommande. Les Figure 62 et Figure 63 montrent le comportement de la servocommande réelle comparé au comportement prédit par la simulation. Les courbes sont très proches ce qui prouve la qualité de la conception. En effet, la réponse harmonique était un des principaux critères de validation de la servocommande.

Enfin, pour des raisons marketing, Eurocopter a initié un certain nombre d'évolutions mineures sur les spécifications de la servocommande. Ainsi malgré le très faible impact de la vitesse maximale à vide sur le confort de pilotage, celle-ci a été revue à la hausse car c'est une performance importante dans l'esprit du client. Une nouvelle vitesse maximale a donc été imposée quitte à devoir revoir à la hausse le critère de consommation maximale. Afin de répondre à ce nouveau besoin, deux modifications ont été apportées :

- La course du levier a été augmentée de 15%. Le gain étant conservé, le diagramme de Bode n'est pas impacté.
- Un diamètre de restriction de 1,25mm a dorénavant été choisi produisant une consommation maximale potentielle à 4,7L/min.

En conclusion de ce chapitre, le design de distributeur en mode nominal a été présenté dans ce chapitre. Les paramètres de design du distributeur ont été calculés à partir d'une analyse par plan d'expérience basé sur des résultats expérimentaux. Un distributeur a ainsi été fabriqué et testé avec ce design. Celui-ci a été validé pour des valeurs extrêmes du domaine de fonctionnement et les résultats expérimentaux ont permis de recaler le modèle de distributeur. La mixabilité a ainsi pu être évaluée sur tout le domaine de fonctionnement. L'analyse a révélé que cette exigence n'était pas satisfaite. Une géométrie originale d'orifice de distribution a donc été proposée en utilisant une méthode basée sur un modèle de simulation. L'innovation a consisté en la définition de la bonne géométrie d'orifice pour assurer la spécification de mixabilité. Un orifice trapézoïdal a été sélectionné grâce au modèle de distributeur, a été fabriqué puis validé par des essais. La conception du distributeur a été finalement complètement validée grâce aux essais sur la servocommande. Toutes les spécifications ont été satisfaites. Afin de répondre à un nouveau besoin marketing, la conception a partiellement évolué du fait de la modification de certaines spécifications.

4.2 - Introduction

This chapter presents the final design of the valve in the nominal mode. A first set of design parameters are computed from the DOE analysis of the tests on the real valves manufactured using the pre-design results. Moreover these tests are used to update the dynamic valve model and to evaluate the mixability over the full operating domain. It will be shown that this requirement is not met and that a new valve geometry is needed. A model-based approach permits defining the final design that is validated by experimental tests on a new valve.

4.3 - Valve design and valve model update from experiments

4.3.1 - DOE-based selection of the rectangular slot and restriction diameter

4.3.1.1 - Methodology of design

The previous Excel study allowed estimating by computation an optimal operating point defined by a width of slot (l_f = 1.38mm) and a restriction diameter (Ø 1.25mm). This result must be checked by measurements. Real tests will be performed around this point in order to define the real optimal operating point. A study domain with different widths of slot and different restriction diameters including the computed operating point is defined. Since one of the objectives is to limit the numbers of tests, the number of points in the study domain will be limited. Then, an approach with a full factorial design is used in order to analyze the results.

For the DOE, the width of slot and the restriction diameter are considered as inputs. Concerning the outputs, they are determined by the specifications (§ 3.1 - p67):

- Maximal leakage flow rate (Q_{max})
- Maximal speed without load in extension (V_{ext})
- Maximal speed without load in retraction (V_{ret})
- Influence scale of the valve (%pilot)

Note: it is not possible to choose a maximal speed without load and the difference between the two speeds (V_{ext} - V_{ret}) instead of V_{ext} and V_{ret}. Indeed, outputs must have a monotonic behaviour in the domain of study and the speed difference has no reason to be monotonic. That is why V_{ext} and V_{ret} are selected.

4.3.1.2 - Inputs of the design of experiment

a) Width of slot

In order to limit the number of manufactured valves and tests, widths of 1mm and 2mm are chosen since the width of 1.38mm is included between these two values.

b) Restriction diameter

The most important parameter linked to the restriction diameter is the maximal leakage flow rate. The leakage flow rate measured for a restriction diameter of Ø 1.25mm under a loss of pressure of 35bar without other restriction is 4.7l/min (see Table 9). This is the maximal value that can be obtained since any other restriction will make this value decrease. The required leakage flow rate is 4l/min thus tests are repeated with lower diameter until the flow rate of 4l/min is obtained. Step of 0.05mm are chosen between two diameters because of a manufacturing interest. All results are given in Table 9. A restriction diameter of 1.15mm is the minimal value that can be considered. Indeed, it has been explained that the flow rate value can just be smaller with other restriction, which has a negative effect on the dynamics of the servoactuator and on the operating of the valve. In a limit case, if the diameter is very small, the valve would be unnecessary (see §4.3.1.3 - c). In a low cost view, the three restrictions of Table 9 will be tested. If a larger diameter becomes interesting, others tests will be performed.

Restriction diameter	***Flow rate with ΔP=35bar***
1.25mm	*4.7l/min*
1.20mm	*4.4l/min*
1.15mm	*4l/min*

Table 9: Flow rate measured for different restriction diameters under a loss of pressure of 35bar.

4.3.1.3 - Outputs of the design of experiment

a) Maximal leakage flow rate

The safety criterion gives a maximal flow rate of 4l/min. Two flow rates are measured during tests. The first one corresponds to the lever in the centred position with a seizure of the main spool in an extreme position (case (3) in Figure 50). The second one corresponds to the lever in extreme position with a seizure of the main spool in the other extreme position (case (4) in Figure 50).

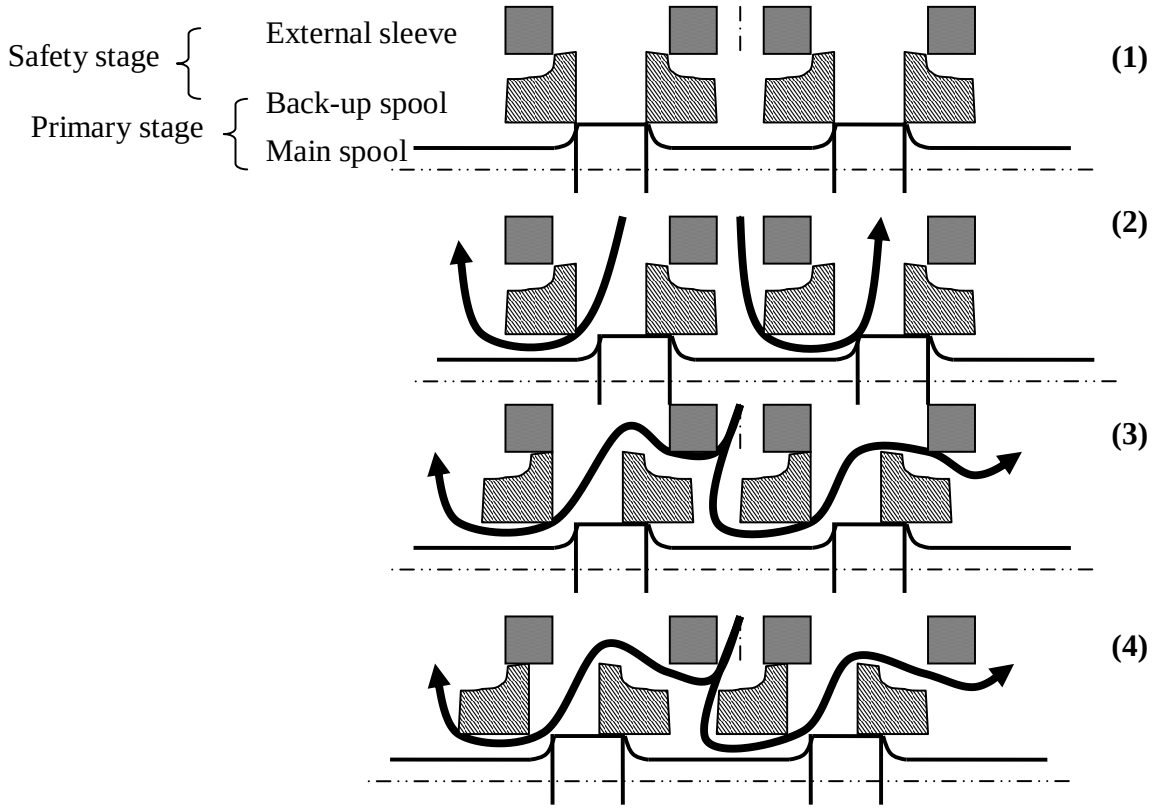

Figure 50: Scheme of the valve main and back-up spool in different configurations

In operation, if the seizure of the main spool appears in extreme position, the back-up spool will have low amplitude (the pilot receives a warning of the seizure). That is why the maximal leakage flow rate has been calculated as the mean of the two measured flow rates.

b) Maximal speed without load (in extension and retraction)

The specifications give a maximal speed without load of [90 – 130mm/s] with a preference for 106mm/s (the most often speed found in use). However, tests are performed on the valve test bench and the measurements give flow gains and not velocity. An Excel method to transform the flow gain of the symmetric valve into a speed gain of a dissymmetrical

servoactuator with the same symmetrical valve has been developed (see annex1). Maximal speed without load is directly extracted from the obtained speed gain curve.

c) Influence scale of the valve

It corresponds to the percentage of the main spool stroke needed to equal the section opened by the valve ($l_f.X_{max}$) and the section of the restriction (σ). The chosen minimal percentage is 70%. The case 100% corresponds to the case where the pilot completely controls the servoactuator with the valve. The value of %pilot is given by the formula:

$$\%pilot = \frac{\sigma}{l_f X_{max}} 100 \tag{55}$$

4.3.1.4 - Measurement results

As there are very few inputs (slot width and restriction diameter), the measurements that correspond to a full factorial design can be performed. The tests have been carried out and the results for the two valves with a slot width of 1mm and 2mm are:

- the measured leakage flow (see Table 10)
- the flow gain curves.

The flow gain measurements are used to update the valve model. The updating is not detailed here not to interrupt the design of experiment sequence. It is explained in §4.3.2 - p114.

With the Excel method validated by the updated valve dynamic model, the flow gain curves are transformed into speed gain curves. V_{ext} and V_{ret} are extracted from these curves (Table 10).

All results are summed up in Table 10.

Inputs (Factors)		**Outputs (Responses)**			
A	B	Y1	Y2	Y3	Y4
l_f (mm)	$Ø_{rest}$ (mm)	Q_{max} (l/min)	V_{ext} (mm/s)	V_{ret} (mm/s)	%pilot (%)
2	1.25	4.7	130	135	65
1	1.2	3.9	85	75	110
1	1.25	4	85	75	120
2	1.2	4.4	125	135	60
1	1.15	3.8	80	75	110
2	1.15	4	120	133	60

Table 10: Summary of the measurement results

a) Optimization

The optimization module in Design-Expert (§2.5.1 - p56) searches the inputs set that meets the required specifications on one output or on multiple outputs.

The optimization has been performed numerically on all the outputs with these constraints on the inputs:

- l_f may vary continuously in the range [1mm ; 2mm]
- $Ø_{rest}$ can take three discrete values {1.15mm; 1.2mm; 1.25mm}

and with the following specifications for the outputs:

- Q_{max} must be lower than 4l/min
- V_{ext} must be in the range [90mm/s; 130mm/s]
- V_{ret} must be in the range [90mm/s; 130mm/s]
- %pilot must be maximized and greater than 70% (if the %pilot is greater than 100%, the valve behaviour is the same than for a % pilot of 100%)

If all the specifications are fully required, the optimization is achieved with a desirability function equal to 1.

The optimization starts with a small value of a penalty function in a downhill simplex (Nelder-Mead) multi-dimensional pattern search [29] which converges at either a stationary point or a design space boundary. Convergence is achieved when the distance moved or objective function change is less than a $10e^{-6}$ ratio.

The optimization gives results showed on Figure 51. The optimal configuration found by the DOE analysis is a slot width of 1.34mm and a restriction diameter of 1.15mm (Figure 51). This configuration satisfies all the criteria on the outputs at their best and corresponds to the maximum of the desirability function. Furthermore the curves of desirability are plotted on Figure 52 functions of the slot width for the three restriction diameters. The curves show a null desirability for the restriction diameters of 1.2mm and 1.25mm. The maximum of desirability (0.872) is located on a point of the curve of null tangency. Consequently, this maximum is a little sensitive to small variations of the slot width. If the slot width varies in the range [1.3mm; 1.41mm], the desirability varies of less than 1.5%.

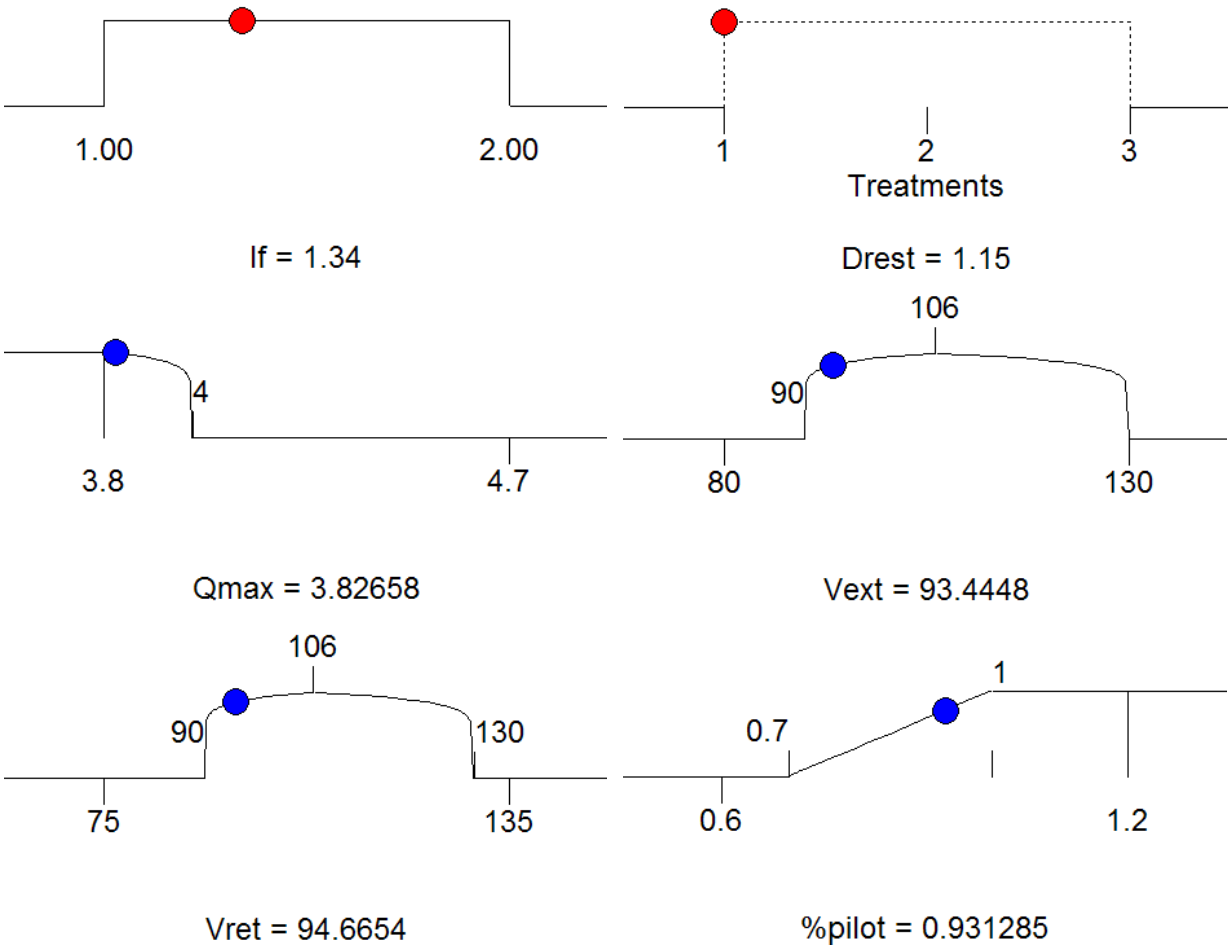

Figure 51: Results of the optimization for all inputs and outputs.

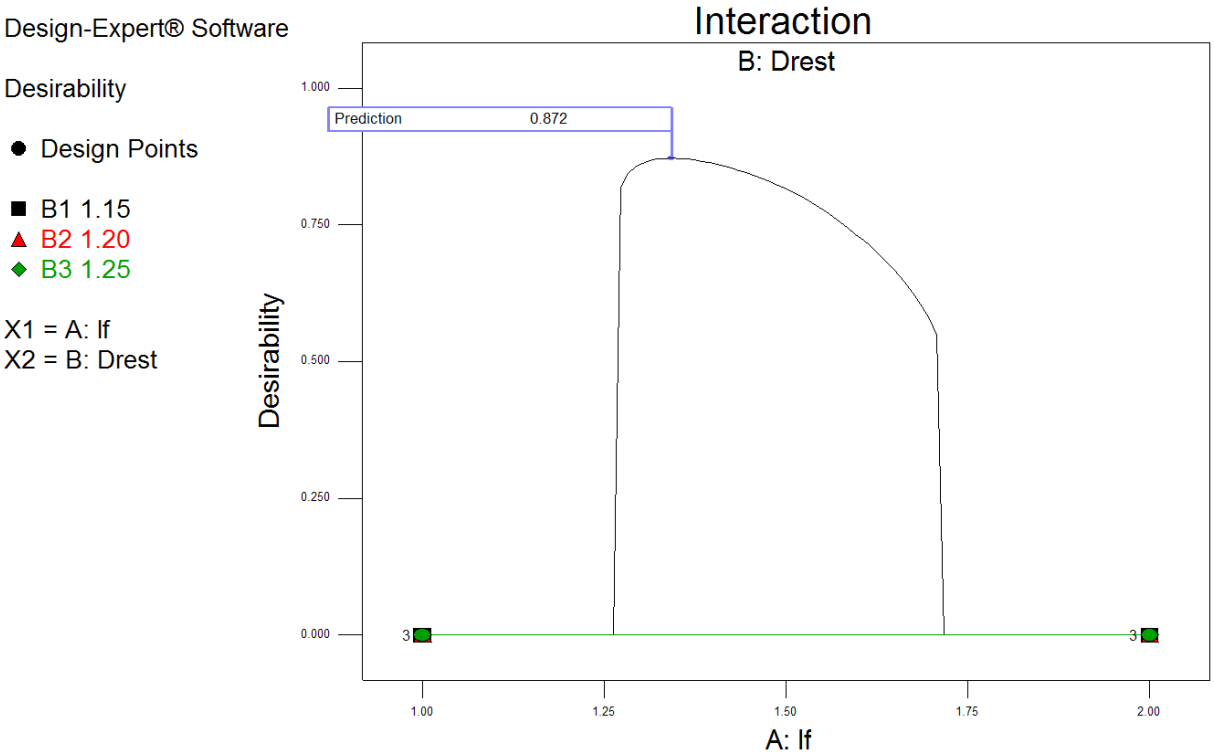

Figure 52: Curve of desirability functions of slot width and for three restriction diameters.

b) Validation of the solution obtained by the design of experiment analysis

In parallel of the tests of the two valves with a slot width of 1mm and 2mm, a third valve with a slot width of 1.38mm is manufactured because of the pre-design results. However, the test results for this third valve can be exploited since the design of experiment has shown that results for slot widths of 1.38mm and of 1.34mm are very close.

The test results for the valve with a slot width of 1.38mm and a restriction diameter of 1.15mm are:

- the measured leakage flow whose maximum is 3.9l/min
- the speed gain curve obtained from the flow measures. The curve gives V_{ext} = 101mm/s and V_{ret} = 99mm/s.

The results of the design of experiment analysis and of the valve test are compared in Table 11.

	Design of experiment prediction	*Test*	*error*
Q_{max} *(l/min)*	*3.8*	*3.9*	*2%*
V_{ext} *(mm/s)*	*95*	*101*	*6%*
V_{ret} *(mm/s)*	*97*	*99*	*2%*
%pilot (%)	*0.9*	*0.9*	*0%*

Table 11: Comparison between the prediction with design of experiment and test on the real valve (slot width of 1.38mm and restriction diameter of 1.15mm)

4.3.1.5 - Conclusion

The valve with a slot width of 1.38mm and a diameter restriction of 1.15mm is the optimum solution which verifies the defined criteria. However a criterion has not yet been checked: the mixability with an existing servoactuator. Indeed, at the beginning of the study, it has been thought that it was sufficient to meet the requirements for the maximal no-load speed in extension and in retraction. Unfortunately, this important criterion is not met with the obtained configuration. Indeed, Figure 53 shows that the two speed curves for the existing and developed servoactuators are only good for the maximal openings but that they are very different for the others openings (around 40% of opening). It appears that a rectangular slot does not permit to satisfy the mixability criterion. The curve of the existing servoactuator seems to indicate that the small openings correspond to a smaller slot width and that the maximal openings correspond to a larger slot width. Consequently, a slot with a width that varies with the opening will be designed and tested.

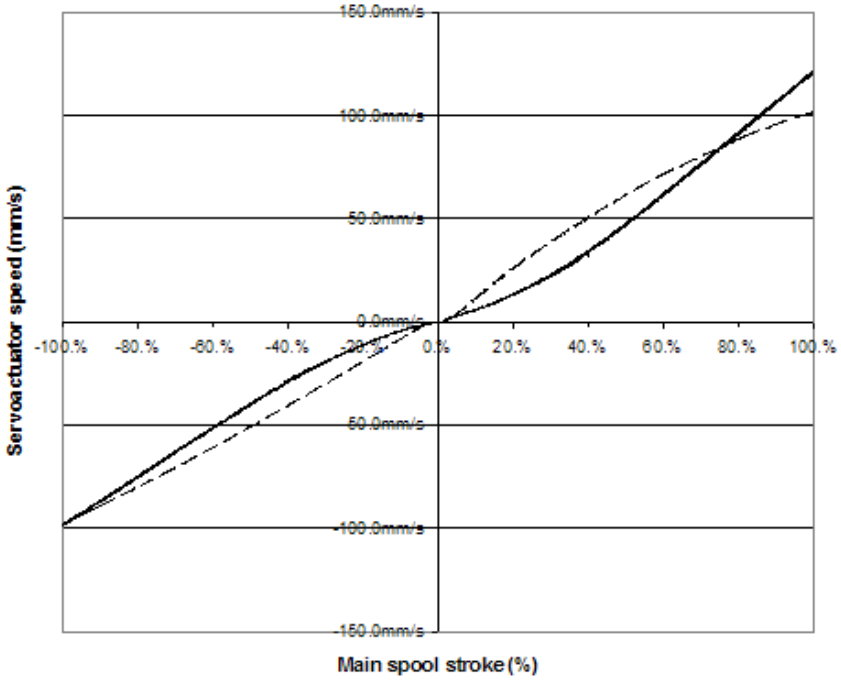

Figure 53: Speed gain of the existing servoactuator (full line) and the new servoactuator with a slot width of 1.38mm and a restriction diameter of 1.15mm (dotted line).

4.3.2 - Update of the dynamic valve model

4.3.2.1 - Methodology:

A dynamic model of the valve has been developed with AMESim in parallel of the pre-design Excel treatment. The model is based on the scheme of the valve with geometrical parameters. When possible, the geometrical parameters that are critical for the modelling (e.g. apparent overlaps) have been checked by metrology. The rounded edge radius cannot exceed 10µm (if superior, the associated edges are grinded).

The model obtained after metrology is simulated to get the flow gain curve and the results are compared to the measured flow gain curve around the null opening. It permits adjusting the dead stroke by modifying the rounded edge radius and the effective overlaps. This is the first update.

The second update concerns the slope of the flow gain as a function of the opening. The equation of flow is:

$$Q = Cq \cdot S \sqrt{\frac{2}{\rho}|\Delta P|} \tag{56}$$

The slope of this equation depends on the flow coefficient *C*q which is a not-known and not-under control parameter of the valve, even if experience and analysis gives 0.6 < *C*q <

1 [27]. The simulated and measured flow gain curves are once more used to update the *C*q such that the two slopes of the curves are identical.

4.3.2.2 - Results for the valve under study

The valve used for the update is one the two valves that have been tested. The update is performed on the valve with a slot width of 2mm and a restriction diameter of 1.15mm. The results are similar with the other valve. The metrology gives:

Edge a (return)	Edge b (supply)	Edge c (supply)	Edge d (return)
25µm	29µm	29µm	26µm

Table 12: Overlap on each edge given by the metrology

These data are implemented in the valve model obtained after metrology. The flow coefficient *C*q is assumed to be equal to 0.78. The simulation gives a first flow-gain curve. This flow gain curve is compared to the measured flow gain (Figure 54). The effective overlap and rounded edge radius are identified to get a better prediction of the dead stroke as explained previously. Furthermore, the flow coefficient is modified in order to adjust the slope of the flow gain. All results are given Table 13.

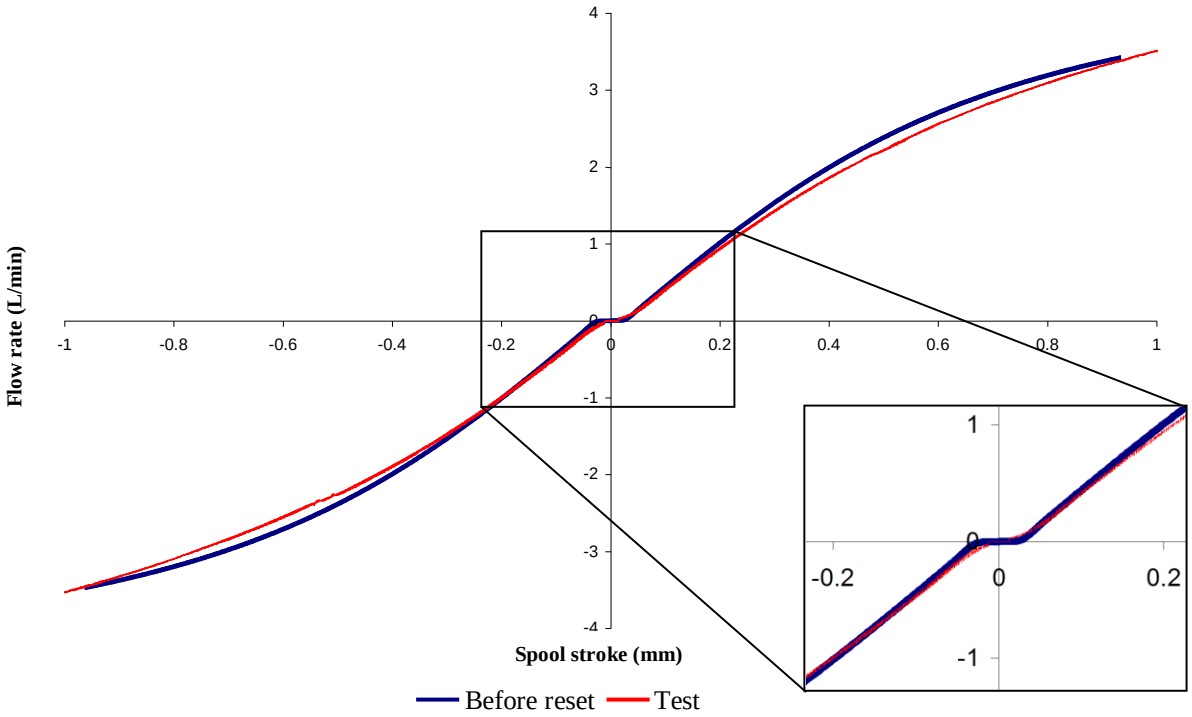

Figure 54: Comparison of the flow gain obtained with tests (red) and extracted from the simulation before update (blue). Width of slot l_f=2mm; restriction diameter Ø=1.15mm.

Edge a (return)				Edge b (supply)				Edge c (supply)				Edge d (return)			
X_{a0}	r	X_{app}	Cq	X_{b0}	r	X_{app}	Cq	X_{c0}	r	X_{app}	Cq	X_{d0}	r	X_{app}	Cq
µm	µm	µm	-	µm	µm	µm	-	µm	µm	µm	-	µm	µm	µm	-
10	**1**	12	0,7	**25**	**1**	27	0,7	**10**	**4**	18	0,7	**22**	**1**	24	0,7

X_{i0} : effective overlap of the edge i
r: rounded edge radius
X_{app} : apparent overlap

Table 13: Overlap and flow coefficient on each edge after update

Figure 55 shows the flow gains extracted from tests and simulation after update. No difference between the two curves is visible. Figure 56 (resp. Figure 57) shows the flow gains extracted from tests and simulation without other update for a different slot width (resp. restriction diameter). Results are excellent and validate the update for the valve model (the results are independent of the restriction diameter).

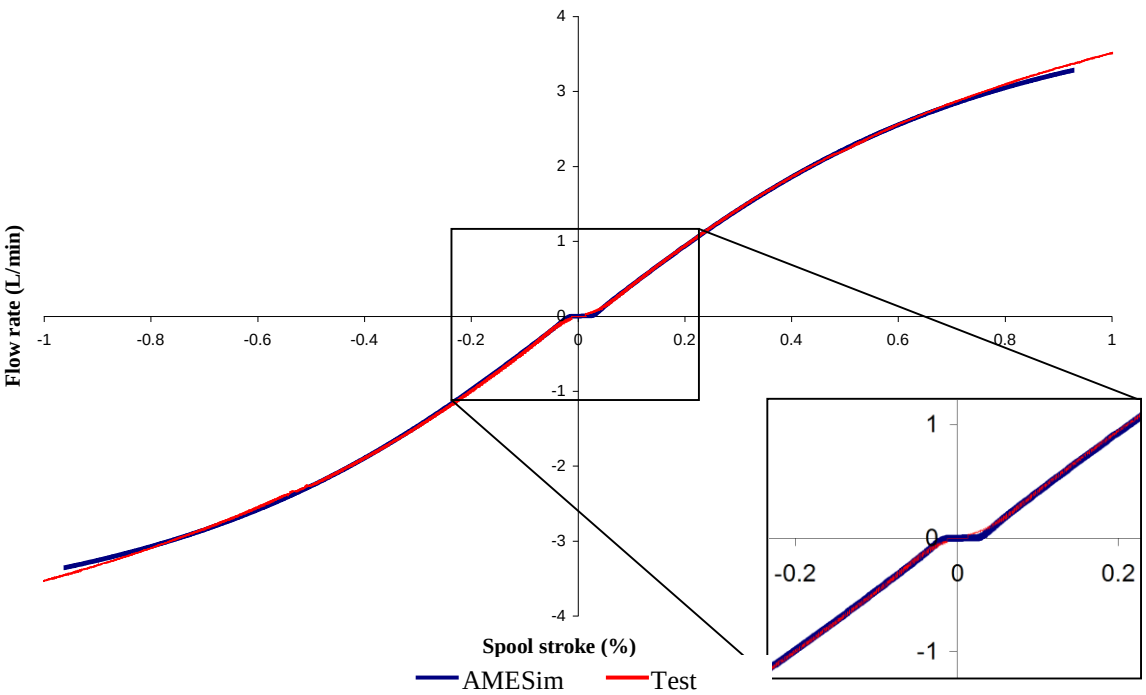

Figure 55: Comparison of the flow gain obtained with tests (red) and extracted from the simulation (blue). Width of slot l_f=2mm; restriction diameter Ø=1.15mm.

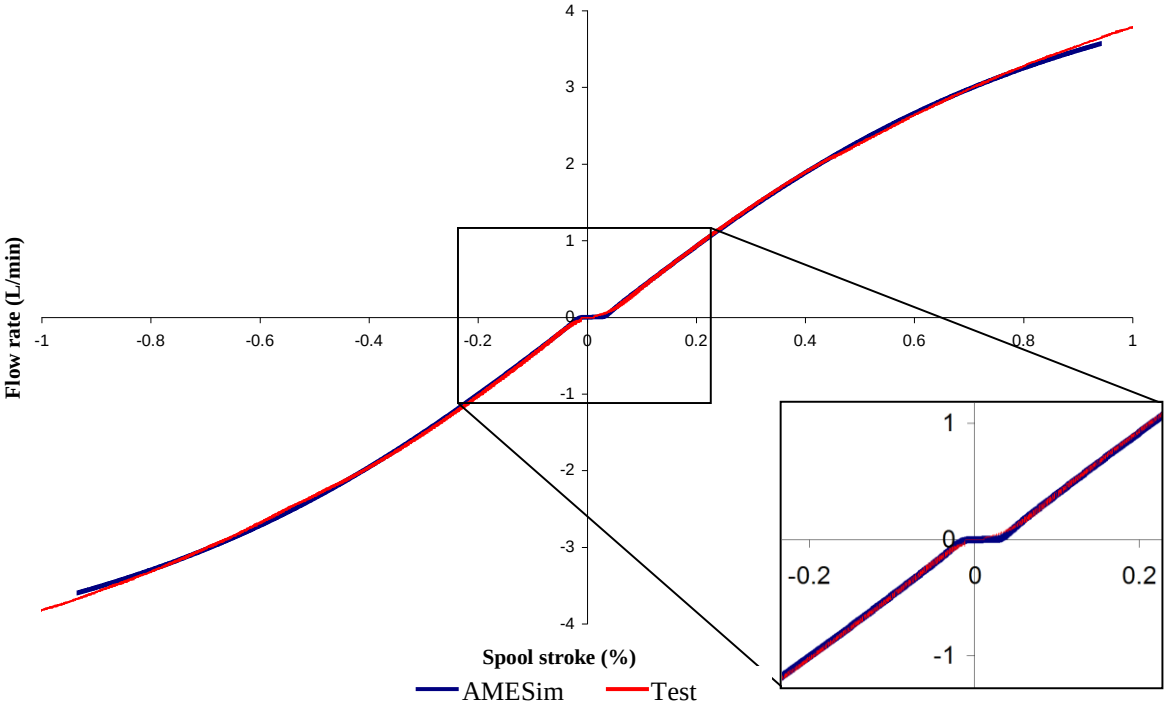

Figure 56: Comparison of the flow gain obtained with tests (red) and extracted from the simulation (blue). Width of slot l_f=2mm; restriction diameter Ø=1.25mm.

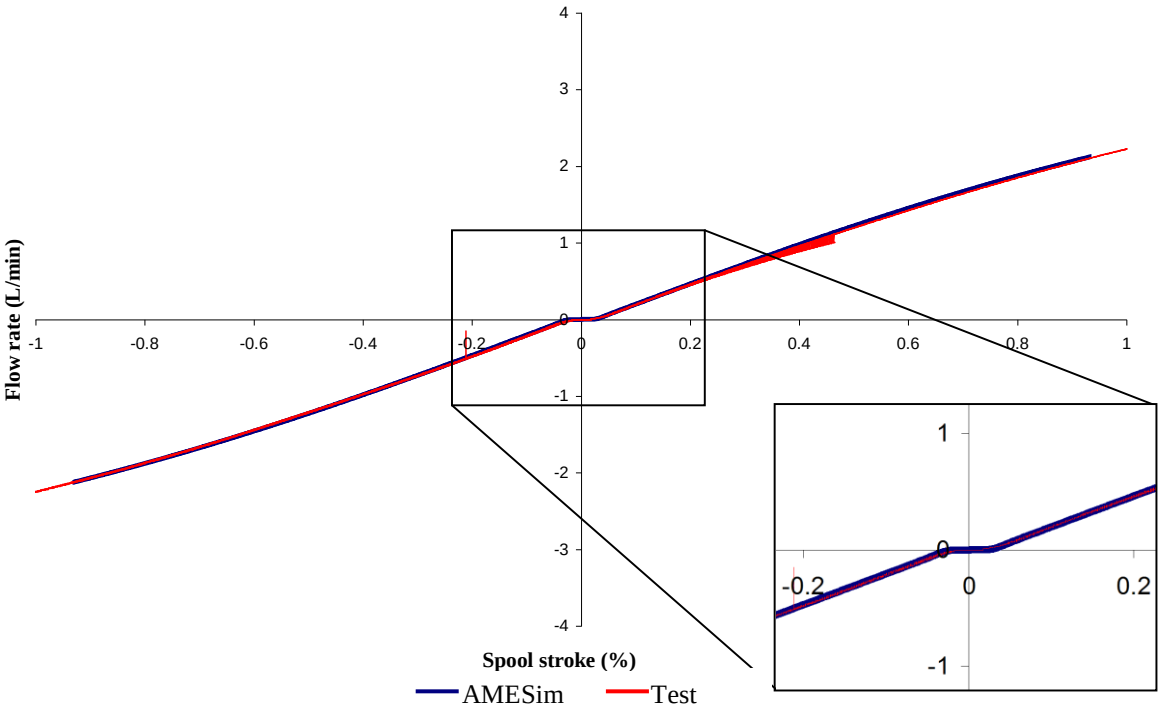

Figure 57: Comparison of the flow gain obtained with tests (red) and extracted from the simulation (blue). Width of slot lf=1mm; restriction diameter 1.15mm.

4.3.2.3 - Conclusion

An update on the flow coefficient of the valve dynamic model has been performed and validated for the computation domain. Concerning the death stroke update, a metrology on the flank overlaps is a good starting point. Then overlaps have to be adjusted in the model to minimize death stroke error between the tested and simulated flow gain. The update must be done for each valve.

A flow coefficient C_q=0.7 is appropriated for such valve geometry (error lower than 5% between simulation and measures in all cases). Consequently this value of flow coefficient will be used for the Excel treatment (from flow gain to speed gain).

4.4 - Valve design update for mixability over the full operating domain

For the new design, the diameter restriction of 1.15mm is kept since it guaranties a maximal leakage flow rate of 4l/min (see Table 9). It has been shown that slots with a constant width are not satisfying and that an original geometry with a changing slot width (function of the opening) seems more satisfying to obtain a similar speed gain between existing and developed servoactuators [24]. A trapezoidal slot is chosen for manufacturing easiness.

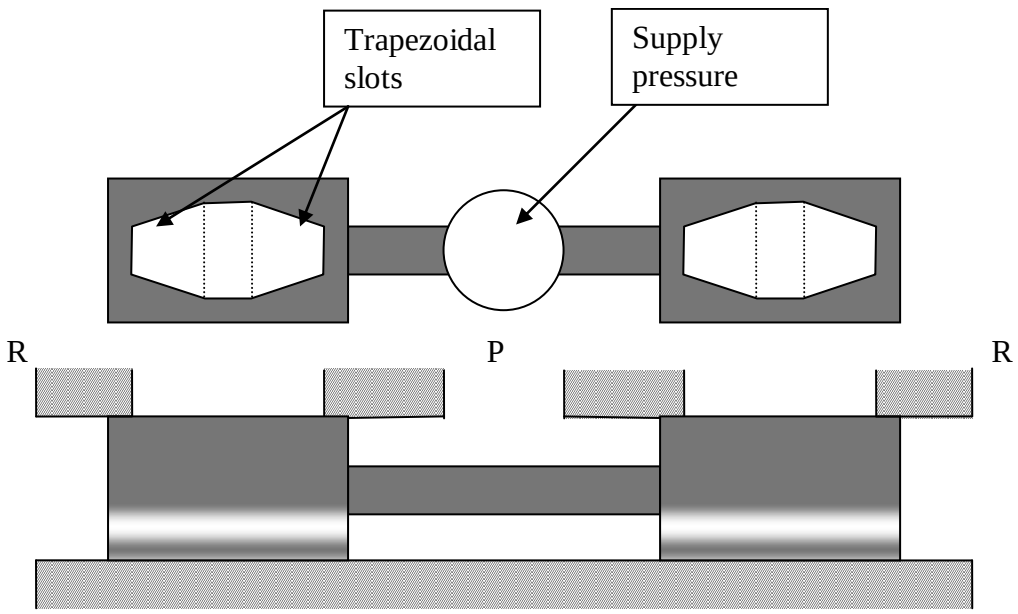

Figure 58: Scheme of the trapezoidal slots

4.4.1 - From rectangular to trapezoidal valve slot

The update model of valve defined in section 4.3.2 - p114 is used as starting point. It is modified to take into account trapezoidal slot. First, equation defining the valve section function of the opening has to be defined.

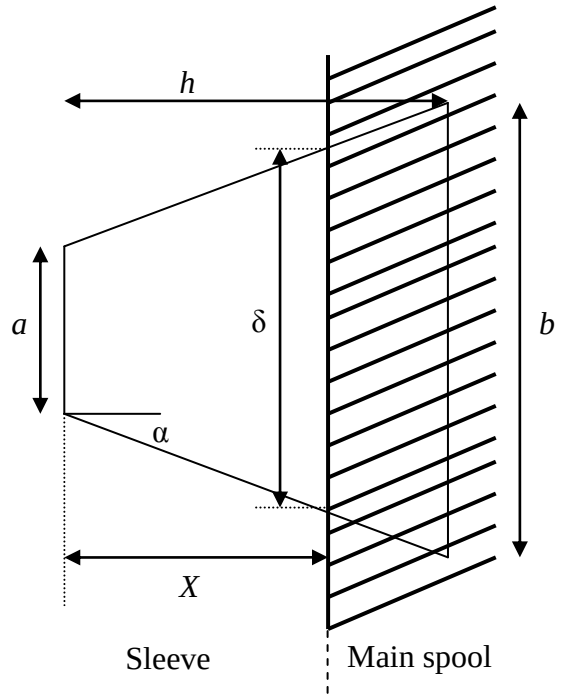

Figure 59: Notation for the computation of the section of the slot in function of the opening.

Section of a trapeze with a small basis a, big basis δ and height X is:

$$S = \frac{a+\delta}{2} X \tag{57}$$

Valve section of a trapezoidal slot at maximal opening can then be deduced:

$$S_{\max} = \frac{a+b}{2} h \tag{58}$$

δ can be eliminated from equation (57). Angle α is introduced:

$$\begin{aligned} &\tan(\alpha) = \frac{\delta - a}{2}\frac{1}{X} = \frac{b-a}{2}\frac{1}{h} \\ &\Rightarrow \delta = X\frac{b-a}{h} + a \end{aligned} \tag{59}$$

Equation (57) becomes:

$$S = \frac{2a + X\dfrac{b-a}{h}}{2} X \tag{60}$$

b is extracted from equation (58):

$$b = \frac{2S_{\max}}{h} - a \tag{61}$$

So the section functions of opening, is obtained from equations (60) and (61):

$$S = \left[a + \frac{X}{h}\left(\frac{S_{\max}}{h} - a \right) \right] X \tag{62}$$

Equation (62) shows that the valve section equation only depends on the small basis a if the maximal stroke (h) and the section at maximal opening (Smax) are known.

The maximal stroke of the valve is the same as for the rectangular slot: h = 0,93mm.

The servoactuator maximal speed without load is required to be around 106mm/s with a low dissymmetry between extension and retraction speeds. The simulation of the servoactuator with the dynamic model permits defining for a rectangular slot, the needed section of the valve to obtain this speed with a restriction diameter of 1.15mm. This area must be the same for the trapezoidal slot (or even with another slot geometry) to reach the target speed. This necessary area obtained by simulation is S_{max} = 1.488mm² (see Figure 60, the curve corresponds to S_{max} = 1.6 x 0.93 = 1.488mm² and gives the best result in term of maximal speed and symmetry between the extension and retraction speeds).

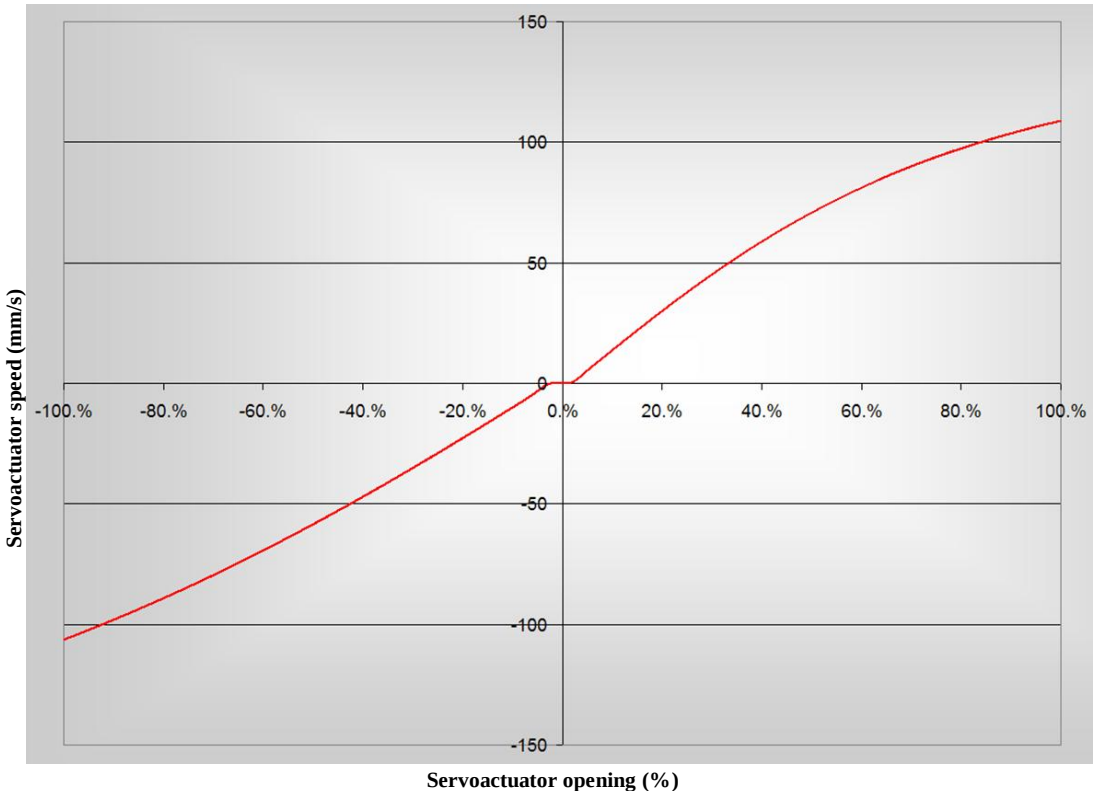

Figure 60: Servoactuator maximal speed without load obtained with the servoactuator dynamic model in order to extract the section at maximal opening (rectangular slots).

4.4.2 - Model-based selection of the basis of the trapezoidal slot

The results obtained in section 4.3.2 - p114 with the valve dynamic model device were excellent. So the updated AMESim model is used for the slot selection before validation with tests on a real valve. The different steps of the method for the slot selection are:

- Evolution of the valve dynamic model to take into account trapezoidal slots
- AMESim simulation for different basis (*a*) and extraction of the gain speed and of the harmonic response
- Selection of the optimal slot with a restriction diameter of 1.15mm
- Manufacturing of the valve with the slots selected by the valve dynamic model
- Checking and validation of the new valve with trapezoidal slots on the test bench

Note 1: The design explorer tool of AMESim has not been used. Indeed, the only parameter is the small basis. In this case, it is easier and faster to find the optimum manually.

Note 2: The harmonic response is an important parameter to assess the real behaviour of the servoactuator. That is why it has been computed from the servoactuator model developed for the speed gain. Two ways were possible to compute the harmonic response: a linear analysis or the transferometer module of AMESim. Linear analysis is faster but is only efficient for linear systems. In this case, the transferometer has so been used as it represents the way that is used during testing.

Two values of small basis for the trapezoidal slot are pointed out that are *a*=0.6mm and *a*=0.8mm (see Figure 61). The value of 0.6mm corresponds to the speed gain the closest to the one of the existing servoactuator. So it is better from a mixability point of view. However, the value of 0.8mm shows more important speeds than for 0.6mm while the difference of speed with the existing servoactuator is acceptable.

The harmonic response is simulated from the servoactuator dynamic model and plotted for these two values (Figure 62 and Figure 63). They correspond to the required behaviour since the curves are included in the domain defined in section 3.3.1 - p73.

Finally, the value of 0.8mm is selected for a control point of view. It has two main advantages on the other value:

- The servoactuator allows the pilot to react faster, in particular for small openings
- The behaviour is more linear, which makes the control easier.

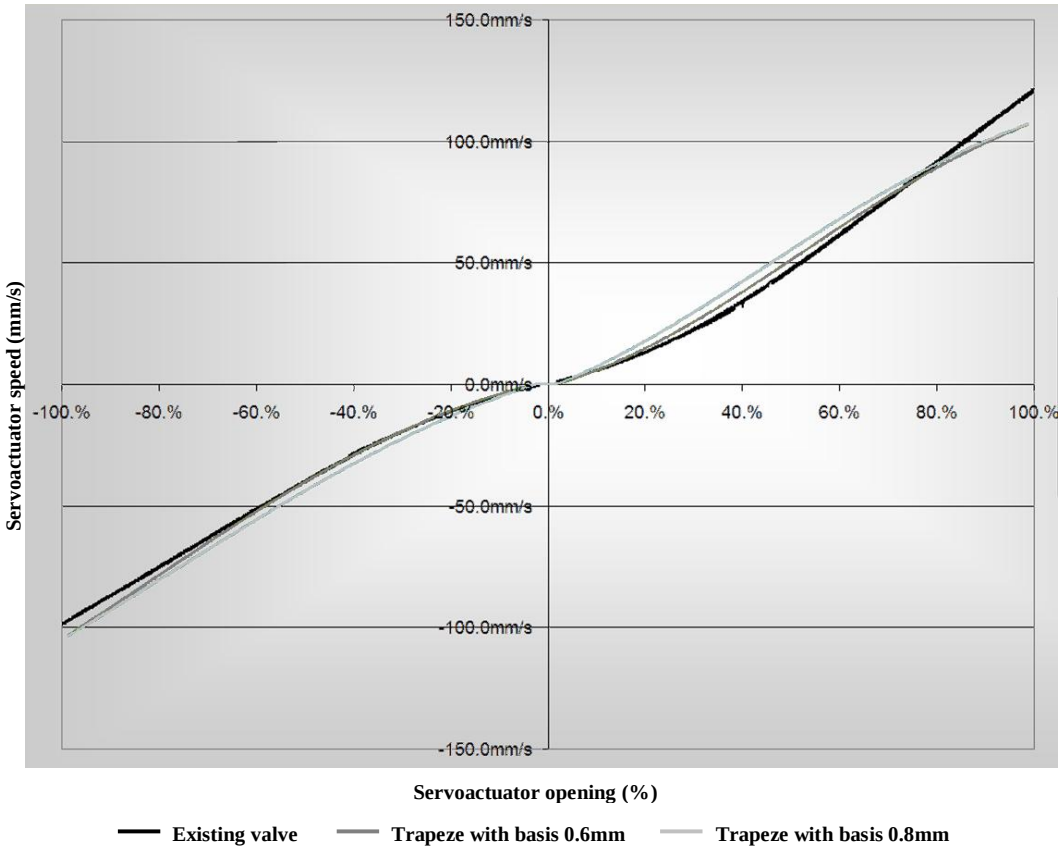

Figure 61: Speed gain for the different basis of trapeze (restriction diameter of 1.15mm).

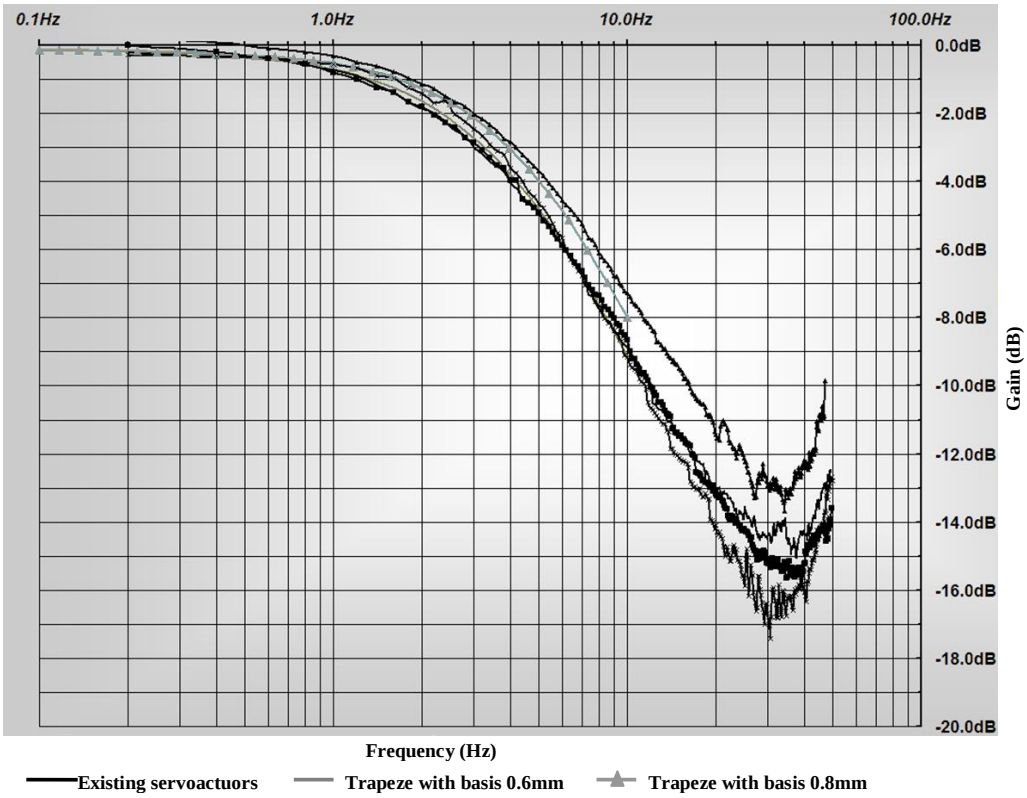

Figure 62: Magnitude of simulated servoactuator with trapezoidal slots and real servoactuators (black curves) - Input magnitude: +/-1mm, restriction diameter Ø1.15mm.

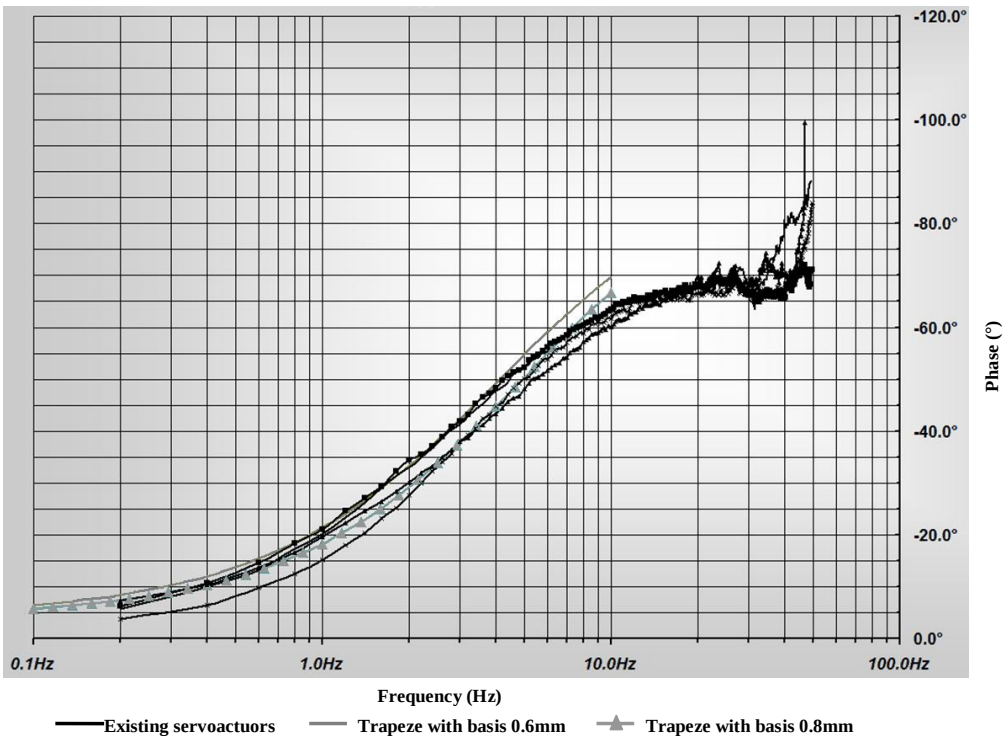

Figure 63: Phase of simulated servoactuator with trapezoidal slots and real servoactuators (black curves) - Input magnitude: +/-1mm, restriction diameter Ø1.15mm.

4.4.3 - Experimental validation of the selected basis

A valve with a trapezoidal slot and a small basis of 0.8mm has so been manufactured and tested on the valve test bench. Figure 64 shows the comparison of the flow gain between the valve simulation and the test.

The gap between the two curves in very small (maximal error lower than 5%): curves are very close which definitely validates the trapezoidal slot with a small basis of 0.8mm.

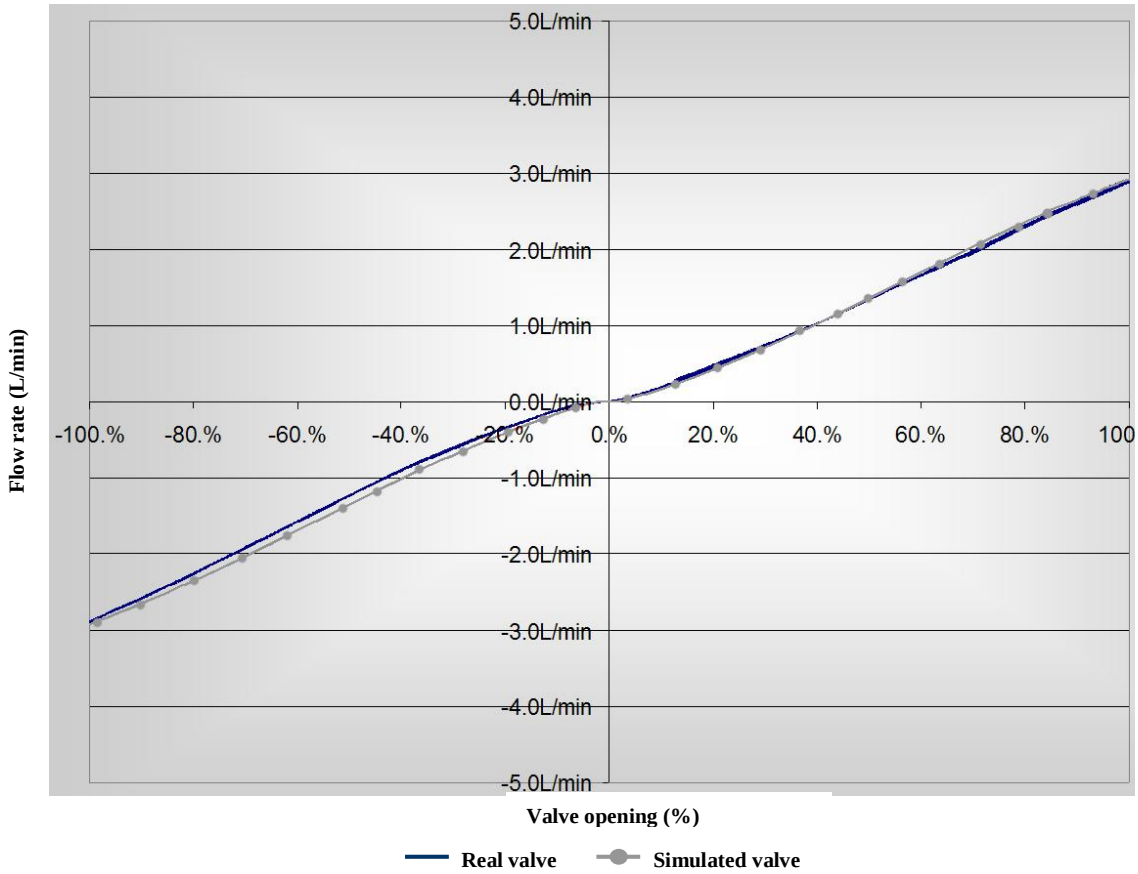

Figure 64: Comparison of the flow gains between simulated and real valve.

4.5 - Servoactuator behavior

4.5.1 - Validation on the servoactuator

A first prototype of servoactuator has been manufactured and now is tested on the servoactuator test bench. The first criterion to be checked is the no-load speed of the servoactuator. The results of this experimental test compared to the servoactuator dynamic model prediction are shown on the Table 14.

	Speed in extension	Speed in retraction
Dynamic model prediction for the new servoactuator	106mm/s	106mm/s
Tests results for the existing servoactuator	122mm/s	117mm/s
Tests results for the new servoactuator	88mm/s	108mm/s

Table 14: Comparison between experimental tests results and servoactuator dynamic model prediction

The results obtained are little different from the servoactuator dynamic model prediction but stay in the specification domain. So the model needs to be update.

The servoactuator dynamic model was based on the valve dynamic model, the scheme of the servoactuator and some supposed data. A metrology analysis has been performed on the prototype to know the real value of the servoactuator parameters (*e.g.* the lever stroke, the body weight) and the supposed data has been changed on the model from the measured data extracted from the test on the prototype (*e.g.* the pressure supply on each body, the seal loads).

After the update on the servoactuator dynamic model, the results of the no load speed between the model and the test are very closed (Table 15). This updated servoactuator model will replace the previous one in the future analyses.

	Seal load	Servoactuator dynamic model prediction	Test speed obtained
Extension	35daN	88mm/s	88mm/s
Retraction	10daN	108mm/s	108mm/s

Table 15: Comparison between experimental tests results and servoactuator dynamic model prediction after updating

The other main response of the system to be checked is the harmonic response of the servoactuator. The Figure 62 and Figure 63 show the behaviour of the real servoactuator tested on the test bench compared to the behaviour predicted by the simulation.

The curves are very close which is proving the quality of the conception. Indeed the harmonic response was one of the main criteria to validate the orifice valve geometry, and the predictions are impressively good.

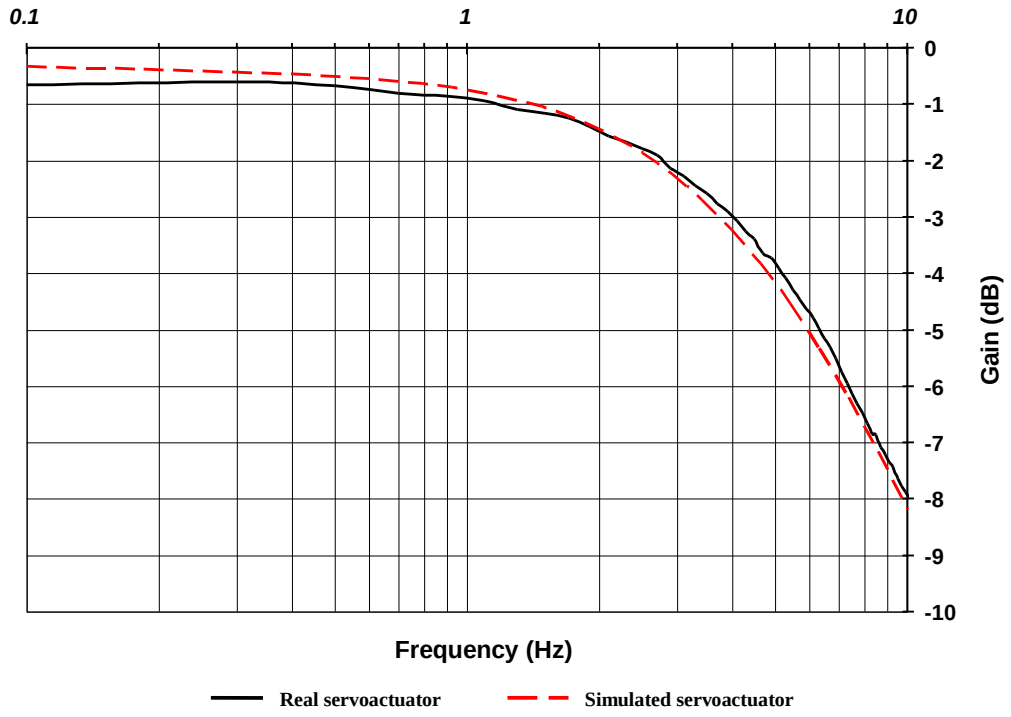

Figure 65: Magnitude of simulated servoactuator compared with the real tested servoactuator - Input magnitude: +/-1mm, restriction diameter Ø1.15mm.

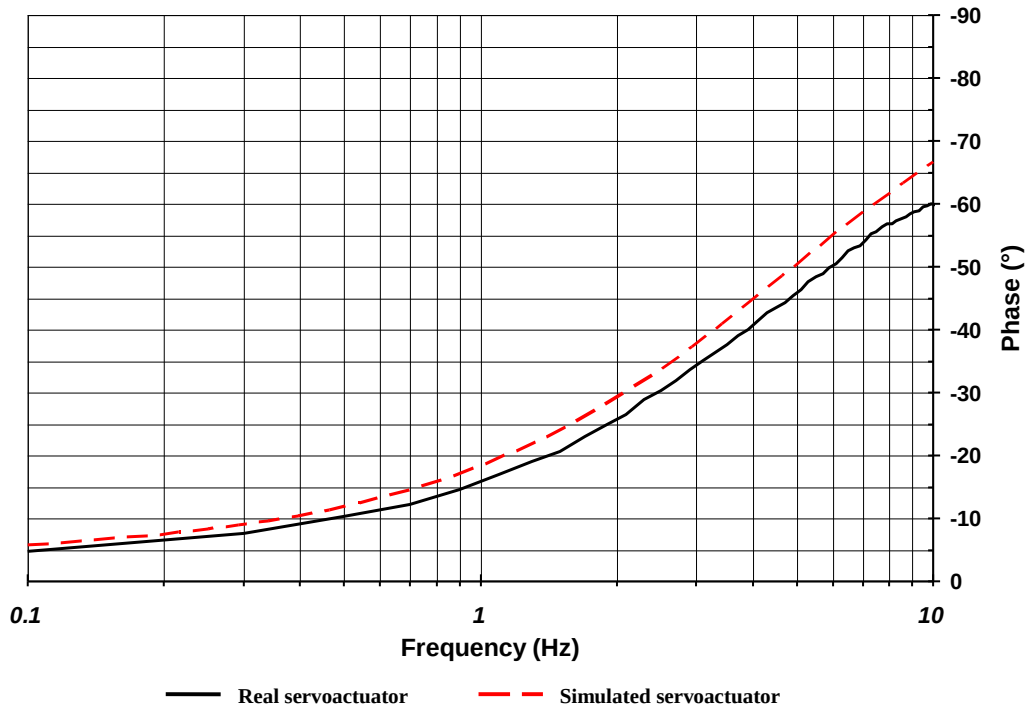

Figure 66: Phase of simulated servoactuator compared with the real tested servoactuator - Input magnitude: +/-1mm, restriction diameter Ø1.15mm.

4.5.2 - Evolution of the project

For marketing reasons, Eurocopter initiates some evolutions on the servoactuator requirements. The maximal speed without load is not as important as the harmonic response for the piloting comfort, but it has a big influence on the customer mind. An increased on the maximal speed without load has so been imposed by the sale department even if the consumption criterion has to be reviewed too.

In order to increase the maximal speed without load which is in the low limit of the specification domain, two modifications have been realized:

- The lever stroke has been increased by 15%. The open loop gain has been kept not to modify the Bode diagram which is very satisfying.
- A restriction diameter with a value of 1.25mm is chosen a priori. In this case, the tests give a maximal flow rate of 4.7l/min. If this case happens with a pump which delivers 6l/min, then 1.3l/min are available to feed the three remaining servoactuators (2 main servoactuators and the tail servoactuator), which gives 0.43l/min by servoactuator (which represent 15mm/s in extension for the main servoactuator).

The new servoactuator load/speed diagram obtained is shown on the Figure 67.

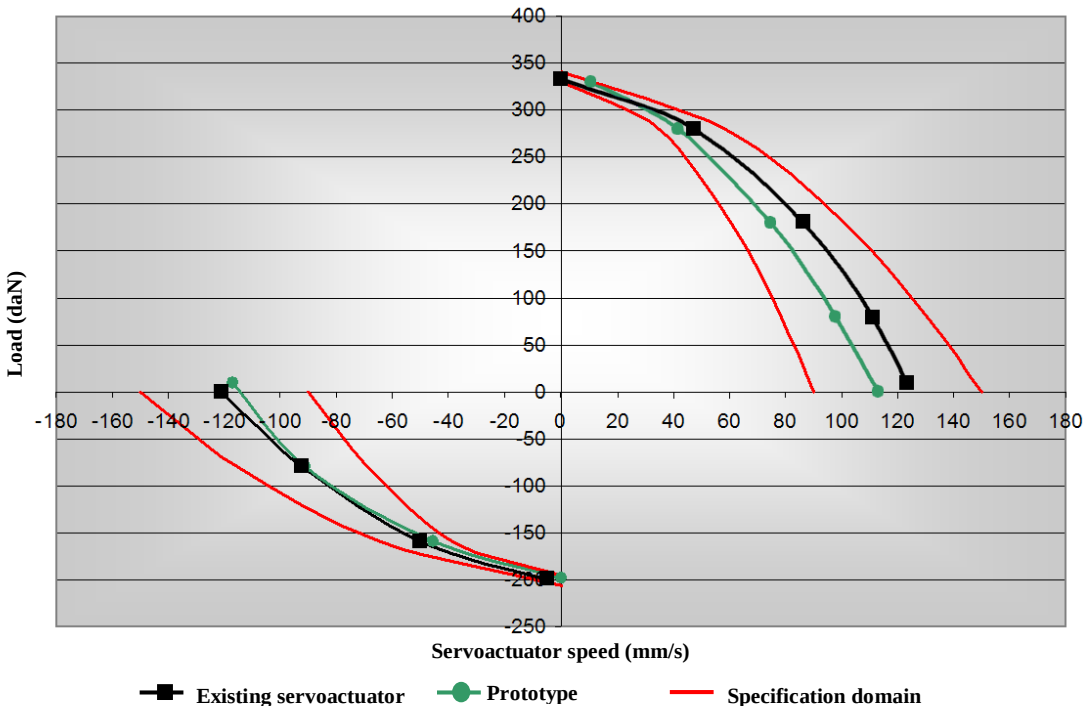

Figure 67: Load/speed diagram of the new servoactuator from simulation obtained with a restriction diameter of 1.25mm.

4.6 - Conclusion

The design of the valve in the nominal mode has been presented in this chapter. The design parameters of the valve have been computed from a DOE analysis based on experimental results. A valve has thus been manufactured and tested with this design. The design has been validated for extreme values of the functional domain and the experimental results have permitted to update the valve dynamic model. The mixability has thus been able to be evaluated over the full operating domain. The analysis point out that this requirement was not reached. An original geometry for the valve width has so been proposed using a model-based approach. The innovation has concerned to define the right geometry to ensure the mixability specification. A trapezoidal slot has been selected with the dynamic model, manufactured and validated by experimental results. Finally and although the requirements are already met, the servoactuator has been upgraded for marketing reasons. The no-load speed of the servoactuator has been increased.

Conclusion

French synthesis

Le principal objectif de la thèse est de concevoir une servocommande à bas coût qui possède des performances similaires à celle de l'hélicoptère le plus vendu : l'EC130. Les performances classiques pour le design de la servocommande sont les vitesses maximales à vide en extension et en rétraction. Les nouvelles exigences requises dans ce travail sont :

- le débit maximal directement lié à la consommation d'huile
- la mixabilité avec la servocommande existante pour éviter d'avoir à changer toutes les servocommandes au même moment durant la maintenance si une d'entre elles est défectueuse. Cette spécification est particulièrement prise en compte durant la conception du distributeur et est une des originalités de ce travail.

L'objectif bas coût conduit à choisir une méthode à partir d'un modèle de simulation afin de limiter les essais expérimentaux et de développer une nouvelle méthode de fabrication. Pour garantir la précision des résultats de simulation, des pièces ont été fabriquées et testées tout au long de l'étude et ont permis de recaler les modèles.

Les architectures de servocommande et de distributeur ont été imposées dans le chapitre un. Concernant les servocommandes, un corps mobile est choisi puisque l'EC130 est un hélicoptère léger avec de faibles charges et par conséquent avec une faible pression d'alimentation. Une servocommande double effet est requise puisque les charges peuvent provenir des deux directions. Finalement, l'actionneur est dissymétrique pour limiter les fuites externes, l'encombrement et autoriser un montage en tandem. De plus, pour des raisons de fiabilité, l'actionneur possède deux corps. Le distributeur est choisi avec une entrée mécanique et un tiroir linéaire pour la robustesse et la simplicité. Comme les raisons de sécurité exigent une solution de by-pass en cas de grippage du tiroir principal, un tiroir secondaire a été ajouté au distributeur.

Dans le chapitre deux, les équations qui définissent le débit à travers les orifices de distributeur ont été présentées. Elles permirent de recenser les paramètres de fluide et géométriques qui influencent le comportement du distributeur et par conséquent de mettre en lumière les paramètres qui peuvent être optimisés pendant la phase de design. Seul un paramètre a été sélectionné, la largeur de fente, pour sa principale influence sur le

comportement dynamique de la servocommande et également parce qu'il peut être ajusté aisément et avec précision. Comme la méthode de design est basée sur un modèle de simulation, il est nécessaire d'établir un modèle de distributeur et de servocommande. Ce chapitre donne le premier modèle dynamique avant recalage.

Dans le chapitre trois, le pré-design du distributeur a été achevé en utilisant une méthode basée sur le modèle statique de distributeur. Les paramètres de design sont la largeur de fente pour les raisons données précédemment et le diamètre d'une restriction ajoutée au distributeur pour garantir la nouvelle spécification sur le débit maximal consommé. Le pré-design permet de calculer ces deux paramètres et de fabriquer des distributeurs. Afin de satisfaire les exigences concernant les coûts de fabrication, une nouvelle méthode pour la rectification des flancs distributeur a été proposée. Elle a été développée en utilisant une analyse par plan d'expérience et est basée sur le comportement asymptotique de la courbe de gain en pression. Cette méthode est bas coût : elle ne requiert qu'un essai pour mesurer la courbe de gain en pression puisque la courbe de gain en débit n'est plus nécessaire. Deux bancs d'essais ont été développés spécifiquement durant la thèse pour procéder aux expérimentations du distributeur et de la servocommande.

Le quatrième chapitre a concerné le design du distributeur en mode nominal. Un plan d'expérience a permis de calculer les paramètres de design depuis les résultats d'essais des distributeurs fabriqués. Un distributeur avec ces valeurs a été fabriqué et les paramètres de design ont été validés grâce aux résultats expérimentaux pour les valeurs extrêmes de la spécification de vitesse maximale à vide. De plus ces essais ont permis de recaler le modèle dynamique de distributeur et d'évaluer la mixabilité sur tout le domaine de fonctionnement. Les résultats de cette évaluation montrent que cette exigence n'est pas atteinte. Afin de résoudre ce problème, une nouvelle géométrie de distributeur a été proposée. La géométrie innovante proposée concerne un distributeur avec des fentes trapézoïdales qui répondent au critère de mixabilité sur tout le domaine de fonctionnement. Les nouveaux paramètres de design sont la petite et la grande base des fentes trapézoïdales. Ces paramètres ont été calculés grâce à la simulation du modèle dynamique recalé de distributeur. Finalement, un nouveau distributeur a été fabriqué et les essais ont permis de valider la nouvelle géométrie. Le distributeur a ensuite été monté sur la servocommande puis l'appareil complet a été testé sur le banc d'essai servocommande. Ceci a permis de recaler le modèle dynamique de servocommande. Les résultats expérimentaux ont complètement validé le design de distributeur. Deux légères modifications ont néanmoins été apportées pour des raisons purement marketing : l'augmentation de la course levier et de la limite de consommation afin d'augmenter la vitesse maximale à vide.

La conclusion finale de la thèse est le succès de l'étude. En effet le seul élément au départ de ce travail fut la servocommande existante conçue il y a plus de 20 ans et quelques spécifications. Il n'y avait aucun plan ni aucune règle de conception. Le Passage de client acheteur à fabricant a donc été un travail délicat. L'approche choisie pour atteindre les objectifs de conception et de fabrication de distributeur à bas coût est basée sur l'interaction entre les modèles de simulation et les essais expérimentaux des distributeurs fabriqués. Ces modèles ont permit de gagner du temps et de l'argent et de produire un appareil efficient au final.

La conception du distributeur a été basée sur le modèle dynamique réalisé. Pour le développement des futures servocommandes, il serait judicieux d'utiliser plus avant le logiciel de simulation. L'analyse de robustesse de la conception pourrait ainsi être automatisée en combinant un outil de modélisation prédictive et un outil d'optimisation. Ceci permettrait d'aller plus loin dans les objectifs de diminution des coûts de conception et des surcoûts de fabrication à cause des tolérances non justifiées.

Thesis conclusion

The thesis main objective is to design a low cost servoactuator which has similar performances as the one of the most sold Eurocopter helicopter: the EC130. The usual main performances for the servoactuator design are the no-load speeds in extension and in retraction. The new requirements to meet in this work are:

- the maximal flow rate that influences the consumption
- the mixability with existing servoactuators to avoid changing all the servoactuators at the same time during the maintenance. This specification is scarcely taken into account in the valve design and is one of the originalities of this work.

The low-cost objective led to choose a model-based design to limit the experimental tests and to develop a new manufacturing method. In order to guaranty the results of the model-based method, the devices have been manufactured and tested along the study to update the models.

The architectures of the servoactuator and of the valve have been selected in chapter one. Concerning the servoactuator, a moving body is chosen since the EC130 is a light helicopter with low loads and thus with a low supply pressure. A double effect servoactuator is required since loads can be in two sides. Finally, the actuator is dissymmetrical to limit the external leakages and the space occupied. Moreover, for reliability reasons, the actuator has two bodies. The valve is chosen with a mechanical input and a linear spool for robustness and simplicity. As the safety requires a by-pass solution in case of the main spool seizure, a back-up spool has been added to the valve.

In the chapter two, the equations that define the flow through the valve orifices have been presented. It permits to take an inventory of the fluid and geometrical parameters that influence the valve behavior and consequently to highlight the parameters that can be optimized during the design. Only one parameter has been selected, the slot width, because it influences mainly the servoactuator dynamic and also because it can be adjusted easily and with accuracy. As the design method is model-based, it is necessary to establish a static model of the valve and dynamic models of the valve and of the servoactuator. This chapter gives the first dynamic models before updating.

In chapter three, the pre-design of the valve has been achieved using a method based on the valve static model. The design parameters are the slot width for the reasons given above and the diameter of a restriction added to the valve to guaranty the new specification on the maximal flow rate. The pre-design allows to compute these two parameters and to manufacture valves. To meet the requirement on the manufacturing cost, a new method for the spool grinding has been proposed. It has been developed using a DOE analysis and is based on the asymptotic behavior of the pressure gain curve. The method is low-cost: it only requires one test to measure the pressure gain curve since the flow gain curve is not necessary. Two test-benches have been developed specifically during the thesis to get experimental results on the valve and on the servoactuator.

The fourth chapter concerns the design of the valve in the nominal mode of the servoactuator. A DOE analysis has permitted to compute the design parameters from experimental results on manufactured valves. A valve with these values has been manufactured and the design parameters have been validated thanks to experimental results for the extreme values of the no-load speed specification. Moreover these tests are used to update the dynamic valve model and to evaluate the mixability over the full operating domain. The results of this evaluation point out that this requirement is not reached. In order to solve this problem, a new valve geometry has been proposed. The innovating proposed geometry concerns the valve trapezoidal slots that ensure the mixability requirement over the full operating domain. The new design parameters are the small and large bases of the trapezoidal slots. These parameters have been computed by a model-based approach on the valve updated dynamic model. Finally, a new valve has been manufactured and tests permit to valid the new geometry. The valve has next been mounted on the servoactuator and the full device has been tested on the servoactuator test bench. It has allowed to update the servoactuator dynamic model. The experimental results have completely validated the valve design. For marketing reasons, two minor changes have nevertheless been added: the lever stroke and the maximal consumption have been increased in order to increase the no load speed.

The final conclusion of the thesis is that the study is successful. Indeed the only initial element to start the work was the existing servoactuator and they were few specifications, no designs scheme and no design rules. The work was thus difficult. The chosen approach to complete the objective of designing and manufacturing a low-cost valve is based on the interaction between simulation model and experimental tests of real manufactured valves. It permits to save time and money and to produce a final efficient device.

The valve has been design from a model-based approach. For the development of the future servoactuator, the robustness analysis of the conception could be automated using a predictive tool like the servoactuator model developed during the thesis, and an optimization tool. By this way, the conception and manufacturing (unjustified tolerances) cost could be decreased.

Bibliography

[1] "Conditions d'homologation des servocommandes hydraulique de gouvernes", Direction technique des constructions aéronautiques, AIR8520A, 1973

[2] "Mobil Aero HF Series – Aviation Hydraulic Fluids", ExxonMobil Aviationlubricants, 2008

[3] "National Aerospace Standard", Aerospace Industries Association, NAS1638, 1964

[4] Adams, H.W., "aircraft hydraulics", Mc Graw Hill, 1943

[5] AMESim, "reference manual", Rev9, nov 2009

[6] Attar, B., "Modélisation réaliste en conditions extrêmes des servovalves électrohydrauliques utilisées pour le guidage et la navigation aéronautique et spatiale", Thèse INSA de Toulouse, 2008

[7] Baz A., Barakat A., Rabie G., "Effect of radial clearances in hydraulic spool valves on the static and dynamic characteristic of servomechanism", Proceedings of the 5th world congress on Theory of Machines and Mechanims, ASME, 1979, pp 785-788

[8] Blackburn, J.F., Reethof, G., Shearer, J.L., "Fluid Power Control", John Wiley, 1960

[9] Donohue, J., "Experimental designs for simulation", Proceedings of Winter Simulation Conference, 1994

[10] Ellman, A., Virvalo, T., 1996, "Formation of Pressure Gain in Hydraulic Servovalves and its Significance in System Behavior", Fluid Power Systems and Technology, ASME FPST-Vol. 3, November, pp. 77–81, Atlanta, GA.

[11] Eryilmaz, B., Wilson, B.H., 2000, "Modelling the Internal Leakage of Hydraulic Servovalves", International Mechanical Engineering Congress and Exposition, ASME, Vol. DSC-69.1, pp. 337-343, Orlando, USA.

[12] Faisandier, J., 2006, Mécanismes Hydrauliques et Pneumatiques, 9°ed. Paris. Dunod.

[13] Guillon, M., "Commande et asservissement hydraulique et électrohydraulique", Lavoisier, 1992

[14] Hatami, S., Cowley, E., Morey, C., "Using experimental design to improve the efficiency of simulation modelling – a manufacturing perspective", Proceedings of Winter Simulation Conference, 1990

[15] Keller, G., "Aircraft hydraulic design", Applied Hydraulic Ed, 1957

[16] Kleijnen, J., "Sensitivity analysis and optimization in simulation: design of experiments and case studies", Proceedings of Winter Simulation Conference, 1995

[17] Lafortune, G., "Commandes de vol hydraulique servocommandes", E/T.M 610, Eurocopter, 1997

[18] Lefort, P., Hamann, J., "L'hélicoptère théorie et pratique", 2007, ed Chiron

[19] Lewis, C.W., “Some Factors Influencing the Speed of Response of Hydraulic Position Servomechanisms”, Aeronautical research council reports and memoranda, 1958

[20] Louvet, F., Deplanque, L., “Les plans d’expériences: une approche pragmatique et illustrée”, 2005

[21] Maré, J-C., “Actionneurs hydrauliques – Commande”, Article S7531, Série Mesure et Régulation, Encyclopédie des Techniques de l’Ingénieur, septembre 2002

[22] Maré, J-C., “Actionneurs hydrauliques – Conception”, Article S7530, Série Mesure et Régulation, Encyclopédie des Techniques de l’Ingénieur, juin 2002

[23] Mare, J-C., Attar B., 2008, “Enhanced model of four ways servovalves characteristics and its validation at low temperature”, International Journal of Fluid Power, Vol 9 N°2, pp 35-43, ISSN 1439-9776

[24] Marger, T., Budinger, V., Maré, J-C., Malburet, F., “Designing redundant metering valves for hydraulic actuators under mixability and low cost-constraints”, AIAA-ATIO

[25] Marger, T., Budinger, V., Maré, J-C., Malburet, F., “managing the hydraulic characteristics of control spool valves through simplified manufacturing process”, ASME

[26] Martin, H.R., Cloy, D.Mc, “Control of fluid power”, Ellis Horwood, 1980

[27] Merritt, H.E., 1967, “Hydraulic Control Systems, John Wiley & Sons”, New York, New York

[28] Padfield, G., “Helicopter flight dynamics”, ed Blackwell science, 1996

[29] Press, W.H., Flannery, B.P., Teukolsky, S.A., Vetterling, W.T., “Numerical recipes in Pascal: the art of scientific computing”, Cambridge University Press, 1989

[30] Stat-Ease, www.statease.com, 2007

[31] Thayer, W.J., “Specification standards for electrohydraulic flow control servovalves, Technical bulletin 117, Moog, 1962.

[32] THM, “Chaine de commande Ecureuil”, Eurocopter

[33] THM, “Chaine de commande SuperPuma”, Eurocopter

[34] Thomson, J.E., Campbel, R.B., “Manual for aircraft hydraulics”, aviation press, 1942

Annex1:
method to compute the speed gain curve from the flow gain test

The initial point is the data issues from the flow gain test. During it, the two chambers are connected across a flowmeter (see Figure 68) and the stroke is measured by a LVDT sensor.

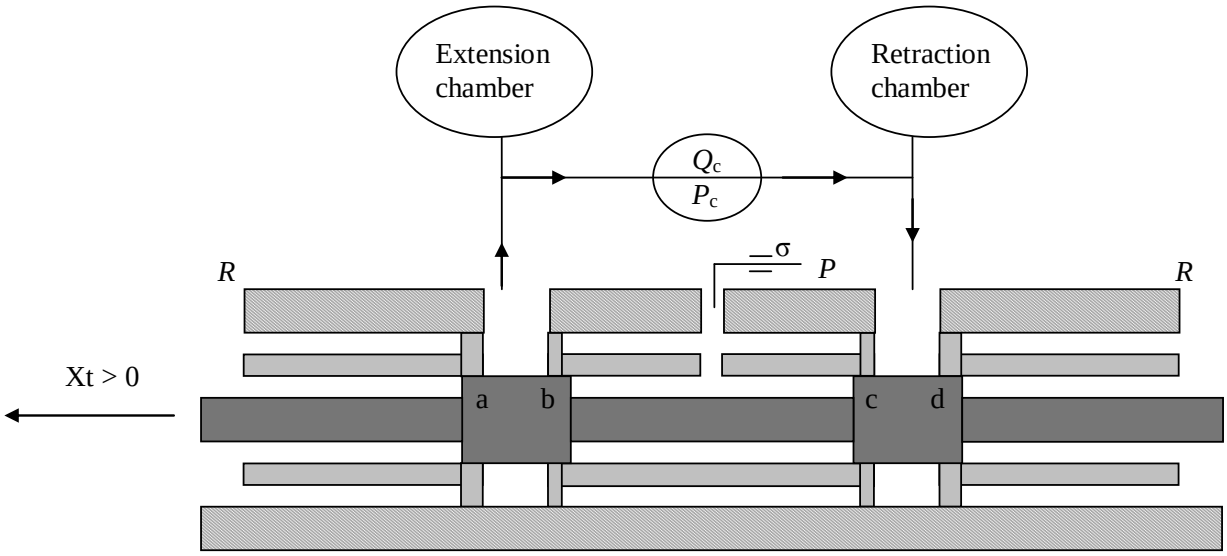

Figure 68: Outline of the flow gain test

First step of the method is to extract all the pressure and the sections during this test.
In extension, the flow rate through edge d is:

$$Q_c = C_q S_d \sqrt{\frac{2}{\rho}(P_c - R)} \tag{63}$$

It is equal to flow rate through edge b:

$$Q_c = C_q \frac{1}{\sqrt{\frac{1}{\sigma^2} + \frac{1}{S_b^2}}} \sqrt{\frac{2}{\rho}(P - P_c)} \tag{64}$$

In retraction, the flow rate through edge a is:

$$Q_c = C_q S_a \sqrt{\frac{2}{\rho}(P - P_c)} \tag{65}$$

It is equal to flow rate through edge c:

$$Q_c = C_q \frac{1}{\sqrt{\frac{1}{\sigma^2} + \frac{1}{S_c^2}}} \sqrt{\frac{2}{\rho}(P - P_c)} \tag{66}$$

Note : S_a, S_b, S_c and S_d (overlaps and clearance can be taken into account) vary with the stroke of the main spool and can be computed with equations (63 to 66).

Pressure Pc can be deduced from equations 63-64 (resp. 65-66) for extension (resp. retraction). Pc is calculated from the return edges (a and d) and not pressure edges (b and c) so that the computation does not depend on the restriction.

i) Computation of the speed in extension

The aim is to compute the speed gain of the dissymmetrical servoactuator with the flow gain of the symmetrical valve defined above. Two bodies, the restriction and seals loads are taken into account. Figure 69 shows the servoactuator in the case of extension and the notations used.

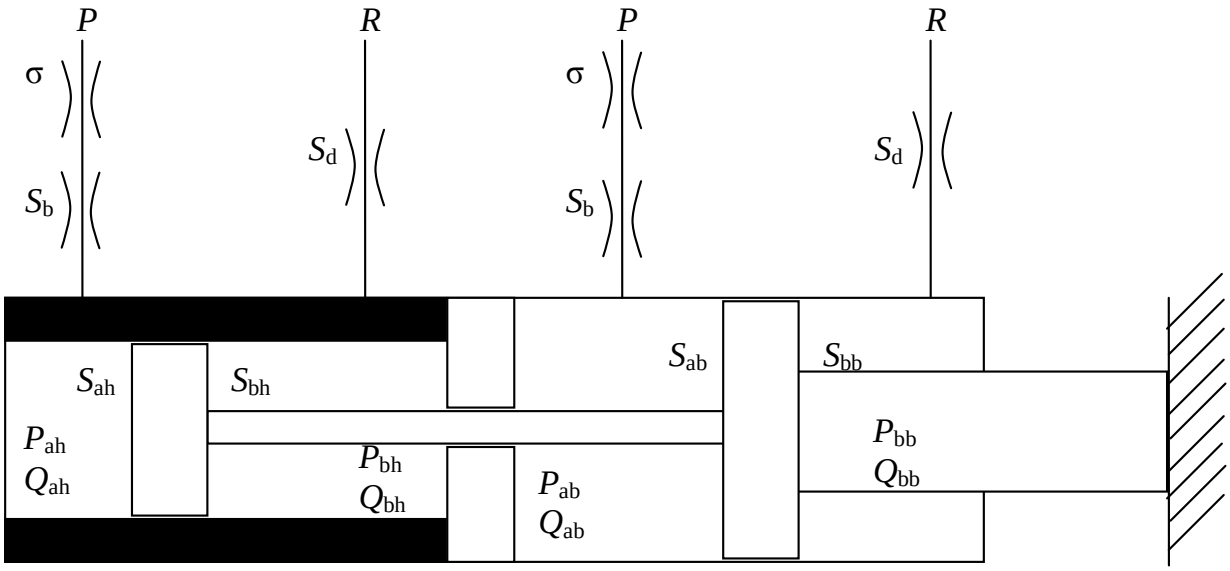

Figure 69 : Servoactuator in extension

The equation defining the speed of the servoactuator is:

$$\dot{X} = \frac{Q_{ah}}{S_{ah}} = \frac{Q_{bh}}{S_{bh}} = \frac{Q_{ab}}{S_{ab}} = \frac{Q_{bb}}{S_{bb}} \tag{67}$$

The flow rate equations applied at the four edges of the valves give:

$$Q_{ah} = C_q \frac{1}{\sqrt{\frac{1}{\sigma^2} + \frac{1}{S_b^2}}} \sqrt{\frac{2}{\rho}\left(P - P_{ah}\right)} \tag{68}$$

$$Q_{bh} = C_q S_d \sqrt{\frac{2}{\rho}\left(P_{bh} - R\right)} \tag{69}$$

$$Q_{ab} = C_q \frac{1}{\sqrt{\frac{1}{\sigma^2} + \frac{1}{S_b^2}}} \sqrt{\frac{2}{\rho}\left(P - P_{ab}\right)} \tag{70}$$

$$Q_{bb} = C_q S_d \sqrt{\frac{2}{\rho}\left(P_{bb} - R\right)} \tag{71}$$

Some hypotheses are needed:

- Same low coefficient (Cq) for all edges
- The two symmetrical valves are strictly identical (upper and lower) => Q_c and P_c identical.

Equations (64) and (68) become:

$$Q_{ah} = Q_c \sqrt{\frac{P - P_{ah}}{P - P_c}} \tag{72}$$

Equations (63) and (69) become:

$$Q_{bh} = Q_c \sqrt{\frac{P_{bh}}{P_c}} \tag{73}$$

Equations (64) and (70) become:

$$Q_{ab} = Q_c \sqrt{\frac{P - P_{ab}}{P - P_c}} \tag{74}$$

Equations (63) and (71) become:

$$Q_{bb} = Q_c \sqrt{\frac{P_{bb}}{P_c}} \tag{75}$$

Equation (67) combined with equations (72), (73), (74) and (75) gives the system below:

$$\dot{X} = \frac{Q_c}{S_{ah}}\sqrt{\frac{P-P_{ah}}{P-P_c}} = \frac{Q_c}{S_{bh}}\sqrt{\frac{P_{bh}}{P_c}} = \frac{Q_c}{S_{ab}}\sqrt{\frac{P-P_{ab}}{P-P_c}} = \frac{Q_c}{S_{bb}}\sqrt{\frac{P_{bb}}{P_c}} \tag{76}$$

Q_c, P_c, P, S_{ah}, S_{bh}, S_{ab}, S_{bb} known, calculation of P_{ah} or P_{bh} or P_{ab} or P_{bb} is necessary to compute the speed of the servoactuator.

Load equilibrium in the jack gives:

$$P_{ah}S_{ah} + P_{ab}S_{ab} = P_{bh}S_{bh} + P_{bb}S_{bb} + F_{joints} \tag{77}$$

Pressure P_{bb} can be deduced from the system (76) and the equation (77):

$$P_{bb} = f(P_c, P, F_{joints}, S_{ah}, S_{bh}, S_{ab}, S_{bb}) \tag{78}$$

So, the speed of the servoactuator is obtained from:

$$\dot{X} = \frac{Q_c}{S_{bb}}\sqrt{\frac{P_{bb}}{P_c}} \tag{79}$$

ii) Computation of the speed in retraction

Method is identical as the speed in extension, only initials conditions are different.

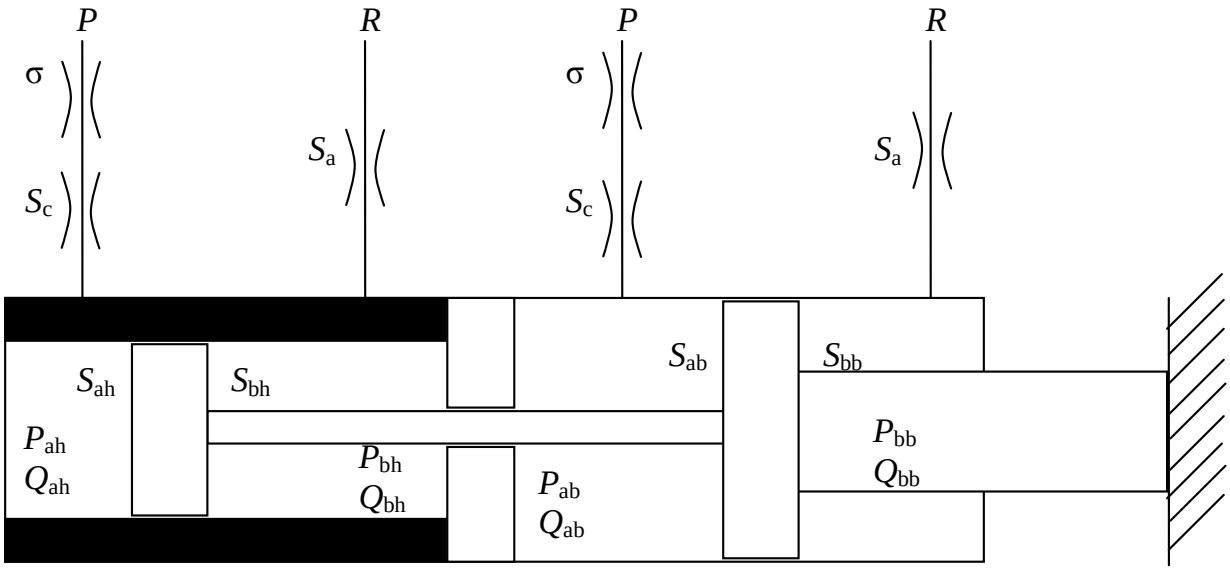

Figure 70 : servoactuator in retraction

Equation (67) about the speed is identical. Equations of edges (68), (69), (70), (71) and the equation of loads equilibrium (77) are becoming:

$$
\begin{aligned}
Q_{ah} &= C_q S_a \sqrt{\frac{2}{\rho}\left(P_{ah} - R\right)} \\
Q_{bh} &= C_q \frac{1}{\sqrt{\frac{1}{\sigma^2} + \frac{1}{S_c^2}}} \sqrt{\frac{2}{\rho}\left(P - P_{bh}\right)} \\
Q_{ab} &= C_q S_a \sqrt{\frac{2}{\rho}\left(P_{ab} - R\right)} \\
Q_{bb} &= C_q \frac{1}{\sqrt{\frac{1}{\sigma^2} + \frac{1}{S_c^2}}} \sqrt{\frac{2}{\rho}\left(P - P_{bb}\right)} \\
P_{ah} S_{ah} &+ P_{ab} S_{ab} + F_{joints} = P_{bh} S_{bh} + P_{bb} S_{bb}
\end{aligned}
\tag{80}
$$

Pressure P_{ab} is computed as P_{bb} in the previous case. By analogy, the speed of the servoactuator in retraction is deduced.

CONCEPTION D'UN DISTRIBUTEUR DE SERVOCOMMANDE HYDROMECANIQUE SOUS CRITERES DE COUT ET DE MIXABILITE

RESUME : Les servocommandes aident le pilote à contrôler l'appareil avec précision et peu d'effort au manche. Le travail de thèse concerne le design et la fabrication de servocommandes à entrée mécanique et puissance hydraulique. Le distributeur est la pièce la plus coûteuse et la plus difficile à concevoir et à fabriquer de la servocommande. Cette pièce est également celle qui influence principalement les performances de l'actionneur. Le principal objectif de la thèse est de concevoir une servocommande faible coût qui possède des performances similaires à une servocommande actuellement utilisée. Cet objectif a été scindé en trois étapes :

- Modéliser une servocommande et en particulier l'étage pilote de celle-ci
- Concevoir le distributeur à partir de ce modèle
- Fabriquer des prototypes de servocommande et valider la conception grâce à des essais

Dans le premier chapitre, des solutions techniques du futur design sont sélectionnées pour la servocommande et le distributeur afin de répondre aux exigences de l'application. Le second chapitre présente les modèles et outils pour le design et la fabrication du distributeur de servocommande. Le troisième chapitre concerne le pré-design et la fabrication des premiers distributeurs. La méthode choisie pour le pré-design du distributeur est basé sur une exploitation de modèle. Une nouvelle méthode de fabrication bas coûts est développée basée sur la représentation asymptotique de la courbe de gain en pression. Le dernier chapitre présente le design final du distributeur. L'évaluation à partir d'essais de l'exigence de mixabilité n'étant pas concluante, une nouvelle géométrie de fente pour le distributeur est proposée. Le design est donc mis à jour grâce à une approche basée sur le modèle puis validé par des essais.

Mots clés : conception, servocommande hydromécanique, distributeur, méthode de fabrication

VALVE DESIGN OF HYDRO-MECHANICAL SERVOACTUATOR UNDER COST AND MIXABILITY CRITERIA

ABSTRACT : The servoactuators assist the pilot to control the helicopter with accuracy and small pilot loads. This work concerns the design and manufacturing of hydraulically supplied and mechanically signaled servoactuators. The valve is the most costly servoactuator device. It is difficult to design and to manufacture. This device is also the one that mainly influences the servoactuator performance. The thesis main objective is to design a low cost servoactuator which has similar performances as one of the servoactuators already in service. This objective has been spread in three steps:

- modelling of servoactuator and in particular the power controller stage of the servoactuator
- model-based design of the valve
- manufacturing of servoactuator prototypes and validation through tests

In the first chapter some technological solutions for the future design are selected for the servoactuator and the valve to meet the requirements of the application. The second chapter presents the models and tools for the design and manufacturing of the servoactuator valve. The third chapter deals with the pre-design and the manufacturing of the first valves. The chosen methodology for the valve pre-design is model-based. A new low cost manufacturing process is developed based on the asymptotic representation of the pressure gain characteristic curve. The fourth chapter presents the final design of the valve. As the assessment of the mixability criterion is not concluding, a new valve geometry is proposed. The design is updated using a model-based approach and validated by experimental tests.

Keywords : model-based design, hydro-mechanical servoactuator, valve, manufacturing

ARTS ET MÉTIERS ParisTech

ParisTech INSTITUT DES SCIENCES ET TECHNOLOGIES PARIS INSTITUTE OF TECHNOLOGY